Universidade de Lisboa

Faculdade de Medicina de Lisboa

Characterization of adenosinergic system in Rett Syndrome

Catarina Miranda Lourenço

Mestrado em Neurociências

Dissertação

2015

Universidade de Lisboa

Faculdade de Medicina de Lisboa

Characterization of adenosinergic system in Rett Syndrome

Catarina Miranda Lourenço

Orientadores: Maria José Diógenes (PhD), Cláudia Gaspar (PhD),

Sofia Duarte (MD)

Mestrado em Neurociências

Dissertação

2015

Todas as afirmações efetuadas no presente documento são da exclusiva responsabilidade do seu autor, não cabendo qualquer responsabilidade à Faculdade de Medicina de Lisboa pelos conteúdos nele apresentados.

A impressão desta dissertação foi aprovada pelo Conselho Científico da Faculdade de Medicina de Lisboa em reunião de 22 de Setembro de 2015.

The scientific content of the present thesis is included in the manuscript currently in preparation:

- “Adenosine receptors as new therapeutic targets in Rett syndrome”.

Other papers where the author of this thesis participate during her master:

- Sandau US, Colino-Oliveira M, Parmer M, Coffmana SQ, Liub L, **Miranda-Lourenço C**, Palminha C, Batalha VL, Xu Y, Huo Y, Diógenes MJ, Sebastião AM, Boison D, “Adenosine kinase deficiency in the brain triggers enhanced synaptic plasticity” – *Under review;*

- Ribeiro FF, Xapelli S, Fonseca Gomes J, **Miranda-Lourenço C**, Tanqueiro SR, Diógenes MJ, Ribeiro JA, Sebastião AM, “Nucleosides in neuroregeneration and neuroprotection” – *Submitted.*

Index

Figure index ix

Table Index xi

Abbreviations list xiii

Resumo v

Abstract ix

1. Introduction 1
   - 1.1 Rett Syndrome 1
     - 1.1.1 Genetic Basis 2
   - 1.2 Rett Syndrome disease modelling 7
     - 1.2.1 Mouse models 7
     - 1.2.2 Induced Pluripotent Stem Cells (IPSCs) 8
   - 1.3 Adenosine 12
     - 1.3.1 Adenosine metabolism 13
     - 1.3.2 Adenosine receptors 14
     - 1.3.3 Adenosine and pathology 18
   - 1.4 BDNF 21
     - 1.4.1 BDNF expression 21
     - 1.4.2 BDNF signalling upon TrkB receptors 22
     - 1.4.3 Interaction between adenosine and BDNF 23
2. Aims 25
3. Materials and Methods 27
   - 3.1 Biological Samples 27
     - 3.1.1 Animals 27
     - 3.1.2 *Post-mortem* Brain Sample 27
   - 3.2 Human Induced Pluripotent Stem Cells (hIPSCs) 27
     - 3.2.1 Cell lines 27
     - 3.2.2 Materials 29
     - 3.2.3 Matrigel dish coating 30
     - 3.2.4 Laminin coating 31
     - 3.2.5 hIPSCs expansion 31
     - 3.2.6 Neuronal induction, the dual SMAD inhibition protocol 32
   - 3.3 Molecular Biology Techniques 34
     - 3.3.1 Western-Blot analysis 34

3.3.2 ELISA assay ... 36
3.3.3 Immunohistochemistry ... 36
3.3.4 RNA extraction and cDNA synthesis ... 38
3.3.5 Quantitative PCR ... 39
3.4 Electrophysiology ... 41
3.4.1 *Ex vivo* electrophysiological recordings ... 41
3.5 Data analysis ... 43
4. Results ... 45
4.1 Characterization of adenosine receptors in *Mecp2 KO* mice model ... 45
4.1.1 Rational ... 45
4.1.2 Adenosine receptors changes in *Mecp2 KO* mice ... 47
4.1.3 Adenosine kinase as a possible cause of adenosine impairment in *Mecp2 KO* mice ... 49
4.2 BDNF signalling impairment in *Mecp2 KO* mice ... 51
4.2.1 Rational ... 51
4.2.2 BDNF protein expression level in *Mecp2 KO* mice ... 52
4.2.3 TrkB receptors characterization in *Mecp2 KO* mice ... 52
4.3 Exploring adenosinergic system through neurons-derived from hIPSCs and in human brain sample ... 54
4.3.1 Rational ... 54
4.3.2 Characterization of hIPSCs ... 54
4.3.3 Adenosine receptors expression in hIPSCs and human brain sample ... 60
4.3.4 BDNF signalling impairment ... 63
5. Discussion ... 71
6. Acknowledgments ... 77
7. Bibliographic references ... 79

Figure index

Figure 1.1 - **Onset and clinical manifestations of RTT**. 2

Figure 1.2 - **Structure of *MECP2* gene**. 4

Figure 1.3 - **MeCP2 protein structure, mutations and associated impairments in RTT**. 5

Figure 1.4 - **MeCP2 and its functions**........ 6

Figure 1.5 - **Schematic representation of hIPSCs production and possible applications**. 9

Figure 1.6 – **Phenotypical characteristics of neurons-derived from RTT-hIPSCs**. 10

Figure 1.7 - **Challenges in RTT-IPSCs modelling**. 11

Figure 1.8 - **Adenosine structure**.. 12

Figure 1.9 - **Adenosine formation and catabolism**........ 14

Figure 1.10 - **Adenosine receptors structure**.. 15

Figure 1.11 - **Adenosine signalling pathways**.. 17

Figure 1.12 - **Adenosine receptors are targeted in several disorders**.. 20

Figure 1.13 - **BDNF signalling through TrkB full-length (TrkB-FL) receptors**.. 23

Figure 3.1 - **Schematic representation of neuronal differentiation, described in sections 3.2.5 and 3.2.6.**........ 33

Figure 3.2 - **Extracellular recording from hippocampal slices.** 42

Figure 4.1 - **Changes in fEPSP induced by DPCPX and CPA**. 45

Figure 4.2 - **A_1R protein expression level in *Mecp2 KO* mice**........ 45

Figure 4.3 - ***A_1R* mRNA relative expression in *Mecp2 KO* mice**. 48

Figure 4.4 - ***$A_{2A}R$* mRNA relative expression and protein expression level in *Mecp2 KO* mice.** 48

Figure 4.5 - **ADK protein expression level in *Mecp2 KO* mice**........49

Figure 4.6 - **fEPSP changes induced by ITU and ITU+DPCPX**. 50

Figure 4.7 - **TrkB-FL and TrkB-Tc protein expression level in *Mecp2 KO* mice**........51

Figure 4.8 - **BDNF concentration in *Mecp2 KO* mice.**........ 52

Figure 4.9 - ***TrkB-FL* and *TrkB-T1* mRNA relative expression in *Mecp2 KO* mice**. 53

Figure 4.10 - **Stages of neuronal differentiation and cell type specific markers**........56

Figure 4.11 - **Characterization of the first 3 stages of neuronal induction**. 58

Figure 4.12 - **Characterization of final neuronal differentiation stage**........59

Figure 4.13 - **Neuronal and glial-marker expression in neurons-derived from hIPSCs.**........59

Figure 4.14 - ***A_1R* mRNA relative expression in neurons-derived from hIPSCs and in RTT human brain** 61

Figure 4.15 - ***$A_{2A}R$* mRNA relative expression in neurons-derived from hIPSCs and in RTT human brain** ……62
Figure 4.16 - **ADK protein expression level in neurons-derived from hIPSCs.** ……………………………………63
Figure 4.17 - ***BDNF* mRNA relative expression in neurons-derived from hIPSCs and in RTT human brain** ……64
Figure 4.18 - **BDNF concentration in neurons-derived from hIPSCs.**…………………………………………………65
Figure 4.19 - ***TrkB-FL* mRNA relative expression in neurons-derived from hIPSCs and in RTT human brain**……… 66
Figure 4.20 - **TrkB-FL protein expression level in neurons-derived from hIPSCs.** …………………………… 67
Figure 4.21 - ***TrkB-T1* mRNA relative expression in neurons-derived from hIPSCs and in RTT human brain.** ……… 68
Figure 4.22 - **TrkB-Tc protein expression level in neurons-derived from hIPSCs.**……………………………..69

Table Index

Table 3-1 - **Characterization of hIPSCs lines.** 28

Table 3-2 - **Reagents for hIPSCs expansion and neuronal induction.** 29

Table 3-3 - **Medium formulation for hIPSCs expansion and neuronal induction.** 30

Table 3-4 - **Western-Blot primary antibodies.** 35

Table 3-5 - **Western-Blot secondary antibodies.** 35

Table 3-6 **- Immunohistochemistry primary antibodies.** 37

Table 3-7 - **Immunohistochemistry secondary antibodies.** 38

Table 3-8 - **Primer sequence and annealing temperature for all primer pairs used for quantitative analysis.** 40

Table 3-9 - **Drugs used in electrophysiology.** 43

Table 4-1 - **Neuronal markers used to characterize hIPSCs.** 55

Table 5-1 - **Summary of obtained results.** 71

Abbreviations list

A$_1$R - Adenosine A$_1$ receptor

A$_{2A}$R - Adenosine A$_{2A}$ receptor

A$_{2B}$R - Adenosine A$_{2B}$ receptor

A$_3$R - Adenosine A$_3$ receptor

aCSF - Artificial cerebrospinal fluid

AD - Alzheimer's disease

ADA - Adenosine deaminase

ADK - Adenosine kinase

ADP – Adenosine diphosphate

AKT - Protein kinase B

AMP - Adenosine monophosphate

AR - Adenosine receptors

ATP - Adenosine triphosphate

BDNF – Brain-derived neurotrophic factor

BRN2 - Brain-2

BSA - Bovine serum albumin

CA1-3 - *Cornu Ammonis,* areas 1-3

cAMP - Cycle adenosine monophosphate

cDNA - Complementary DNA

CNS - Central nervous system

CPA - N6-Cyclopentyladenosine

CpG - -C-phosphate-G

CREB - cAMP response element-binding protein

CTD - C-terminal domain

CypA - PPIA peptidylprolyl isomerase A (cyclophilin A)

DAG - Diacylglycerol

dATP - Deoxyadenosine triphosphate

dCTP - Deoxycytidine triphosphate

dGTP - Deoxyguanosine triphosphate

DNA - Deoxyribonucleic acid

DPCPX - 1,3-Dipropyl-8-cyclopentylxanthine

DTT - Dithiothreitol

dTTP - Deoxythymidine triphosphate

DMSO - Dimethyl sulfoxide

EDTA - Ethylenediaminetetraacetic acid

ELISA - Enzyme-Linked Immunosorbent Assay

ER - Endoplasmic reticulum

Erk - Extracellular signal-regulated kinases

FBS - Fetal bovine serum

fEPSP - Field excitatory post-synaptic potential

FOXG1 -Forkhead box protein G1

GABA - γ-AminoButyric Acid

GAPDH - Glyceraldehyde-3-phosphate dehydrogenase

GFAP - Glial fibrillary acidic protein

HD - Huntington's disease

HDACs - Histona deacetilases

hIPSCs - Human induced pluripotent stem cells

ID - Inter domain

IP3 - Inositol 1,4,5-triphosphate

IPSCs - Induced pluripotent stem cells

IRAK1 - Interleukin-1 receptor-associated kinase

K$_m$ - Michaelis menton constant

KO - knockout

LTD - Long-term depression

LTP - Long-term potentiation

MAP2 - microtubule-associated protein 2

MAPK - Mitogen-activated protein kinases

MBD - Methyl binding domain

MeCP2 - Methyl CpG binding protein 2

mTOR - Mammalian target of rapamycin

NF-kB - factor nuclear kappa B

NGF - nerve growth factor

NLS - Nuclear localization signals

NMDA - N-methyl-D-aspartic acid

NT-3(4/5) - neurotrophin-3(4/5)

NTD - N-terminal domain

OCT3/4 - Octamer-binding transcription factor 4/3 (POU5F1)

OMIM - Online Mendelian Inheritance in Man

OTX2 - Orthodenticle homeobox 2

PAX6 - Paired box protein 6

PBS - Phosphate-buffered saline

PD - Parkinson’s disease

PenStrep - Penicillin Streptomycin

PFA - paraformaldehyde

PI3K - Phosphoinositide 3-kinase

PIP2 - Phosphatidylinositol-4,5-bisphosphate

PK - Protein kinase

PLC - Phospholipase C

PLD - Phospholipase D

PNS - Peripheral nervous system

PVDF - Polyvinylidene fluoride

qPCR - Quantitative polymerase chain reaction

RCP - Red Opsin gene

RIPA - Radio-Immunoprecipitation Assay

Rpl13A - Ribosomal protein L13A

RNA - Ribonucleic acid

RT - Reverse transcription

RTT - Rett Syndrome

SAH - S-adenosylhomocysteine

SDS-PAGE - Sodium dodecyl sulphate-polyacrylamide-gel electrophoresis

SIN3A - Paired amphipathic helix protein Sin3a

SNAP25 - Synaptosomal-associated protein 25

SOX2 - Sex determining region Y-box 2

TBR1 - T-box, brain, 1

TBR2 - T-Box, brain, 2

TBS-T - Tris-Buffered Saline and Tween 20

TRD - Transcription repression domain

Trk – tropomyosin-related kinase

Trk(B)-FL - tropomyosin-related kinase (B) full-lengh

TrkB-T1 - tropomyosin-related kinase B T1 isoform

Trk(B)-Tc - tropomyosin-related kinase (B) truncated isoforms

TUJ1 - Neuron-specific class III β-tubulin

UTR - Untranslated region

VGAT - Vesicular GABA transporter

VGLUT - Vesicular glutamate transporter

WT - wild type

XCI -X-chromosome inactivation

ZO1 -Tight junction protein ZO-1

Resumo

A Síndrome de Rett (RTT) é uma doença rara do neurodesenvolvimento e de causa genética que afeta cerca de 1:10000 raparigas em todo o mundo. Esta doença caracteriza-se por um aparente normal desenvolvimento até aos 6 a 18 meses de idade, seguido de uma fase de regressão, na qual ocorre a perda das capacidades já adquiridas. Entre outros sintomas, destacam-se: severa disfunção cognitiva e motora, epilepsia e aparecimento de movimentos estereotipados e repetitivos das mãos com progressiva perda da sua funcionalidade.

Estudos genéticos mostraram que esta síndrome se deve, maioritariamente, a mutações no gene *methyl CpG binding protein 2* (*MECP2)* localizado no cromossoma X. Este gene codifica a proteína MeCP2, um modulador epigenético e regulador da estrutura da cromatina, com funções primordiais no desenvolvimento e maturação do Sistema Nervoso Central (*central nervous system* - CNS). Uma das proteínas cuja expressão é controlada pela MeCP2 é o fator neurotrófico derivado do cérebro (*brain-derived neurotrophic factor* - BDNF), conhecido pelas suas importantes funções na maturação e diferenciação celular, plasticidade sináptica e sobrevivência neuronal. Consequentemente, alterações na MeCP2 podem comprometer os níveis de expressão e função do BDNF.

Estudos em modelos animais, que reproduzem a maioria dos sintomas característicos da RTT, demonstraram que o aumento da expressão do *BDNF* consegue reverter parcialmente algumas das disfunções e sintomas desta síndrome. Contudo, o uso terapêutico de BDNF não é ainda exequível uma vez que a barreira hematoencefálica (*blood-brain barrier* - BBB) é impermeável a este fator neurotrófico, impedindo-o de chegar ao cérebro e desempenhar adequadamente as suas funções. Na tentativa de facilitar os efeitos do BDNF, têm-se desenvolvido novas estratégias envolvendo, por exemplo, a utilização de fármacos que atravessando a BBB potenciem a ação neuroprotetora do BDNF. Um dos fármacos que tem merecido particular atenção é a adenosina. A adenosina é um neuromodulador do CNS que exerce as suas funções através da ativação de quatro recetores, A_1, A_{2A}, A_3 e A_{2B}. Em particular, a ativação dos recetores A_{2A} é fulcral para a manutenção dos níveis de BDNF e do seu recetor, TrkB-FL, assim como para os seus efeitos sinápticos. É de realçar que, o sistema adenosinérgico, para além de ser crucial na sinalização mediada pelo BDNF, também tem um

papel de destaque no controlo da excitabilidade sináptica através da ativação dos recetores inibitórios do tipo $A_{1,}$ reconhecidos como potenciais alvos terapêuticos no controlo da epilepsia. Estas ações da adenosina sugerem a possibilidade de este neuromodulador também estar afetado na RTT. De facto, estudos preliminares, realizados no nosso laboratório, apontam para a existência de uma disfunção do sistema adenosinérgico em associação à desregulação já conhecida da sinalização mediada pelo BDNF na RTT.

Assim, este projeto teve como principal objetivo fazer a caracterização detalhada do sistema adenosinérgico e da sinalização mediada pelo BDNF, através da utilização de: 1) modelo animal, ratinho mutante *Mecp2 knockout* (*KO*); 2) modelo humano, neurónios derivados de células pluripotentes induzidas humanas (*human induced pluripotent stem cells* - hIPSCs) de pacientes com RTT e 3) tecido cerebral humano recolhido durante autópsia realizada a paciente com RTT.

Ensaios de ligação anteriormente realizados já tinham mostrado um aumento dos níveis proteicos dos recetores A_1 em amostras de córtex cerebral de ratinhos *Mecp2 KO* quando comparado com amostras de ratinhos *WT*, não havendo alterações na expressão do seu mRNA. No presente trabalho, ensaios de *Western-Blot* revelaram uma diminuição significativa dos recetores do tipo A_{2A} no córtex cerebral dos ratinhos *Mecp2 KO*, não tendo sido contudo, detetadas alterações nos níveis de expressão do mRNA avaliados por *polimerase chain reaction* (PCR) quantitativo. Curiosamente, registos eletrofisiológicos realizados no hipocampo destes animais sugerem uma diminuição dos níveis de adenosina endógena, que não é atribuível a variações nos níveis proteicos de um dos enzimas responsáveis pela degradação da adenosina, adenosina cinase (*Adenosine Kinase* - ADK).

No modelo animal, os resultados, obtidos por *ELISA*, confirmaram que os níveis proteicos de BDNF estão bastante diminuídos. Semelhante resultado foi obtido para os níveis dos seus recetores TrkB-FL quando avaliados pela técnica de *Western Blot*, não havendo, contudo, alterações significativas nos recetores truncados deste fator neurotrófico (TrkB-Tc). No entanto, os níveis de expressão de mRNA para as duas isoformas do recetor TrkB (TrkB-FL e TrkB-T1 – isoforma truncada) não mostraram alterações significativas.

Em neurónios derivados de hIPSCs, a avaliação dos recetores adenosinérgicos (A_1 e A_{2A}), do BDNF e dos recetores TrkB, efetuada através de PCR quantitativo, demonstrou uma

considerável variabilidade, não sendo por isso possível fazer uma comparação com os resultados obtidos no modelo animal. Relativamente ao estudo dos níveis proteicos de BDNF, neste modelo, observou-se uma tendência para aumento e, pelo contrário, registou-se uma tendência para diminuição dos níveis de expressão dos seus recetores.

Os resultados obtidos a partir da amostra de córtex temporal de uma paciente com RTT mostraram um aumento da expressão de mRNA dos recetores A_1 e uma diminuição da expressão de mRNA dos recetores A_{2A}. No que respeita aos recetores TrkB, observou-se um aumento da expressão do mRNA que codifica para o recetor TrkB-FL. Não se observou contudo alteração no mRNA para o recetor TrkB-T1. Em associação, não foi observada alteração na expressão de mRNA que codifica para o BDNF.

Neste trabalho, o maior problema encontrado foi a variabilidade observada, não só entre as linhas celulares provenientes de indivíduos do mesmo género, como também entre as rondas independentes de diferenciação da mesma linha parental. Parte dessa variabilidade pode estar relacionado com as múltiplas alterações genéticas e epigenéticas que ocorrem durante os procedimentos de reprogramação e de diferenciação, tais como a fixação de mutações aleatórias esporádicas e a inativação aleatória do cromossoma X em linhas femininas. Uma outra importante fonte de variabilidade é a eficiência da produção de neurónios corticais, que é propensa a flutuar comprometendo os resultados. Ainda que alguns resultados mostrem tendências concordantes entre os modelos estudados, é difícil retirar conclusões a partir destes, o que é ainda mais agravado pelo reduzido tamanho da amostra.

Globalmente, os resultados apontam para uma disfunção na sinalização mediada quer pelo BDNF quer pelo sistema adenosinérgico, sugerindo um possível envolvimento de ambos na fisiopatologia da doença. Estas evidências abrem novas perspetivas para a intervenção farmacológica nesta patologia.

Palavras-Chave: Síndrome de Rett; Sistema adenosinérgico; Recetores A_1 e A_{2A}; BDNF; IPSCs

Abstract

Rett Syndrome (RTT) is a genetic neurodevelopmental disorder, with an incidence of 1:10,000 female live births. This disorder is the main genetic cause of intellectual disability in females and it is mainly caused by mutations in the methyl-CpG binding protein 2 (*MECP2*) gene.

The MeCP2 protein, codified by the *MECP2* gene, is an epigenetic modulator that controls chromatin structure. This protein is known to modulate the expression of brain-derived neurotrophic factor (BDNF), a neurotrophin with essential functions in cell differentiation, synaptic plasticity and survival. Furthermore, BDNF overexpression can partially ameliorate some RTT associated symptoms. Thus, therapeutic strategies designed at delivering BDNF to the brain could be a breakthrough for RTT. However, this strategy has been hampered by the inability of BDNF to cross the blood-brain barrier (BBB). The development of new therapeutic strategies is, therefore, of the outmost importance.

The adenosine is a neuromodulator that acts through the activation of four different receptors: A_1R, $A_{2A}R$, $A_{2B}R$ and A_3R. The two most well characterized receptors in the brain are the A_1R and $A_{2A}R$ and their manipulation has been suggested for the treatment of several neurological pathologies. Given that, the activation of $A_{2A}R$ is known to potentiate BDNF synaptic actions in healthy animals, one could anticipate that the activation of these adenosine receptors could be a potential therapeutic strategy. On the other hand, most of RTT patients have epilepsy, a pathology where adenosine system might be affected. However, until recently, there was no available information about the contribution of the adenosinergic system to the pathophysiology of RTT. To overcome this gap in knowledge, our lab has developed a new line of research on this topic. The main goal of this project was to further characterize both the adenosinergic system and the BDNF signalling in RTT. This goal was achieved by using: i) a well-established animal model, *Mecp2 KO* mice; ii) human RTT model, neurons-derived from RTT patients induced pluripotent stem cells (IPSCs) and iii) *post-mortem* human brain samples from a RTT patient.

Even though we found some concordant tendencies between the human and the mouse models, given the high variability observed in the human material, no clear conclusions can be drawn. This is certainly aggravated by the small sample size that, in the future, could be solved by increasing not only the number of patient-derived hIPSCs lines but also by increasing the amount of independent rounds of differentiation. The availability of more *post-mortem* samples would also be an important asset.

Overall, the here presented results clearly show a dysfunction in BDNF signalling and in the adenosinergic system, suggesting that both systems are involved in the pathophysiology logy of the disorder. These evidences open new pharmacological avenues for the treatment of RTT.

Keywords: Rett Syndrome; Adenosinergic system; Adenosine A_1 and A_{2A} receptors; BDNF; IPSCs.

1. Introduction

1.1 Rett Syndrome

Rett Syndrome (RTT, OMIM 312750) is a progressive neurodevelopmental disorder that affects brain development during early childhood (Chahrour and Zoghbi, 2007; Banerjee et al., 2012). This rare syndrome, with an incidence of approximately 1 in 10,000 female live births (Chahrour and Zoghbi, 2007) was first described in 1966 by Dr. Andreas Rett (Rett, 1966) but only 17 years later became recognised by the medical community when Dr. Bengt Hagberg and colleagues described 35 RTT cases (Hagberg et al., 1983). Children have an apparently normal development until 6-18 months of age when a regression phase starts with loss of previously acquired skills (Chahrour and Zoghbi, 2007; Bedogni et al., 2014). Patients develop typical symptoms grouped in 4 clinical stages: i) developmental stagnation; ii) rapid regression; iii) stationary stage and iv) motor deterioration (*Figure 1.1*) (Abreu, 2014; Chahrour and Zoghbi, 2007).

The most prominent features in girls with RTT are the development of stereotypic hand movements with a decline of purposed hand movements, stagnation of neuromotor development, severe cognitive impairment, seizures (epilepsy), autistic features and autonomic dysfunctions (reviewed by Chahrour and Zoghbi, 2007). RTT patients can live until sixty/seventy years of age in spite of their severely affected physical condition (Chahrour and Zoghbi, 2007).

In 1999 Amir and colleagues described mutations in the *MECP2* gene (methyl-CpG binding protein 2) as the cause of RTT (Amir et al., 1999). This gene codifies the MeCP2 protein and is located in X chromosome, explaining the high prevalence of this disorder in the female gender and the low rate of survival in male patients (Liyanage and Rastegar, 2014; Chahrour and Zoghbi, 2007).

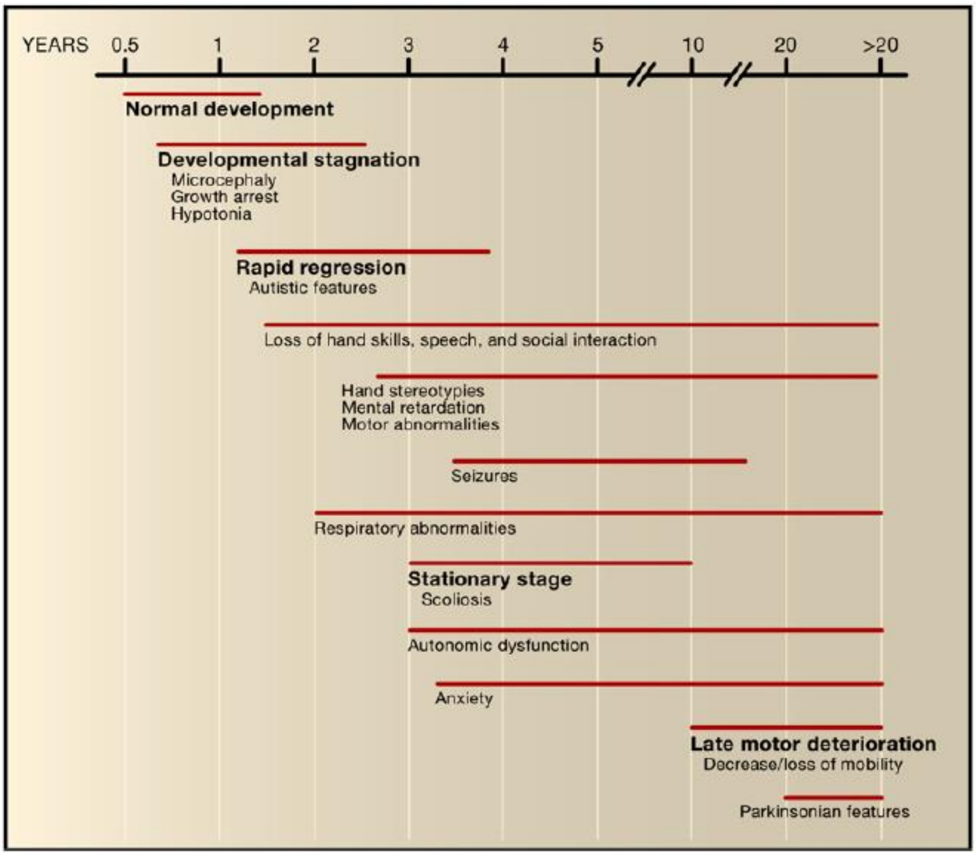

Figure 1.1 - **Onset and clinical manifestations of RTT.** RTT patients have normal development during the first months of life. After this period, starts a phase of developmental stagnation followed by a rapid deterioration with loss of acquired speech, loss of purposeful hand use and midline stereotypies. Autistic features also emerge and, in advanced stages of the disease, the clinical condition deteriorates with loss of motor skills and profound cognitive impairment. In addition, patients suffer from anxiety, seizures, and autonomic abnormalities (Chahrour and Zoghbi, 2007).

1.1.1 Genetic Basis

RTT represents the most common genetic cause of severe intellectual disability in females (Percy and Lane, 2005). About 99% of RTT cases are sporadic, hindering the initial quest of the associated locus (Chahrour and Zoghbi, 2007). However, studies using rare familial cases allowed the identification of the locus Xq28 followed by the identification of mutations in *MECP2* (Amir et al., 1999). Mutations in *MECP2* gene appear in 90% of RTT classical cases (Liyanage and Rastegar, 2014), missense and nonsense mutations represent 70% of all mutations, small C-terminal deletions represent 10% and complex rearrangements 6% of the cases (reviewed in Chahrour and Zoghbi, 2007). The majority of the mutations arise *de novo* in the paternal germline and involve a C to T transition at CpG dinucleotides (Girard et al., 2001; Trappe et al., 2001; Wan et al., 1999). A relationship between RTT phenotype and the type of *MECP2* mutation has already been shown, where truncating mutations and mutations affecting the nuclear localization signals (NLS) of MeCP2 protein are associated with a severe RTT phenotype (Amir and Zoghbi, 2000; Smeets et al., 2005).

Atypical cases of RTT (around 10% of RTT patients), are characterized by mutations in other genes, namely *CDKL5* and *FOXG1* genes and display distinct phenotypes (Neul et al., 2011; Evans et al., 2005; Philippe et al., 2010).

1.1.1.1 MeCP2: gene, protein and its functions

***MECP2* gene**

MeCP2 was first identified in 1992 by Bird and colleagues (Lewis et al., 1992) and it is the most studied protein of the methyl-CpG binding protein family due to its primordial functions and link to this specific disorder (reviewed in Liyanage and Rastegar, 2014 and Bedogni et al., 2014).

The *MECP2* gene spans approximately 76 Kb, between the Interleukin-1 receptor associated kinase gene (*IRAK1*) and the Red Opsin gene (*RCP*) (Liyanage and Rastegar, 2014). The structure of *MECP2* gene, both in human and mouse, is comprised of 4 exons (exon 1-4) and 3 introns (intron 1-3) and two different isoforms are generated by alternative splicing: MeCP2_e1 and MeCP2_e2 differing only in N-terminal sequence (*Figure 1.2*) (Cheng and Qiu, 2014; Liyanage and Rastegar, 2014).

These two isoforms have redundant and also non-redundant functions and their expression pattern is distinct. MeCP2_e1 is 10 times more abundant in the postnatal human brain than MeCP2_e2 and expression studies in the adult mouse brain showed that MeCP2_e2 expression is exclusive to the thalamus and cortex layers (reviewed in Liyanage and Rastegar 2014). Loss of MeCP2_e2 isoform does not cause typical symptoms of RTT, suggesting that this isoform alone is not responsible for RTT pathology (Itoh et al., 2012).

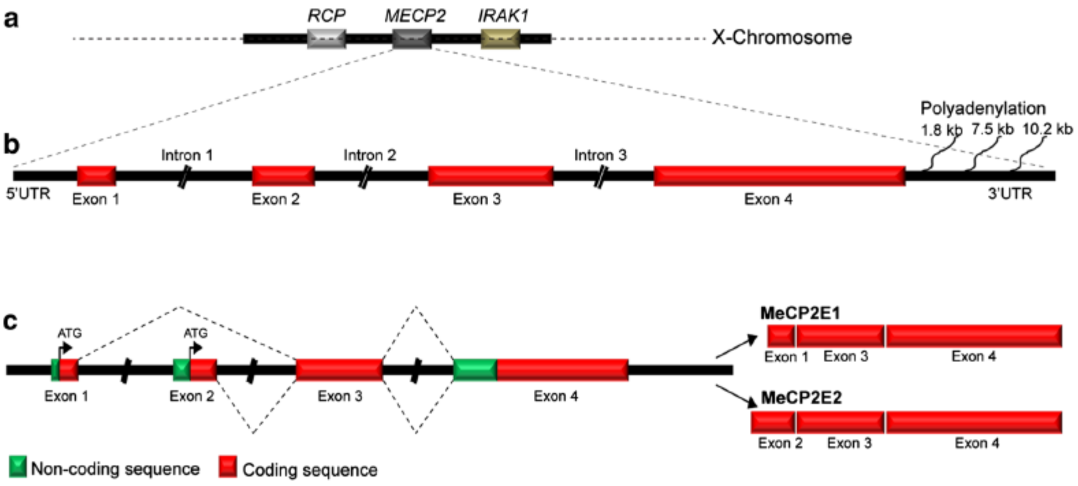
a
RCP
MECP2
IRAK1
X-Chromosome
b
Polyadenylation
1.8 kb
7.5 kb
10.2 kb
Intron 1
Intron 2
Intron 3
5'UTR
Exon 1
Exon 2
Exon 3
Exon 4
3'UTR
c
ATG
ATG
Exon 1
Exon 2
Exon 3
Exon 4
MeCP2E1
Exon 1
Exon 3
Exon 4
MeCP2E2
Exon 2
Exon 3
Exon 4
Non-coding sequence
Coding sequence

Figure 1.2 - **Structure of *MECP2* gene**. **a –** *MECP2* is found in the X chromosome (Xq28), between *RCP* and *IRAK1* genes**. b –** *MECP2* is composed of four exons (exons 1-4), three introns (1-3) and three polyadenylation sites at the 3’UTR. **c –** Alternative splicing generates two isoforms: MeCP2_e1, encoded by exons 1, 3 and 4 and MeCP2_e2 by exons 2, 3 and 4. Translation start site (arrows); coding region (red bars); non coding-sequence (green bars) (adapted from Liyanage and Rastegar, 2014).

MeCP2 protein

The protein structure of MeCP2 is constituted by 5 domains: N-terminal domain (NTD), methyl binding domain (MBD), inter domain (ID), transcription repression domain (TRD) and C-terminal Domain (CTD) (*Figure 1.3**a***) (Liyanage and Rastegar, 2014).

Most of the missense mutations in MeCP2-related disorders affect the MBD, required for methylation-dependent chromatin binding (Galvão and Thomas, 2005; Kudo et al., 2003), explaining the inability of MeCP2 to locate and cluster into heterochromatin and its retention in the cytoplasm (Stuss et al., 2013). Mutations in the TRD and CTD domain are also present in MeCP2-related disorders (*Figure 1.3**b***) (Liyanage and Rastegar, 2014; Bedogni et al., 2014).

MeCP2 is mainly detected in neurons but it is also present in astrocytes, oligodendrocytes and microglia (reviewed in Liyanage and Rastegar, 2014; Zachariah et al., 2012). Its expression is high during embryonic development and low during neuronal maturation and synaptogenesis. *MECP2* expression starts to increase over to the first 3 postnatal weeks, reaching a plateau phase until later adult life, where a new increase of MeCP2 expression takes place (Shahbazian et al., 2002).

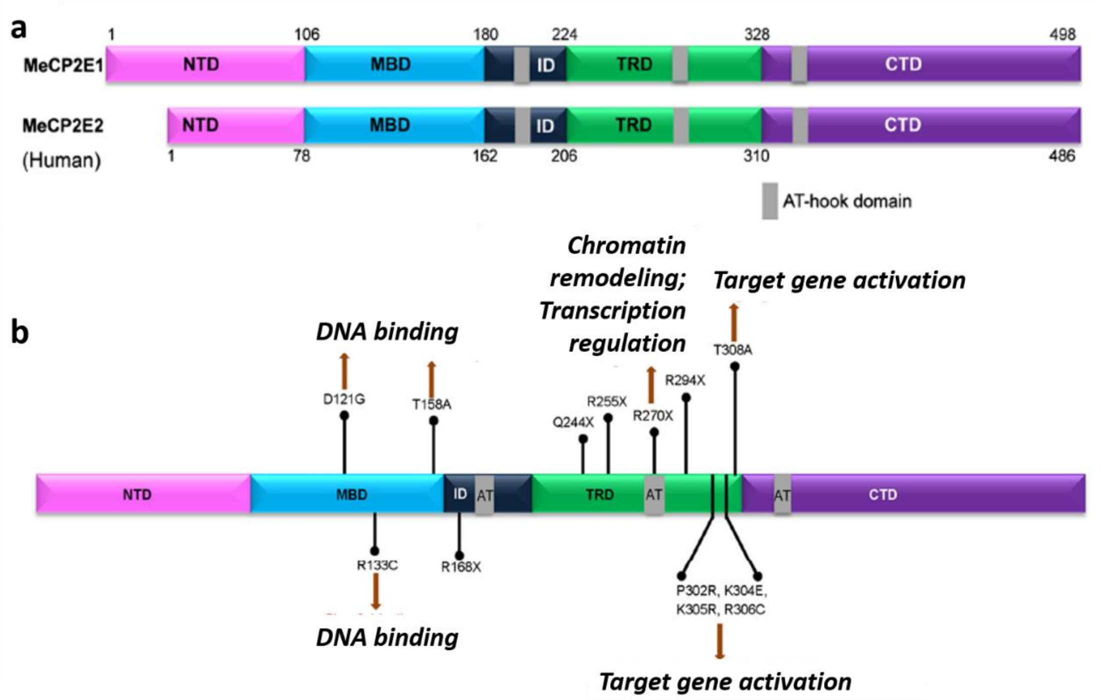
a
MeCP2E1
1
106
180
224
328
498
NTD
MBD
ID
TRD
CTD
MeCP2E2
(Human)
1
78
162
206
310
486
AT-hook domain
b
DNA binding
D121G
T158A
Chromatin remodeling; Transcription regulation
Target gene activation
T308A
R294X
R255X
R270X
Q244X
NTD
MBD
ID
AT
TRD
AT
AT
CTD
R133C
R168X
P302R, K304E,
K305R, R306C
DNA binding
Target gene activation

Figure 1.3 - **MeCP2 protein structure, mutations and associated impairments in RTT**. **a** – MeCP2_e1 and MecP2_e2 protein has 498 and 486 amino acids, respectively. Both isoforms have the some functional domains: methyl-CpG-binding domain (MBD), transcriptional regression domain (TRD), C-terminal domain (CTD) and N-terminal domain (NTD). AT-hook, in grey, allows binding to AT rich DNA. **b** – Frequently reported mutations in *MECP2* and affected domains (adapted from Liyanage and Rastegar, 2014).

MeCP2 functions

MeCP2 is a multifunctional protein involved in transcriptional regulation and modulation of chromatin structure. The two prominent MeCP2 functional domains, MBD and TRD, enable multiple functions through direct DNA binding, interaction with other proteins or recruitment of essential factors (see Liyanage and Rastegar, 2014; Banerjee et al., 2012; Bedogni et al., 2014). Post-translational modifications have been found to regulate protein stability and modulate protein activity (reviewed in Liyanage and Rastegar, 2014; Cheng and Qiu, 2014).

The precise role of MeCP2 in transcriptional repression or activation remains controversial. MeCP2 was first identified as a transcription repressor since MeCP2 was located at methylated promoters and recruited co-repressors like SIN3A and histone deacetylases (HDACs) 1 and 2, promoting a global compaction of chromatin (Nikitina et al., 2007; Klose and Bird, 2004). On the other hand, MeCP2-mediated transcriptional gene activation occurs in association with activator complexes containing cAMP response element-binding protein (CREB) (Chahrour et al., 2008). The regulation of *brain-derived neurotrophic factor* (*Bdnf*) gene by MeCP2, is an example of the paradoxical role of MeCP2 upon transcriptional regulation. Binding of MeCP2 to the *Bdnf* promoter represses its expression but in *Mecp2*-deficient mice, BDNF expression levels are decreased (see section 1.4.1) (reviewed in Li and Pozzo-Miller, 2014).

Furthermore, MeCP2 plays also an important role in the regulation of RNA splicing, microRNA regulation, and in the regulation of protein synthesis through AKT/mTOR pathway, relevant to neuronal differentiation and maturation (*Figure 1.4*) (see Cheng and Qiu, 2014; Liyanage and Rastegar, 2014; Bedogni et al., 2014).

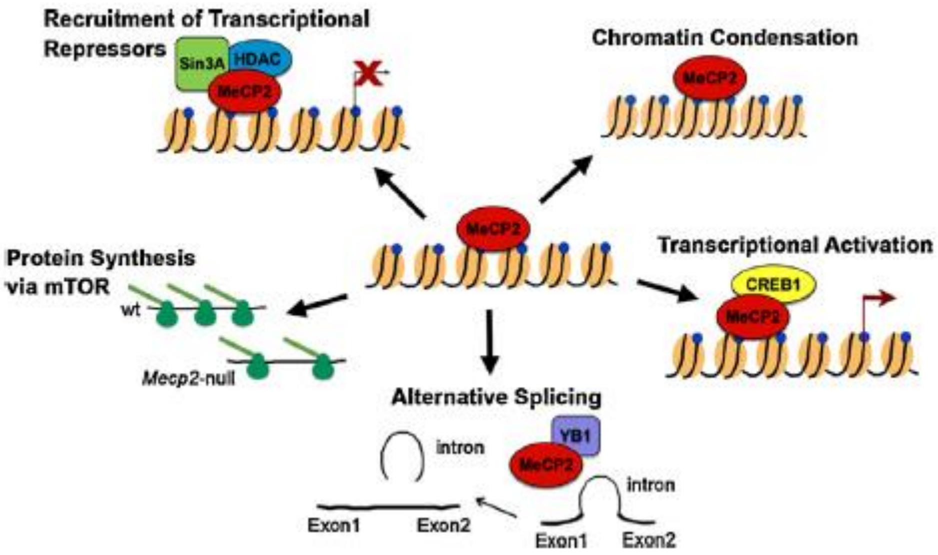
Recruitment of Transcriptional Repressors
Sin3A
HDAC
MeCP2
Chromatin Condensation
MeCP2
MeCP2
Protein Synthesis via mTOR
wt
Mecp2-null
Transcriptional Activation
CREB1
MeCP2
Alternative Splicing
intron
YB1
MeCP2
intron
Exon1
Exon2
Exon1
Exon2

Figure 1.4 **MeCP2 and its functions**. Multiple MeCP2 functions are schematized. Involvement of MeCP2 in transcriptional repression and activation is associated with specific factors, such as Sin3A and HDAC in repression and CREB1 in activation. MeCP2 has also an active role on protein synthesis via AKT/mTOR pathway, in chromatin condensation and in alternative splicing (Bedogni et al., 2014).

Given the wide range of cellular activities of the MeCP2, alterations in its functions result in impaired brain development and function (Banerjee et al., 2012; Liyanage and Rastegar, 2014). However, the exact mechanisms caused by MeCP2 dysfunction that result in RTT related pathophysiological features remain undisclosed. To this end, the use of *MECP2*-deficient models is of the outmost importance.

1.2 Rett Syndrome disease modelling

Several models are currently available to study RTT. The majority of them have been developed in mice where the insertion of specific mutations or deletion of large portions of the gene result in *MECP2* dysfunction (Liyanage and Rastegar, 2014). The recent breakthrough in reprogramming of patient-derived fibroblasts into human induced pluripotent stem cells (hIPSCs) together with the ability to promote differentiation into specific neuronal populations, allows the generation of human disease relevant cell lines as disease models. In this chapter, the advantages and disadvantages of each model are discussed.

1.2.1 Mouse models

Several mouse models have been generated in order to understand the cellular mechanisms and behavioural traits underlying RTT. The same models have also been used to develop and test possible therapeutic strategies (Katz et al., 2012; Liyanage and Rastegar, 2014; Banerjee et al., 2012). A good model is characterized by its ability to recapitulate the disease phenotype and its utility in translational studies. Therefore, it is important that a considerable overlap between the mouse and human phenotypical traits exist as well as reproducibility and robustness between laboratories, as discussed in (Katz et al., 2012).

The established models include mice carrying global alleles and conditional null alleles. In the first group, we can distinguish the null mutations (Guy et al., 2001; Chen et al., 2001), that are similar to the large deletions found in 10% of RTT patients; truncations and single-nucleotide mutations, that are more approximate to the mutations found in the majority of RTT patients and point mutations (reviewed in Katz et al., 2012). The second group is characterized by mice models where: *Mecp2* deletions or mutations are cell type specific (Calfa et al., 2011b).

The majority of RTT mice models used are the null despite of only 10% of RTT patients present large deletions.

Due to X chromosome inactivation (XCI), girls affected with RTT present mosaicism for the expression of the mutant allele resulting in different degrees of severity. To avoid this confounding effect experiments are typically done in male mice which do not mimic this genetic mosaicism but simplify data interpretation (Stearns et al., 2007; Robinson et al., 2012). *Mecp2*-null male mice exhibit consistent early abnormalities in motor behaviour, within 6 weeks of age, and more severe than in heterozygous females (Pratte et al., 2011; Stearns et al., 2007). Other characteristics in common with the human disease are: breathing and cardiac abnormalities (Mccauley et al., 2011; Pratte et al., 2011); cognitive impairments; anxiety and alterations in social behaviour (Stearns et al., 2007). These animals also have reduced brain volume (Stearns et al., 2007) and prototypical features of human RTT neuropathology such as smaller neurons, higher neuronal packing density, reduced dendritic arbour and abnormal dendritic spines (reviewed in Katz et al., 2012).

1.2.2 Induced Pluripotent Stem Cells (IPSCs)

Due to the constraints of isolating neurons from living subjects, initial studies using the human brain were performed on *post-mortem* tissues that are not always well preserved, accessible and often represent an end-stage of the disease. On the other hand, animal models, fail to recapitulate in full, the complexity of the human pathology (Jang et al., 2014; Amenduni et al., 2011; Chailangkarn et al., 2012).

Pluripotent human embryonic stem cells were for the first time successfully generated from early stages of the human embryo in 1998 (Thomson et al., 1998). To develop cellular models of human disease it is essential to generate cell lines genetically predisposed to disease. In 2006, it was demonstrated that the expression of 4 transcription factors (*OCT4*, *SOX2*, *KLF4* and *c-MYC*) was sufficient to reprogram mice somatic cells, like fibroblasts, to a pluripotent state – Induced Pluripotency (Takahashi and Yamanaka, 2006). A similar protocol was also successfully applied to generate hIPSCs (Takahashi et al., 2007). Most IPSCs lines are derived by retroviral transduction of dermal fibroblasts due to its availability and high reprogramming efficiency (Saporta et al., 2011; Jang et al., 2014; Dajani et al., 2013; Cheung et al., 2012). IPSCs are pluripotent and can differentiate into any cell type by manipulation of the culture environment with growth factors, small molecules and extracellular matrix proteins guiding their differentiation into the cell-type of interest (Dajani et al., 2013; Saporta et al., 2011)

Recently, neurons-derived from IPSCs emerged as a promising alternative providing a new paradigm for the generation and study of human disease-specific neurons with a predominant role in certain neurological/neurodevelopment/neuropsychiatric pathologies (Saporta et al., 2011). Once its validity as a model has been demonstrated, it could even be used in translational studies and in the screening of potential therapeutic strategies (*Figure 1.5*) (Saporta et al., 2011; Freitas et al., 2012; Jang et al., 2014; Chailangkarn et al., 2012).

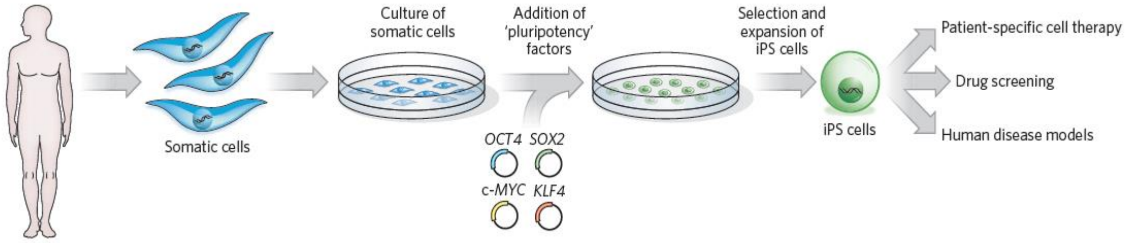
Somatic cells
Culture of somatic cells
Addition of 'pluripotency' factors
OCT4
SOX2
c-MYC
KLF4
Selection and expansion of iPS cells
iPS cells
Patient-specific cell therapy
Drug screening
Human disease models

Figure 1.5 - **Schematic representation of hIPSCs production and possible applications**. To generate IPSCs, reprogramming of somatic patient-derived cells is achieved using retroviral transduction of four pluripotency factors (*OCT4*, *SOX2*, *c-MYC* and *KLF4*). IPSCs can be differentiated into the desired cell type that allows human disease modelling, to investigate patient-specific cell therapy and drug screening (Yamanaka and Blau, 2010).

In the specific case of RTT, this *in vitro* human neurodevelopmental model, offers an excellent opportunity to recapitulate the early stages of development and mimic specific biochemical and cellular features of the disease difficult to reproduce in other models (Freitas et al., 2012).

The first RTT-IPSCs were generated in 2009 (Hotta et al., 2009) and multiple studies have followed in order to study RTT neuronal and glial phenotype from a neurodevelopmental point of view. In these studies, neurons-derived from RTT-hIPSCs recapitulate some of the phenotypes already described in the mouse models and observed in patients (reviewed in Dajani et al., 2013). These include, reduced soma/nuclear size, lower expression of neuronal markers, reduced dendrite spine density, reduced glutamatergic synapse number, altered neuronal morphology, reduction in the transient rise of intracellular calcium and decrease in the frequency/amplitude of spontaneous excitatory and inhibitory postsynaptic currents (*Figure 1.6*) (Marchetto et al., 2010). The high overlap between the characteristics observed in these studies and the human disease provides strong support to the utility of neurons-derived from IPSCs as a model to study RTT.

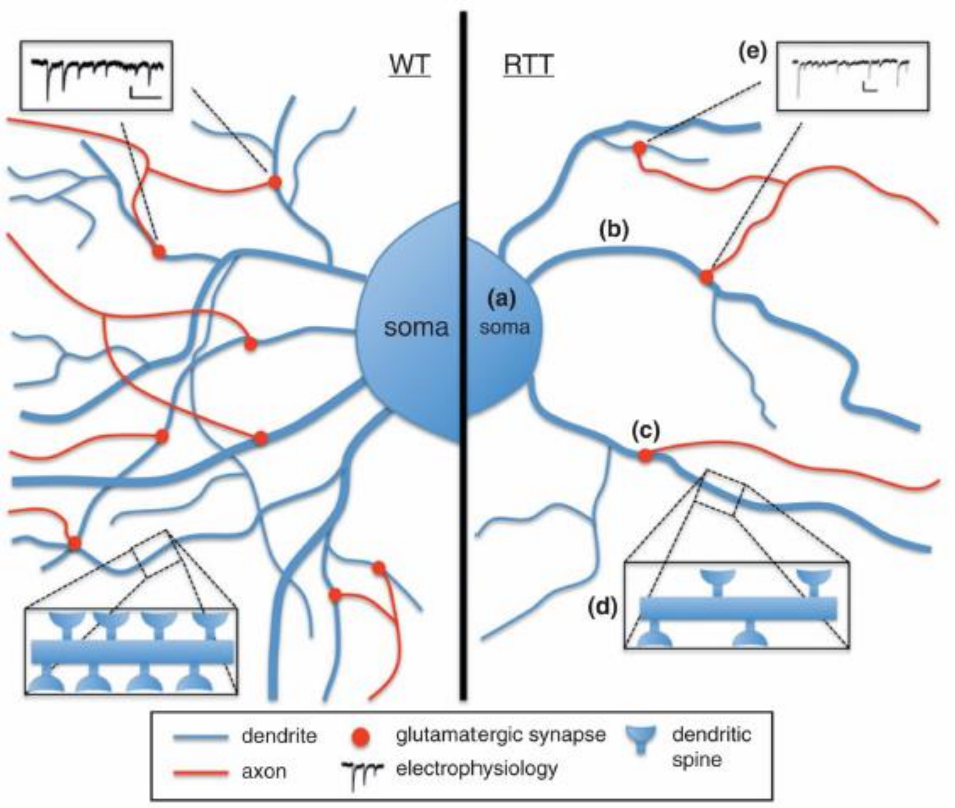

Figure 1.6 **Phenotypical characteristics of neurons-derived from RTT-hIPSCs**. As observed in other RTT models, neurons derived from RTT-hIPSCs exhibit **(a)** smaller soma size; **(b)** reduced dendritic branching; **(c)** less glutamatergic synapses; **(d)** fewer dendritic spines and **(e)** decreased frequency of spontaneous postsynaptic currents (Chailangkarn et al., 2012).

Nevertheless, it is important to take into account that this model still requires improvement given the newness of this technique. One of the challenges of using hIPSCs is to produce differentiated and functional specific cell types. However, the protocols used generally result in a heterogeneous cell population, neurons and glia. This could be an advantage given the improved neuronal survival when cultured in mixed populations but it can create difficulties in data analysis. Therefore, biochemical and gene expression analysis cannot be performed without a careful normalization for cell type and their proportions (Saporta et al., 2011). Secondly, epigenetic memory of the original cell (fibroblast) might not be fully erased, affecting the differentiation potential. Variability between cell lines and clones from the same individual in proliferation and differentiation potential have been observed, which affect data interpretation (Chailangkarn et al., 2012).

Nevertheless, this can be partially solved by using different clones from the same individual or improving of differentiation protocols (Dajani et al., 2013).

Another specific challenge in X-linked diseases is the random X chromosome inactivation process that is not epigenetically stable demanding screening of cellular lines to evaluate the proportion of cells expressing the mutant allele (Cheung et al., 2012; Kim et al., 2011). Nevertheless, this outcome can also be considered as an advantage since isogenic clones expressing either the *wild type* allele (*WT*) or the mutant allele can be studied (Ananiev et al., 2011). Finally, generation of individual IPSCs is an expensive and time-consuming process which can be exceeded with collaborations between laboratories and institutes (*Figure 1.7*) (Chailangkarn et al., 2012).

The continuous improvement of this model could have enormous impact in health by contributing to personalized medicine, making predictions about the efficiency of certain drugs in individuals, to regenerative medicine and cell-replacement therapies overcoming rejection issues (Chailangkarn et al., 2012; Jang et al., 2014).

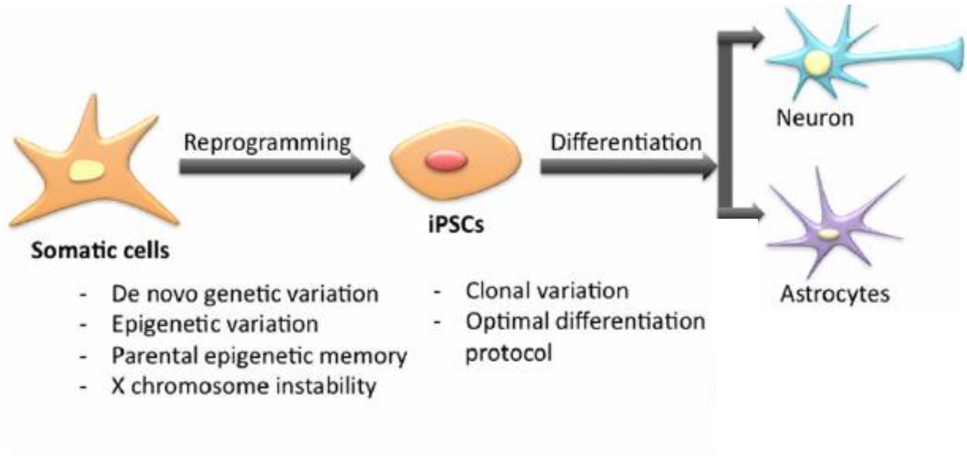
Reprogramming
Differentiation
Neuron
Somatic cells
iPSCs
Astrocytes
- De novo genetic variation
- Epigenetic variation
- Parental epigenetic memory
- X chromosome instability
- Clonal variation
- Optimal differentiation protocol

Figure 1.7 - **Challenges in RTT-IPSCs modelling**. During reprogramming, *de novo* genetic and epigenetic variation appears as a possible problem as well as parental epigenetic memory. In female IPSCs X-chromosome instability has also to be considered and followed throughout the process. During differentiation, clonal variation and optimal differentiation protocol should be taken into account when interpreting experiment results (adapted from Dajani et al., 2013).

1.3 Adenosine

Adenosine is an endogenous purine nucleoside, constituted by an adenine attached to a ribose (*Figure 1.8*) and is ubiquitously distributed throughout the body (Sachdeva and Gupta, 2013; Chen et al., 2007). This purine has an essential and vital role in several physiologic functions, acting in the synthesis of nucleic acids and ATP, blood supply, glucose homeostasis and can produce pharmacological effects in peripheral and central nervous system (PNS) (reviewed in Sachdeva and Gupta, 2013). Adenosine has the particularity of acting both as a neuromodulator and as a homeostatic modulator in a wide variety of systems. As a neuromodulator, adenosine, controls the information flow through neuronal circuits and as a homeostatic modulator sends paracrine signals that can tone metabolic activity in specific cells of a tissue, allowing a trans-cellular coordinated response to changes in the tissue workload (reviewed in Gomes et al., 2011).

Extracellular adenosine acts through multiple G-protein coupled receptors and it is constitutively present in extracellular space at low concentrations (nanomolar range) that markedly rise in stressful conditions, like ischemia, hypoxia, excitotoxicity and inflammation, having a cytoprotective role (Boison, 2013; Jacobson and Gao, 2012; Chen et al., 2007).

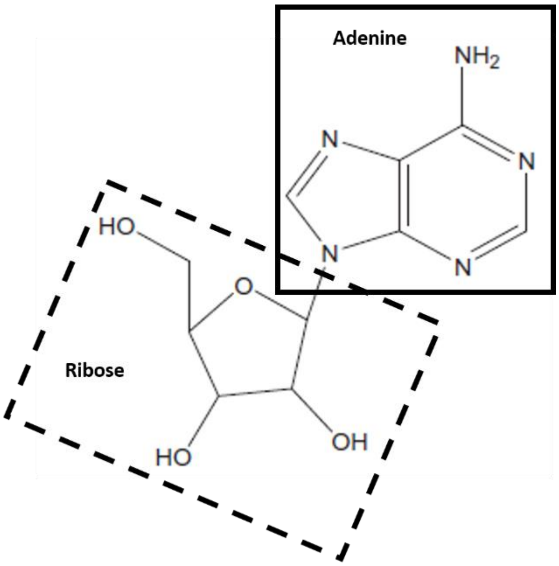

Figure 1.8 - **Adenosine structure**. Adenosine is composed by an adenine (filled line) attached to a ribose (spaced line).

1.3.1 Adenosine metabolism

Adenosine can be formed intra and extracellularly by the action of the enzyme 5’-nucleotidase on adenosine monophosphate (AMP) (Phillips and Newsholme, 1979) or intracellularly by the hydrolysis of S-adenosylhomocysteine (SAH) (Nagata et al., 1984) catalysed by SAH hydrolase.

The intracellular levels of adenosine are controlled by adenosine kinase (ADK), which phosphorylates adenosine to produce AMP, and by adenosine deaminase (ADA) resulting in the formation of inosine. Small changes in ADK activity rapidly cause dramatic changes in intracellular adenosine concentration (Bontemps et al., 1983; Bontemps et al., 1993). Several studies have shown that ADK is the primordial enzyme for adenosine clearance under baseline conditions, once it has a low-capacity and a low-K_m. ADA with an high-capacity and high-K_m acts in adenosine clearance when adenosine levels are excessive (Boison et al., 2010).

Adenosine does not accumulate in synaptic vesicles like the classical neurotransmitters, but it is instead released from the cytoplasm into the extracellular space through a nucleoside transporter (see e.g. Ribeiro et al., 2002).

In summary, adenosine homeostasis is determined by three major pathways working in a concerted manner: 1) adenosine formation, 2) adenosine removal and 3) adenosine uptake by transmembrane transporters (reviewed in Boison, 2013 and Boison et al., 2010). The activity of the transporters depends on the intracellular metabolic clearance rate to maintain adenosine uptake. This means that under steady-state conditions of adenosine production, extracellular adenosine concentration is controlled by intracellular adenosine clearance rate (Greene, 2011). In parallel, since ADK is the main enzyme involved in adenosine clearance and the enzymatic reaction is ATP dependent, adenosine homeostasis is largely influenced by the energetic status of the cell (Boison, 2013). During metabolic stress, the huge increase in adenosine concentration is achieved by the release and degradation of adenine nucleotides, such as adenosine triphosphate (ATP), adenosine diphosphate (ADP) and AMP by a cascade of ecto-5’nucleotidases, namely CD39 and CD73 (*Figure 1.9*) (Sachdeva and Gupta, 2013).

Interestingly, enzymes involved in adenosine degradation have been considered promising pharmacological targets for disorders where adenosine levels are deregulated, such as epilepsy (Boison, 2012; Boison, 2013). In addition, alterations in the mechanisms that control adenosine levels have also been reported, in particular the overexpression of ADK has been detected in epileptogenic brain areas (Gouder et al., 2004), highlighting the use of this particular enzyme as a possible pharmacological target.

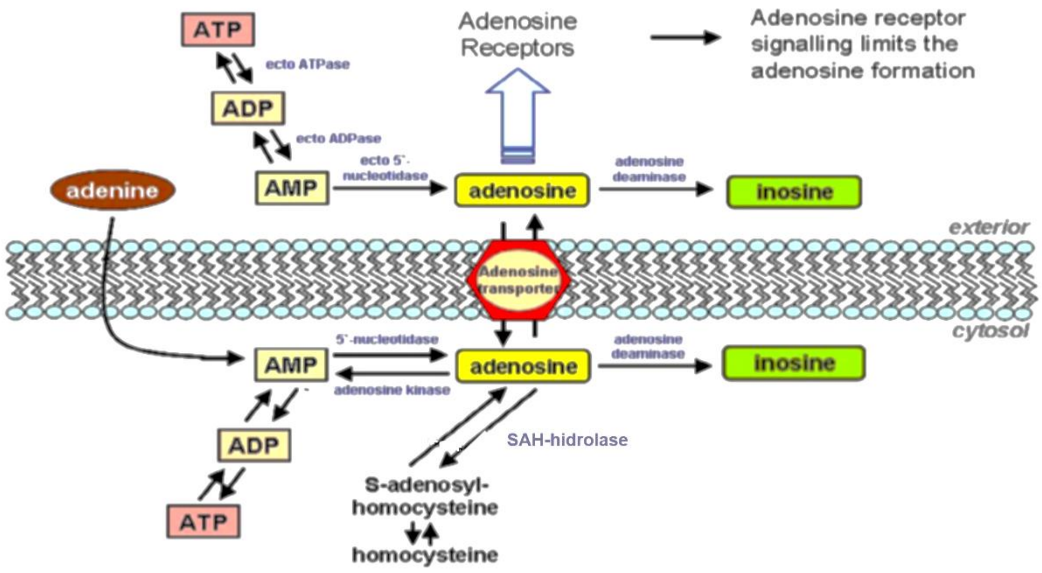
ATP
ecto ATPase
ADP
ecto ADPase
AMP
ecto 5´-nucleotidase
adenine
Adenosine Receptors
Adenosine receptor signalling limits the adenosine formation
adenosine
adenosine deaminase
inosine
exterior
Adenosine transporter
cytosol
5´-nucleotidase
AMP
adenosine kinase
adenosine
adenosine deaminase
inosine
ADP
ATP
SAH-hidrolase
S-adenosyl-homocysteine
homocysteine

Figure 1.9 - **Adenosine formation and catabolism**. Schematic representation of the multiple processes involved in the formation, transport and removal of adenosine. Adenosine can be synthetized intracellularly by AMP dephosphorylation via nucleotidases or by cleavage of S-adenosylhomocysteine via SAH-hydrolase. Extracellularly, adenosine is formed by ectonucleotidades that dephosphorylate AMP, ADP and ATP. Adenosine clearance is performed by the adenosine deaminase, intra- and extracellularly and by adenosine kinase, only intracellularly. All these processes produce inosine. Adenosine transport between cytosol and extracellular space occurs via membrane nucleotide transporters. **ADP** - adenosine diphosphate; **AMP** - adenosine monophosphate; **ATP** - Adenosine triphosphate; **SAH** - S- adenosylhomocysteine (adapted from Sachdeva and Gupta, 2013).

1.3.2 Adenosine receptors

To the present date, four different receptors have been cloned A_1, A_{2A}, A_{2B} and A_3 (R). A_1R and A_3R are mainly coupled to G_i proteins, while the A_{2A}R and A_{2B}R act mainly through activation of G_s proteins (Ralevic and Burnstock, 1998) though coupling to G_q can also occur.

Adenosine receptors (AR) have an extracellular domain comprised of the N-terminal and 3 extracellular loops and by an intracellular domain that comprises the C-terminal and 3 intracellular loops (*Figure 1.10*) (Sachdeva and Gupta, 2013). In humans, the similarity between receptors is greater between A_1R and A_3R and between $A_{2A}R$ and $A_{2B}R$ (Jacobson and Gao, 2012).

A_1R and $A_{2A}R$ are considered to be the high affinity receptors for adenosine, and in basal conditions are probably tonically activated (Dunwiddie and Masino, 2001). Given the higher density of A_1R and $A_{2A}R$ in the brain comparing to the other adenosine receptors, these receptors probably have higher impact in cerebral function (reviewed by Gomes et al., 2011).

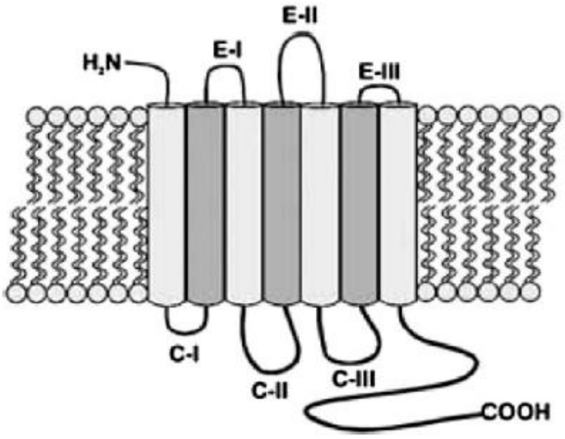

Figure 1.10 - **Adenosine receptor structure**. Adenosine receptors are constituted by an N-terminal extracellular domain, 3 extracellular loops (E-I, E-II and E-III), a C-terminal intracellular domain and 3 intracellular loops (C-I, C-II and C-III) (Sachdeva and Gupta, 2013).

Adenosine A_1 receptors

A_1R are the most abundant adenosine receptors in the central nervous system (CNS), with higher expression density in the neocortex, cerebellum, hippocampus and dorsal horn of spinal cord. They are pre-, post- and nonsynaptically located (Fredholm et al., 2005). When located postsynaptically they can influence excitatory response controlling both N-type Ca^{2+} channels and NMDA receptors (Mendonça et al., 1995). If located nonsynaptically they control the K^+ current resulting in neuronal hyperpolarization (Greene and Haas, 1991). Besides being expressed in neurons they can also be found in astrocytes and microglia (reviewed by Gomes et al., 2011). Moreover, these receptors can also be found in adipose tissue, heart muscle and inflammatory cells like neutrophils (reviewed in Sachdeva and Gupta, 2013).

The activation of A_1R promotes the inhibition of adenylyl cyclase due to the activation of toxin-sensitive G_i proteins. It can also promote the inhibition of G-protein coupled-activation of voltage dependent Ca^{2+} channels and induce PLC activation (*Figure 1.11*) (Rogel et al., 2005).

A_1R activation selectively depresses excitatory transmission and also can decrease miniature events in excitatory synapses (Scanziani et al., 1992).

Adenosine A_{2A} receptors

$A_{2A}R$ are mostly coupled to G_s, which consequently increase intracellular cAMP. In the striatum they are also coupled to G_{olf} (Corvol et al., 2001) and, in the hippocampus, there is evidence that these receptors can be coupled to G_i/G_o (*Figure 1.11*) (Cunha et al., 1999). Besides being postsynaptically highly expressed in the striatopallidal GABAergic neurons and in the olfactory bulb (see e.g. Fredholm et al., 2001), the $A_{2A}R$ are also expressed in the hippocampus and cortex (see e.g. Ribeiro et al., 2002). These adenosine receptors are mostly found in synapses (pre- and postsynaptically) and also in glial cells (reviewed in Gomes et al., 2011).

The $A_{2A}R$ do not have a marked effect on basal synaptic transmission but they play an important role in synaptic plasticity (reviewed in Gomes et al., 2011), specially in aged animals (Costenla et al., 1999). The ability of $A_{2A}R$ to enhance the activity-dependent efficiency of excitatory synapses has been argued to result from: 1) an enhanced release of neurotransmitters (Lopes et al., 2002; Rebola et al., 2003) 2) a localized desensitization of A_1R-mediated inhibition (Lopes et al., 1999); 3) a facilitation of brain-derived neurotrophic factor-induced signalling (Fontinha et al., 2008; Diógenes et al., 2011); and 4) from an enhanced responsiveness of N-methyl-d-aspartate (NMDA) receptors (Rebola et al., 2008).

Adenosine A_{2B} and A_3 receptors

A_{2B}R, like A_{2A}R, are positively coupled to adenylyl cyclase and PLC, through G_q proteins (Linden et al., 1999), and are mostly expressed in gastrointestinal tract, bladder, lung and mast cells (reviewed in Sachdeva and Gupta 2013). Even though the closest structure between A_{2A}R and A_{2B}R and their capacity to activate adenylyl cyclase (*Figure 1.11*), these two receptors have very different functions, being postulated that A_{2B}R could act by a different transduction system than adenylyl cyclase. The affinity of these receptors is also low, being activated predominantly when adenosine levels are increased (in µM order) (Sachdeva and Gupta, 2013).

A_3R can be found in liver, lung, mast cells, eosinophils, neutrophils, testis, heart and brain cortex. Similarly to the A_1R, A_3R activation inhibits adenylyl cyclase and activates phospholipase C and D (*Figure 1.11*) (Abbracchio et al., 1995). They also can promote Ca^{2+} influx and its release from intracellular stores (Jacobson, 1998). Furthermore, given the link between A_3R and the MAPK pathway, the A_3R play an important role in cancer, cell growth, survival and death (Boison, 2013; Sachdeva and Gupta, 2013).

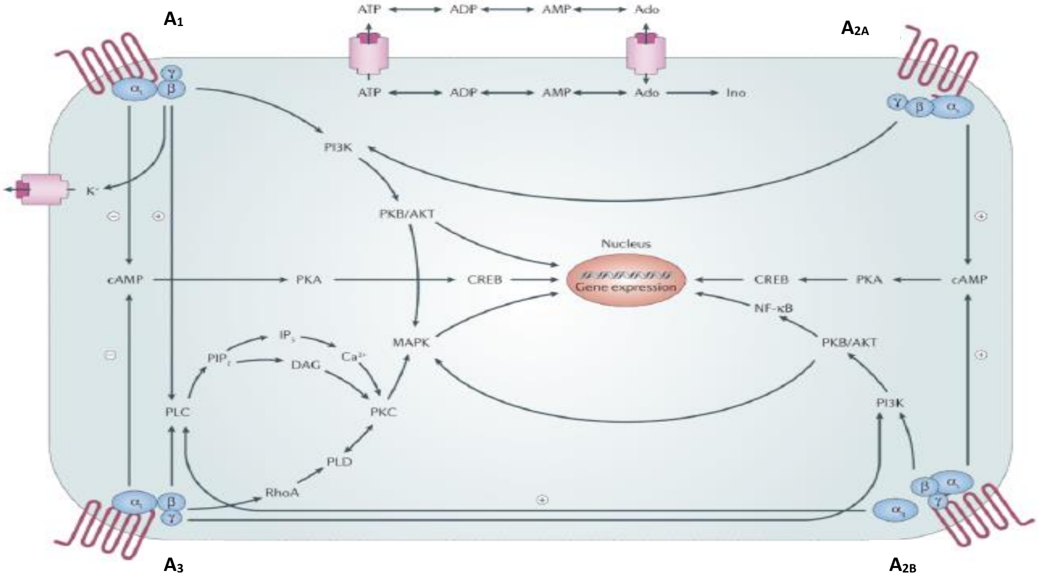

Figure 1.11 **Adenosine signalling pathway**. Schematic representation of the pathways activated by adenosine. Activation of A_1R and A_3R inhibits adenylyl cyclase activity through activation of toxin-sensitive G_i proteins, increasing PLC activity via $G_{\beta\gamma}$ subunits. A_{2A}R and A_{2B}R activation leads to adenylyl cyclase increased activity by G_s protein activation. A_{2A}R activation induces inositol phosphate formation in some situations, probably via Gα15 and Gα16 proteins. A_{2B}R activation induces PLC through G_q. All four adenosine receptors can couple to MAPK. **Ado** - adenosine; **ADP** - adenosine diphosphate; **AKT** - protein kinase B**; AMP** - adenosine monophosphate; **ATP** - adenosine triphosphate; **CREB** - cAMP response element binding protein; **DAG** - diacylglycerol; **Ino** - inosine; **IP3** - inositol 1,4,5-trisphosphate; **MAPK** - mitogen-activated protein kinases; **PI3K** - phosphatidylinositol 3-kinase; **PIP2** - phosphatidylinositol-4,5-bisphosphate; **PK** - protein kinase; **PLD** - phospholipase D; **NF-κB** - nuclear factor-κB (Jacobson and Gao, 2012).

1.3.3 Adenosine and pathology

Dysfunction in the adenosinergic signalling has been associated with several pathologies. Therefore, adenosine and its receptors have been pointed out as promising pharmacological targets in several disorders: cardiovascular, renal, pulmonary, inflammatory, endocrine and neurologic (*Figure 1.12*) (reviewed in Jacobson and Gao, 2012).

Within the neurologic disorders, epilepsy, Huntington’s, Parkinson´s and Alzheimer´s diseases are the ones receiving more attention.

In epilepsy, the role of adenosine as an anti-epileptic drug has been extensively studied. Initial evidence came from studies showing that the inhibitory A_1R are enriched in excitatory synapses, where they were responsible for the inhibition of glutamate release, decreasing therefore glutamatergic responsiveness and hyperpolarising neurons. These events are highly desirable to counteract epilepsy, characterized by an exacerbated and repetitive excitation (see for review Gomes et al., 2011). In addition, levels of extracellular adenosine rise during seizures, which could be a hint that adenosine plays an important role as an endogenous anti-epileptic molecule (During and Spencer, 1992; Berman et al., 2000). Subsequently, several studies have shown that the administration of compounds that increase the extracellular levels of adenosine, such as inhibitors of adenosine transporters or ADK inhibitors (briefly explored above in chapter 1.3.1), and agonists of A_1R, attenuate seizures and convulsive activity in animal models (reviewed in Boison et al., 2013). However, it was also shown that synaptic A_1R have decreased density and efficiency in animal models of epilepsy (Glass et al., 1996; Ekonomou et al., 2000) which could complicate the manipulation of A_1R receptors to modulate inhibition of this pathology. Nowadays, the inhibition of the excitatory $A_{2A}R$ is appearing as a new strategy to control chronic epilepsy and its blockage, by the use of antagonists, could be an alternative (El Yacoubi et al., 2008).

In Huntington’s disease (HD) the available data points to a possible involvement of $A_{2A}R$ on the pathophysiology of this disorder given that several alterations were detected in the $A_{2A}R$ gene as well as in the expression levels of the $A_{2A}R$ protein (Varani et al., 2001; Tarditi et al., 2006). Moreover, it is known that $A_{2A}R$ have an important role in motor control, in glutamatergic transmission, in neuroinflammation, on metabolism and mitochondrial function, all of them altered in HD (reviewed in Gomes et al., 2011). Thus $A_{2A}R$ antagonists have been explored as a potential therapeutic strategy since they improve motor function and also act as a neuroprotective agent decreasing glutamate levels and consequently controlling glutamatergic synapses. However, this topic brings some controversy since some studies refer $A_{2A}R$ agonists as a preferential therapeutic target in HD, because $A_{2A}R$ activation by its agonists could also facilitate BDNF functions, that are impaired in HD, through TrkB transactivation (Sebastião and Ribeiro, 2009) (explored in chapter 1.4.3) and at the same time, $A_{2A}R$ antagonism, initially suggested, potentiate NMDA-mediated toxicity. (Popoli et al., 2002).

The role of adenosine in the pathology of Parkinson’s disease (PD) has also been described. Since $A_{2A}R$ are involved in motor control (reviewed in Chen et al., 2007), in glutamatergic transmission control, neuroinflammation, metabolism and mitochondrial function, known to be impaired in PD, modulation of $A_{2A}R$ improves PD. The use of $A_{2A}R$ antagonists in PD is more accepted than in HD, and it is now being evaluated in clinical trials with the propose to ameliorate motor impairments and promote neuroprotection (LeWitt et al., 2008; Hauser et al., 2003).

The capacity of adenosine to control and integrate cognition and memory, through A_1R and $A_{2A}R$, provides the link between adenosine impairment and Alzheimer’s Disease (AD), a disorder characterized by the progressive impairment in these two functional capacities (Cunha and Agostinho, 2010). It was shown that A_1R and $A_{2A}R$ change their density and localization pattern in AD brain and that the chronic stress found in these patients also upregulates $A_{2A}R$ suggesting that its manipulation could promote neuroprotection (reviewed in Gomes et al., 2011). The capacity of $A_{2A}R$ to modulate learning and memory, are vastly studied in AD, where an epidemiologic relationship between caffeine consumption and AD risk has been shown (Maia and Mendonça, 2002). This relationship suggests that the $A_{2A}R$ antagonism achieve by caffeine ($A_{2A}R$ antagonist) consumption could decrease AD risk.

Even though the $A_{2A}R$ antagonism is beneficial in the above described neurodegenerative disorders, the $A_{2A}R$ agonism has emerged as a replacement strategy once it can potentiate BDNF functions, through TrkB facilitation (Numakawa, 2014). This is an important breakthrough since BDNF is impaired in these disorders but cannot be administrated due to pharmacokinetic issues.

Despite above mentioned pathologies share some phenotypical traits with RTT, the adenosinergic system in RTT has not yet been fully characterized.

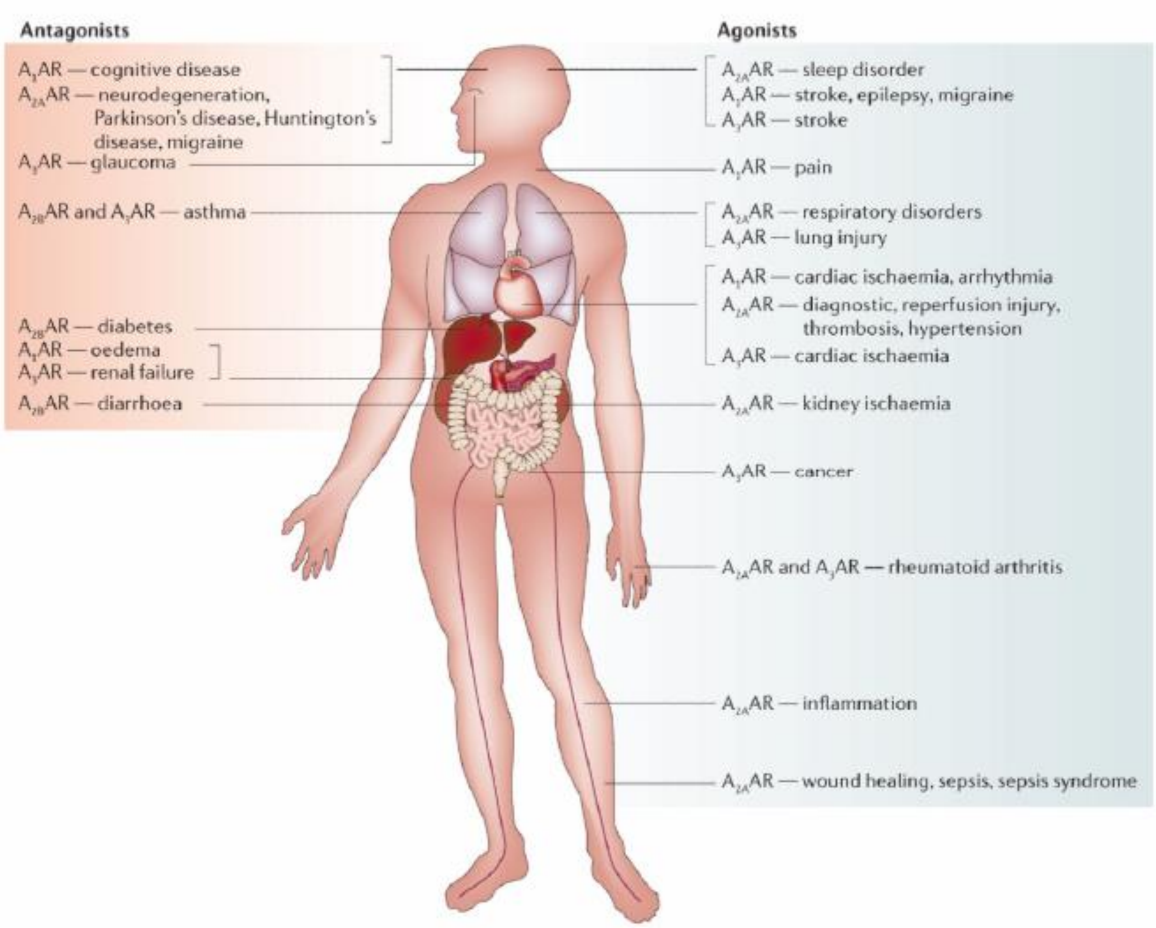
Antagonists
A_1AR — cognitive disease
A_{2A}AR — neurodegeneration, Parkinson's disease, Huntington's disease, migraine
A_3AR — glaucoma
A_{2B}AR and A_3AR — asthma
A_{2B}AR — diabetes
A_1AR — oedema
A_1AR — renal failure
A_{2B}AR — diarrhoea
Agonists
A_{2A}AR — sleep disorder
A_1AR — stroke, epilepsy, migraine
A_3AR — stroke
A_1AR — pain
A_{2A}AR — respiratory disorders
A_3AR — lung injury
A_1AR — cardiac ischaemia, arrhythmia
A_{2A}AR — diagnostic, reperfusion injury, thrombosis, hypertension
A_3AR — cardiac ischaemia
A_{2A}AR — kidney ischaemia
A_3AR — cancer
A_{2A}AR and A_3AR — rheumatoid arthritis
A_{2A}AR — inflammation
A_{2A}AR — wound healing, sepsis, sepsis syndrome

Figure 1.12 - **Adenosine receptors are targeted in several disorders**. Use of adenosine receptors antagonists, agonists or both is widely explored and already applied in the treatment of some disorders (Jacobson and Gao, 2012).

1.4 BDNF

BDNF was discovered in 1982 (Barde et al., 1982) and it is a member of the neurotrophin family that in mammals includes nerve growth factor (NGF), neurotrophin-3 (NT-3), and neurotrophin-4/5 (NT-4/5) (Cohen-cory et al., 2011). Axon targeting, neuron growth, synapses maturation and synaptic plasticity are some of essential functions executed by these signalling molecules, in particular by BDNF (Binder and Scharfman, 2004).

1.4.1 BDNF expression

The *Bdnf* gene is composed by four untranslated 5’ exons associated to different promotors and one 3’ exon (Li and Pozzo-Miller, 2014; Binder and Scharfman, 2004). Eight different transcripts can be transcribed from this locus but all of them are translated into an identical BDNF protein (Li and Pozzo-Miller, 2014). BDNF is synthetized in the endoplasmic reticulum (ER) as a precursor protein, pro-BDNF, and proper protein folding takes place in the Golgi apparatus. Pro-BDNF is then cleaved both intra- and extracellularly, near synapses to produce the mature and active BDNF form (14 kDa) (Binder and Scharfman, 2004; Lee et al., 2001). However, some studies have demonstrated that pro-BDNF is also present in the extracellular space, with a negative regulator function promoting apoptosis, inhibiting dendritic complexity and promoting long-term depression (LTD) by the activation of the p75 receptor (Barker, 2004). In the rodent brain, BDNF levels are low during prenatal development and rise drastically in the postnatal period (Kolbeck et al., 1999). Interestingly, this expression pattern coincides with MeCP2 expression pattern. Remarkably, it was also observed that BDNF expression remains unaffected during presymptomatic stage in *Mecp2 knockout* (*KO*) mice (Chang et al., 2006). In addition, *Bdnf*-deficient mice have a phenotype similar to that found in *Mecp2 KO* models (Chang et al., 2006). Besides, the positive correlation between BDNF and MeCP2 expression, it has also been shown that MeCP2 binds to *Bdnf* at methylated CpG sites adjacent to A/T runs (Klose et al., 2005), which could occur in association with repressor factors, such as HDACs, indicating a negative relation between these two molecules (Martinowich et al., 2003). How MeCP2 can modulate BDNF expression has not been fully addressed and therefore the “Dual operation model”, that proposing a dual action of MeCP2 upon BDNF expression is widely accepted (see Li and Pozzo-Miller, 2014).

1.4.2 BDNF signalling upon TrkB receptors

Neurotrophins can bind to one or more tropomyosin-related kinase (Trk) receptors members (Binder and Scharfman, 2004). Their action is mediated by the high-affinity full-length receptors (Trk-FL), which signal through their intrinsic tyrosine kinase activity. Neurotrophin binding induces receptor dimerization, which results in kinase activation and receptor autophosphorylation on multiples tyrosine residues. This creates binding sites for intracellular target proteins via the SH2 domain (Huang and Reichardt, 2003). Truncated isoforms of Trk receptors (Trk-Tc), formed by alternative splicing, can also bind neurotrophins, but cannot activate classical pathways of full-length receptors. This happens because truncated isoforms do not have the intracellular kinase domain (Allen et al., 1994). They are also thought to act as negative effectors of full-length Trk receptors (Luikart et al., 2003) and may have their own signalling properties (see e.g. Rose et al., 2003).

Mature BDNF has high-affinity to TrkB receptors, activating signal transduction through these. There are at least three signalling transduction pathways that BDNF can trigger: 1) PLC γ pathway, associated to synaptic plasticity BDNF-mediated, which leads to protein kinase C activation; 2) PI3K pathway, related to cell survival BDNF functions, which activates serine/threonine kinase AKT and 3) MAPK pathway, linked to growth and differentiation BDNF functions, that activates several downstream effectors as shown in (*Figure 1.13*) (Huang and Reichardt, 2003).

Three different truncated isoforms of TrkB receptor (TrkB-Tc) can be consider: TrkB-T1, the most abundant truncated isoform in the brain, TrkB-T2 and TrkB-Sch (Luberg et al., 2010). All of them can inhibit the BDNF activity by acting as dominant negative inhibitors of TrkB-FL receptors (Eide, 1996).

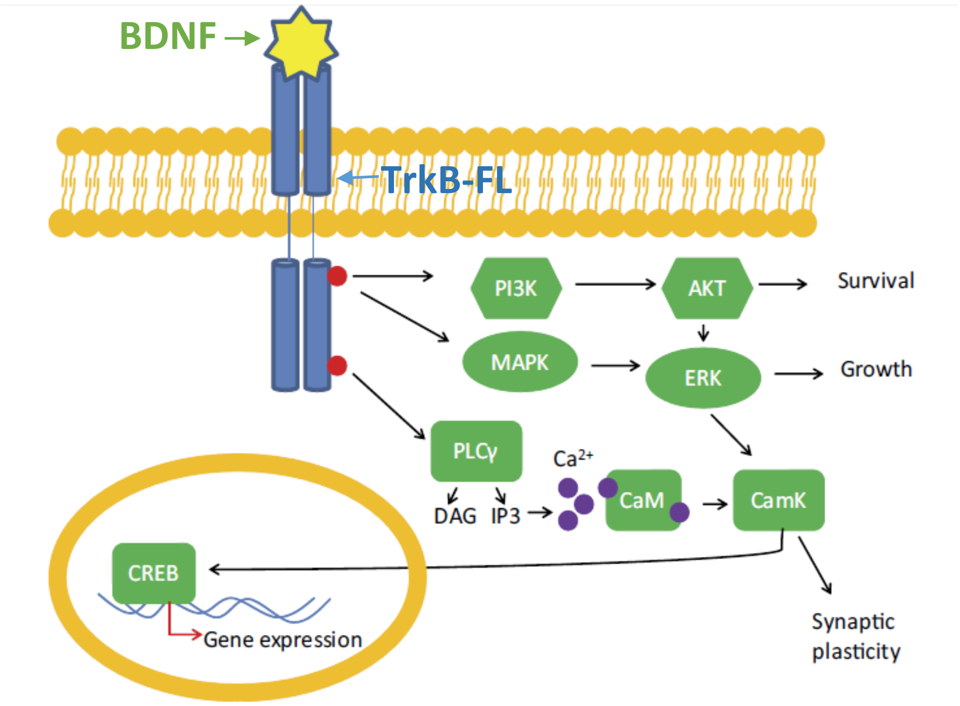

Figure 1.13 **BDNF signalling through TrkB full-length (TrkB-FL) receptors**. BDNF binding to TrkB-FL receptor promotes receptor autophosphorylation and dimerization, activating downstream signalling pathways: PI3K (promotes cell survival); MAPK pathway (promotes cell growth and differentiation); and PLCγ (activates IP3, which is related with synaptic plasticity). These pathways activate CREB, a transcription factor that up-regulates gene expression. **Akt** - protein kinase B **CREB** - cAMP response element binding protein; **DAG** - diacylglycerol; **Erk** - extracellular signal-regulated kinases **IP3** - inositol 1,4,5-trisphosphate; **MAPK** - mitogen-activated protein kinases; **PI3K** - phosphatidylinositol 3-kinase; **PLC** - phospholipase C (adapted from Autry and Monteggia, 2012).

1.4.3 Interaction between adenosine and BDNF

A close relationship between adenosine receptors and neurotrophic factors, namely BDNF, has been found.

Presynaptic depolarization, that leads to an increase in adenosine extracellular levels and consequently to an enhancement of cAMP by $A_{2A}R$ activation trigger hippocampal synaptic actions of BDNF (Diógenes et al., 2004). At the same time, $A_{2A}R$ activation can transactivate TrkB receptors in the absence of the neurotrophin (Rajagopal et al., 2004; Lee and Chao, 2001). It was also seen that $A_{2A}R$ activation can mediate neuroprotection, by increasing cell survival through Trk-dependent and PI3K/AKT pathway, in hippocampal neurons after BDNF and NGF withdrawal (Lee and Chao, 2001). Interestingly, it is also known that $A_{2A}R$ are required for normal BDNF expression levels in the hippocampus (Tebano et al., 2008).

During high neuronal activity, such as long-term potentiation (LTP), higher release of adenosine or its precursor, ATP, is observed creating the ideal conditions for the interplay between $A_{2A}R$ and TrkB-FL receptors (Sebastião and Ribeiro, 2009). Indeed, when $A_{2A}R$ activity is blocked or extracellular adenosine is depleted, the facilitatory action of BDNF upon LTP is completely lost (Fontinha et al., 2009; Fontinha et al., 2008; Jerónimo-Santos et al., 2014).

Decreased BDNF levels might be involved in neurodegenerative disorders (Connor and Dragunow, 1998), diabetic neuropathies (Nitta et al., 2002) and RTT (reviwed in Li and Pozzo-Miller, 2014) making the use of BDNF very promising for their treatment. However, until now the pharmacological administration of BDNF has not been easy mainly due to pharmacokinetic problems. Therefore, the discovery that the activation of $A_{2A}R$ potentiates BDNF actions opened a new avenue for potential therapeutic strategies for these disorders, in particular for RTT.

2. Aims

RTT is genetic disorder with severe intellectual disabilities among other symptoms. It is known that in RTT brain-derived neurotrophic factor (BDNF) signalling is impaired. Therefore, restoring BDNF signalling could be a great breakthrough in the treatment of RTT, but it has been hampered by the difficulty of BDNF to reach its target tissue. Given that, the activation of $A_{2A}R$ is known to potentiate BDNF synaptic actions in healthy animals, one could anticipate that the activation of these adenosine receptors could be a potential therapeutic strategy. On the other hand, most of RTT patients have epilepsy, a pathology where adenosine system might be affected and has been largely explored as a potential therapeutic target. However, until recently, there was no available information about the contribution of the adenosinergic system to the pathophysiology of RTT. To overcome this gap in knowledge, our lab has developed a line of research on this topic.

The present thesis was developed within a broader project that aims at:

i) the characterization of the adenosinergic system and BDNF signalling in RTT;

ii) investigating whether drugs that mediate the activation of adenosine receptors, could be a breakthrough in RTT treatment by controlling epilepsy through the activation of A_1R, and potentiating BDNF effects by the activation of $A_{2A}R$.

In particular, the main goal of this project was to further characterize both the adenosinergic system and the BDNF signalling in RTT. This goal was achieved by using:

1) a well-established animal model, *Mecp2 KO* mice;

2) human RTT model, neurons-derived from RTT patients IPSCs;

3) *post-mortem* human brain samples from a RTT patient.

3. Materials and Methods

3.1 Biological Samples

3.1.1 Animals

The experiments were performed in adult mice, 6 to 10 weeks old, Mecp2tm1.1Bird/J (*Mecp2 knockout (KO)*, deletion of exons 3 and 4 of the *Mecp2* gene) (Guy et al., 2001), and in *wild type* (*WT*) littermates that were used as control. The genotype of animals was determined by polymerase chain reaction, as previously described (Guy et al., 2007).

The animals were housed on a 12 hours light/dark cycle, with food and water provided *ad libitum*. Experiments involving animals were taken into careful consideration in order to reduce the number of animals sacrificed. All animals were handled according to the Portuguese law on Animal Care and European Union guidelines (86/609/EEC).

3.1.2 *Post-mortem* Brain Sample

The brain tissue of an 11 year-old girl affected with RTT (MeCP2 mutation - R255X) who died after a severe pneumonia was dissected and different anatomic regions were immediately frozen at -80˚C. Age and sex-matched cortical tissue was kindly provided by the biobank of Hospital San Juan de Deu (HSJD). Parent informed consent and ethical approval from (HSJD) were obtained.

For the present study samples from the temporal cortex were used for RNA extraction (QIAGEN), cDNA synthesis and subsequent quantitative PCR analysis.

3.2 Human Induced Pluripotent Stem Cells (hIPSCs)

3.2.1 Cell lines

Cortical neurons were obtained from hIPSCs. Five cell lines were used in this study: two from healthy controls and three derived from RTT patients. Two lines were derived from RTT female patients with known MeCP2 mutations: EMC23i (named as RF1, R306C) and

EMC24i (named as RF2, R255X) were kindly provided by Joost Gribnau (Erasmus Medical School, Rotterdam, Netherlands). The cell line Rett-male (RM) was derived from a male patient (Q83X) and was a gift of Professor Alysson Muotri (University of California, San Diego, USA). Two control hIPSCs lines were used from healthy donors: Ct1 was reprogrammed in lab of Luis Pereira de Almeida (Centro de Neurociências e Biologia Celular, Coimbra) and derived from a healthy female donor. Ct2 was kindly provided by TCLab (Évora) and was derived from a healthy male donor (Table 3-1).

Patient-derived fibroblasts were reprogrammed using a protocol described by Warlich, fluorescence-based lentiviral reprogramming, using the four human genes: *OCT4*, *SOX2*, *C-MYC* and *KLF4* (Warlich et al., 2011).

Table 3-1 – **Characterization of hIPSCs lines** (F - Female; M - Male; y-years).

Cell line	Abbreviation	Age (y)	Sex	MeCP2 Mutation	Origin
F7	Ct1	7	F	No	Luis Pereira de Almeida, CNBC
WT-Évora F0000B13	Ct2	3	M	No	TCLab
EMC23i/R1	RF1	6	F	R306C	Joost Gribnau, Erasmus Medical School
EMC24i/R2	RF2	8	F	R255X	Joost Gribnau, Erasmus Medical School
Rett Male	RM	3	M	Q83X	Alysson Muotri, University of California

3.2.2 Materials

All reagents to generate cortical neurons from patient and healthy control-derived hIPSCs are described in tables 3-2 and 3-3.

Table 3-2 – **Reagents for hIPSCs expansion and neuronal induction**.

Material	Description	Preparation	Supplier
Accutase	Mixture of proteolytic and collagenolytic enzymes used for the detachment of cells and tissues. It was used to perform single-cell passaging of hIPSCs-derived neural precursors.	Ready-to-use solution. Stored at -20˚C.	STEMCELL^{TM} Technologies
EDTA	It is an aminopolycarboxylic acid that acts as a hexadentate ("six-toothed") ligand and chelating agent. Used to passage cells.	Prepared by mixing 500 µl of 0.5M of EDTA stock, 500 ml of sterile PBS (Sigma®) and 0.9g of NaCl (Sigma®) to adjust osmolality.	Sigma®
FGF2	Promotes proliferation of neural progenitors in rosettes.	Aliquots (20 ng/ml) stored at -20˚C. Working solution, diluted in 0.5 ml N2B27. Supplemented medium at 1:100.	PeproTech
Laminin	ECM protein used as coating matrix.	Slowly thawed at 4˚C and then diluted in sterile PBS (Sigma®), to a final concentration of 20 µg/ml.	Sigma®
LDN-193189	Small molecule which inhibits BMP signalling, allowing ectoderm differentiation.	Diluted in DMSO to final concentration of 10 mM. Stored at -20˚C. Working dilution: 100 µM solution in DMSO. Supplemented medium at 1:1000.	STEMCELL^{TM} Technologies
Matrigel® coating	Commonly used substrate for supporting the growth and self-renewal of hIPSCs. Composed mainly of laminin, collagen IV, heparin sulfate proteoglycans, entactin and growth factors.	Aliquoted and frozen at -20˚C. For use read 3.2.3 section	BD (Becton, Dickinson and Company)
Penicillin Streptomycin (PenStrep; P/S)	Antibiotic mixture used in culture to prevent bacterial contaminations.	PenStrep (P/S), 5.000 units of penicillin and 5.000µg/ml of streptomycin. Store at -20˚C.	Life Technologies
Phosphate buffered saline (PBS)	Buffer solution containing sodium phosphate, sodium chloride and, in some formulations, potassium chloride and potassium phosphate. The osmolality and ion concentrations of the solutions match those of the human body.	Ready-to-use solution	Sigma®

Poly-L-ornithine	Culture substrate that increases attachment of neural cells.	Diluted in ddH$_2$O to a final concentration of 1.5 mg/ml (100x), filtered, aliquoted and stored at -20˚C.	Sigma®
SB-431542	Potent inhibitor of ALK5, ALK4 and ALK7, preventing differentiation to mesoderm.	Diluted in DMSO to a final concentration of 10 mM. Stored at -20˚C. Supplemented medium at 1:1000.	Life Technologies

Table 3-3 – **Medium formulation for hIPSCs expansion and neuronal induction.**

Medium	Description	Preparation
mTeSR™	Complete and defined serum-free medium, with high concentrations of bFGF, TGF-β, GABA, pipecolic acid, lithium chloride. mTeSR™1 is not xeno-free as it contains bovine serum albumin.	To prepare 500 ml of mTeSR1, 100 ml of thawed mTeSR™1 5X supplement was mixed with 400 ml of mTeSR™1 basal medium. Aliquots stored at -20˚C. (STEMCELL™ Technologies)
N2B27	Chemically-defined serum-free medium generally used for neuronal differentiation.	Composed by 50% (v/v) of N2 medium and 50% (v/v) of B27 medium. **N2 medium**: 242.5 ml of DMEM/F12, 250 µl of insulin (20µg/ml), 2.5 ml of P/S (1%), 4 ml glucose 10% and 2.5 ml N2 supplement (1%) **B27 medium**: 241.25ml of Neurobasal, 5ml of B27 supplement (2%), 2.5 ml of L-Glutamine (1mM) and 1.25 µl of P/S (1%) and 5 ml of B27 (2x) supplement. All from Life Technologies.
Washing Medium	Thaw hIPSCs.	250ml of washing medium: 218.5ml of KO-DMEM (Life Technologies); 25ml of KO-SR (Life Technologies), 2.5ml of MEM non-essential aminoacids (1%), 1,25ml of L-Glutamine (1mM), 250µl of β-Mercaptoethanol (0.1mM) and 2.5ml of P/S (1%). All from Life Technologies.

3.2.3 Matrigel dish coating

Matrigel® was diluted in cold DMEM/F12 (4˚C) (1:30) supplemented with PenStrep (1:100) and then used to coat the wells of a 6-well plate (1 ml per well of a 6-well plate).

The plate was incubated for at least 3 hours at room temperature. After the incubation at room temperature, the plate was store at 4˚C until further use. Medium was removed prior to cell seeding.

3.2.4 Laminin coating

Plates were incubated with poly-L-ornithine (15 µg/ml) at 37˚C, for at least 4 hours. Next, poly-L-ornithine was removed and replaced by laminin solution (20µg/ml diluted in PBS) and incubated at 37˚C for at least 4 hours. Laminin solution was removed before cell plating.

3.2.5 hIPSCs expansion

Initially cells were thawed adding drop-by-drop 1 ml of pre-heated (37˚C) washing medium, transferring them into a tube with warm medium and then centrifuged for 5 minutes at 120g. The supernatant was discarded and cells were resuspended in pre-warmed mTeSR^{TM}1 supplemented with PenStrep (1:150) and plated on Matrigel®-coated plates.

Cells were expanded for a few passages with a splitting-ratio of 1:3. Passages were performed when colonies were reaching 80% confluency. Cell passaging was performed using an enzyme-free method. The cell culture medium was removed from the well and cells were washed once with 0.5mM EDTA, followed by an incubation for 3-5 minutes with 1.0 ml of 0.5mM EDTA. Cells were scraped from the well using the tip of the pipette, resuspended in 1 mL of mTeSR^{TM}1 supplemented with PenStrep and transferred to a Falcon^{TM} tube taking special care not to get single-cell suspension. During the expansion phase medium was changed every day.

Cells were cryopreserved using also the non-enzymatic procedure to help detach cells. Cells were washed with 1 mL of 0.5mM EDTA per well and then incubated with the same volume of EDTA for 3-5 minutes. Cells were then carefully scraped using the tip of the pipette, resuspended in 1 mL of washing medium and transferred to a Falcon^{TM} tube and centrifuged at 120g for 5 minutes. The supernatant was discarded and the cells were resuspended with freezing medium (10% DMSO in Knockout Serum Replacement – KO-SR - (Life Tecnhologies)). Resuspended cells were then transferred to a cryovial and placed in a Mr. Frosty at -80˚C over-night. After this, cells were placed in liquid nitrogen (*Figure 3.1*).

3.2.6 Neuronal induction, the dual SMAD inhibition protocol

Several protocols have been described to obtain neurons. The dual SMAD inhibition protocol has been shown to be the most efficient since it combines two small molecules that inhibit TGF and BMP signalling: SB-431542 and LDN-193189. This protocol has been designed to obtain cortical glutamatergic neurons (Shi et al., 2012).

Cells were expanded and plated according to the protocol described above. Final plating was performed on 2 wells of one 6-well plate (1 well for Protein extraction and 1 well to carry on the differentiation) and on 4 wells of a 12-well plate (for immunostaining checkpoints), all previously coated with Matrigel®.

IPSCs were plated on Matrigel® coated plates (see section 3.2.3) and medium (mTeSR^{TM}1) was changed every day until cells became confluent. On day 1, mTeSR^{TM}1 was replaced by N2B27 medium supplemented with the small molecules, SB-431542 and LDN-193189 (1:1000) (Shi et al., 2012) preventing differentiation into endoderm and mesoderm lineages. Until day 12 of neuronal induction, medium was changed every day and was supplemented with the small-molecules. At day 12, cells were split 1:3 using EDTA (0.5mM) and seeded on laminin-coated plates (see below section 3.2.4). Cells were plated with N2B27 medium supplemented with the small molecules for 24h and after this medium was changed every day using non-supplemented N2B27.

Between days 12-17 of neuronal induction, the first neuronal rosettes appeared and at this point the N2B27 medium was supplement with 20ng/mL of FGF2 for 4 consecutive days. Between day 17-20 cells were again split using EDTA (0.5mM) and replated on laminin-coated plates.

The last passage was performed around day 30, when the first neurons begin to accumulate at the periphery of the rosettes. At this stage, cells were single-cell passaged using accutase and replated on laminin-coated plates at a density of 50.000 cells/cm^2. Cells were plated on a glass coverslip coated with laminin and a total of 18 wells of 24-well plate were used. Briefly, wells were washed twice with PBS. Then, 1 mL of accutase was added and plates were incubated for 5-10 minutes at 37˚C. Cells were resuspended in washing medium, transferred to a Falcon^{TM} tube and centrifuged at 120g for 5 minutes, at room temperature. The supernatant was discarded and the pellet resuspended in culture medium, N2B27.

From day 30 on, cell medium was change every other day leaving 1/3 of the old medium in the well. After day 60, N2B27 was supplemented with laminin (1:200) once a week to promote and maintain cell adherence to the glass coverslip (*Figure 3.1*).

We have generated cortical neurons from all the hIPSCs lines. In the case of RM and RF1 two independent rounds of differentiation were performed, referred to as RM-1, RM-2 and RF1-1 and RF1-2.

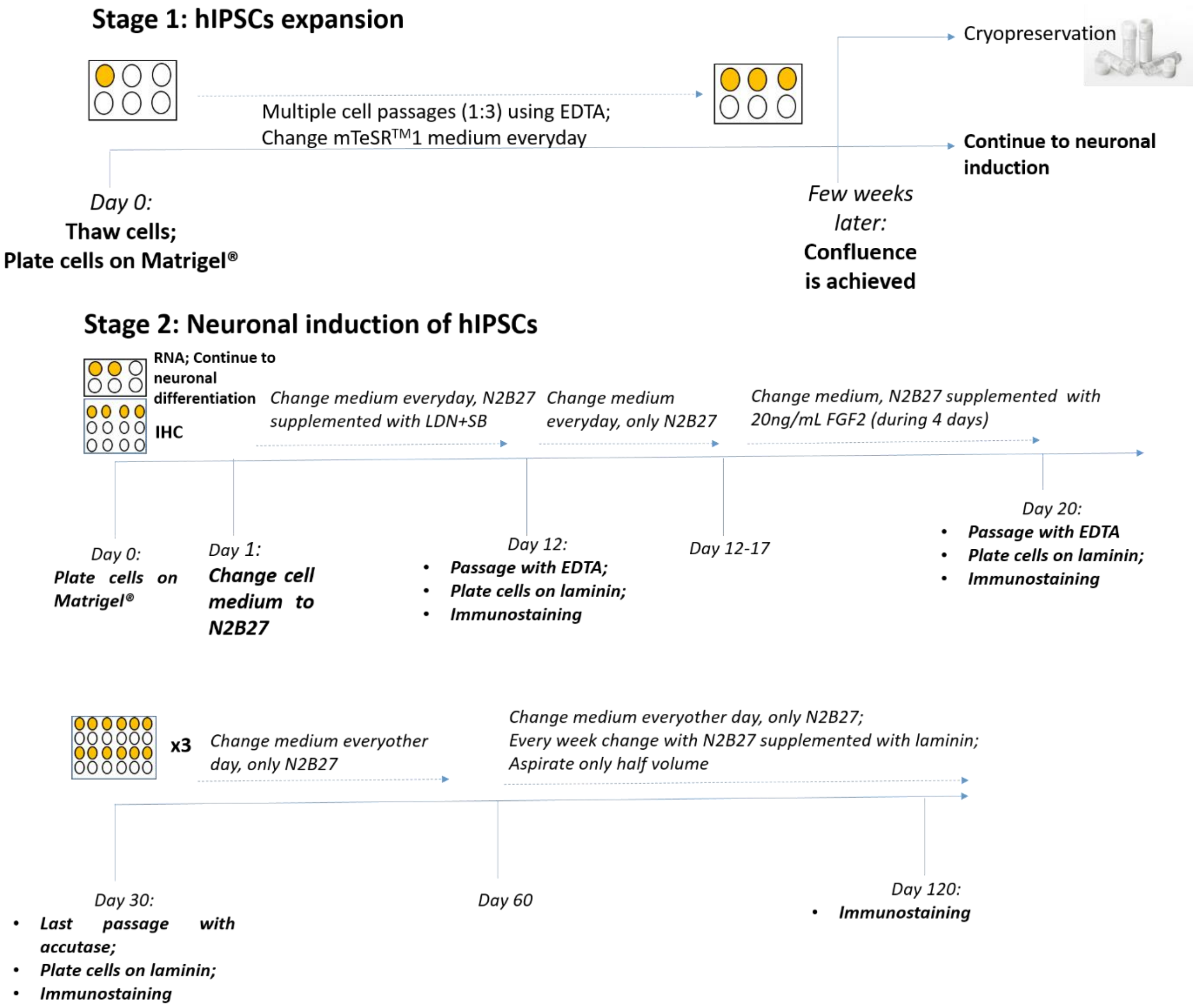
Stage 1: hIPSCs expansion
Cryopreservation
Multiple cell passages (1:3) using EDTA;
Change mTeSR™1 medium everyday
Continue to neuronal induction
Day 0:
Thaw cells;
Plate cells on Matrigel®
Few weeks later:
Confluence is achieved
Stage 2: Neuronal induction of hIPSCs
RNA; Continue to neuronal differentiation
IHC
Change medium everyday, N2B27 supplemented with LDN+SB
Change medium everyday, only N2B27
Change medium, N2B27 supplemented with 20ng/mL FGF2 (during 4 days)
Day 0:
Plate cells on Matrigel®
Day 1:
Change cell medium to N2B27
Day 12:
Passage with EDTA;
Plate cells on laminin;
Immunostaining
Day 12-17
Day 20:
Passage with EDTA
Plate cells on laminin;
Immunostaining
x3
Change medium everyother day, only N2B27
Change medium everyother day, only N2B27;
Every week change with N2B27 supplemented with laminin;
Aspirate only half volume
Day 30:
Last passage with accutase;
Plate cells on laminin;
Immunostaining
Day 60
Day 120:
Immunostaining

Figure 3.1 - **Schematic representation of neuronal differentiation, described in sections 3.2.5 and 3.2.6.**

3.3 Molecular Biology Techniques

3.3.1 Western-Blot analysis

Protein Extraction

Protein extracts for Western-Blot analysis were prepared from snap-frozen mice cortex and from differentiated neurons-derived from hIPSCs (day 120).

Neurons-derived from IPSCs. Cells were washed with iced-cold PBS and lysed with radio-immunoprecipitation assay (RIPA) buffer: 50mM Tris-HCl (pH 7.5), 150mM NaCl, 5mM ethylenediamine tetra-acetic acid (EDTA), 0.1% SDS and 1%Triton X-100 and protease inhibitors cocktail (Mini-Complete EDTA-free; Roche Applied Science).

Mouse cortex. Snap-frozen cortex samples were first disrupted with a Teflon pestle in 50 mM sucrose-Tris (pH 7.6) supplemented with protease inhibitors cocktail (Mini-Complete EDTA-free; Roche Applied Science).

All lysates were then vortexed and sonicated (3 cycles of 15 seconds), and clarified by centrifugation (13000g, 10min). The protein content in the supernatant was determined by Bio-Rad DC reagent, a commercial Bradford assay (Sigma®).

Protein Electrophoresis, Transfer and Detection/Quantification

Equal amounts of protein were loaded (*neuron-derived from hIPSCs*: 30-45 µg; *mice cortices:* 70 µg except for $A_{2A}R$ blot: 200 µg) and separated on 10% sodium dodecyl sulphate-polyacrylamide gel electrophoresis (SDS-PAGE) and then transferred to polyvinylidene fluoride (PVDF) membrane (GE Healthcare). To check protein transfer efficiency, membranes were stained with Ponceau S solution. After blocking with a 5% non-fat dry milk solution in TBS-T (20 mM Tris base, 137 mM NaCl and 0.1% Tween-20), membranes were washed three times with TBS-T, before incubation with the primary antibody, diluted in 3% BSA solution in TBS-T (overnight at 4˚C) and secondary antibodies diluted in blocking solution (1 hour at room temperature).

Immunoreactivity was visualized using ECL chemiluminescence detection system (Amersham-ECL Western Blotting Detection Reagents from GE Healthcare) and band intensities were quantified by digital densitometry (*ImageJ* 1.45 software). α-tubulin or β-actin bands were used as loading control.

Antibodies

Table 3-4 – **Western-Blot primary antibodies***.*

Protein	Primary Antibody	Dilution	Supplier
$A_{2A}R$	$A_{2A}R$	1:1500	Upstate cell signalling solutions (05-717)
ADK	Rabbit polyclonal anti-ADK	1:6000	Kindly provided by Detlev's (Gouder et al., 2004)
GAPDH	Mouse monoclonal anti-GAPDH	1:5000	Ambion® by life technologies (AM4300)
TrkB-FL and TrkB-Tc	Mouse monoclonal anti-TrkB	1:1500	BD Transduction Laboratories (610101)
α-tubulin	Rabbit polyclonal anti-α-Tubulin	1:3000	Abcam® (ab4074)

Table 3-5 – **Western-Blot secondary antibodies***.*

Secondary Antibody	Dilution	Supplier
Goat anti-mouse IgG-HRP	1:10000	Santa Cruz Biotechnology (sc-2005)
Goat anti-rabbit IgG-HRP	1:10000	Santa Cruz Biotechnology (sc-2004)

3.3.2 ELISA assay

To determine BDNF protein concentration in mice hippocampi and in neurons-derived from hIPSCs, ELISA assays using BDNF Emax® ImmunoAssay System (Promega, USA) were performed.

Lysates were prepared with 200 µl of lysis buffer (137mM NaCl; 20mM Tris-HCl (pH 8.0); 1% NP40; 10% glycerol; 1mM PMSF; 10µg/ml aprotinin; 1µg/ml leupeptin; 0.5mM sodium vanadate) and homogenised in a sonicator (Vibra-Cell, Sonics & Materials, Inc). RIPA buffer (described in section 3.3.1) was used to prepare the protein lysates from neurons-derived from hIPSCs. To improve BDNF detection, samples were acidified with HCl 1M, until reaching approximately pH 2.6. After 10 to 20 minutes NaOH was added to neutralise samples to 7.6 pH.

Nunc-Immuno™ MaxiSorp™ plates were used to execute the technique and all steps were done according to manufacturer's instructions.

3.3.3 Immunohistochemistry

Immunohistochemistry was only performed with hIPSCs-derived neurons in order to follow their neuronal differentiation, using appropriate cell-type specific markers (section 4.3.2). Cells were washed with PBS and fixed with 2% paraformaldehyde (PFA) during 1 hour, followed by 5minutes incubation with methanol. Cellular permeabilization and blocking were performed using 10% fetal bovine serum (FBS) with 0.1% Triton in PBS (Sigma®) for 30 minutes. Primary antibodies were diluted in blocking solution and incubated overnight at 4˚C. Cells were then washed three times for 5 minutes with TBS-T (described in section 3.3.1). Secondary antibodies were diluted in blocking solution and cells were incubated for 1 hour at room temperature. After secondary antibody incubation cells were washed three times in TBS-T and DAPI (1:1000 dilution in PBS; Sigma®) counterstaining was used to label the nucleus for 10 minutes. Cells were mounted with Mowiol (Sigma®) and observed with Axiovert 200M (Zeiss) or with confocal LSM 710 (Zeiss).

Antibodies

Table 3-6 – **Immunohistochemistry primary antibodies.**

Protein	Primary Antibody	Dilution	Supplier
BRN2	Goat polyclonal anti-Brn2	1:200	Santa Cruz (SC-6029)
CTIP2	Rat monoclonal anti-CTIP2	1:400	Abcam (ab18465)
FOXG1	Rabbit polyclonal anti-FOXG1	1:1000	Abcam (ab18259)
GFAP	Rabbit polyclonal anti-GFAP	1:800	Sigma (HPA056030)
MAP2	Mouse monoclonal anti-MAP2	1:200	Sigma (M4403)
Oct3/4 (POU5F1)	Mouse monoclonal anti-OCT3/4	1:400	Santa Cruz (sc-5279)
OTX2	Rabbit polyclonal anti-OTX2	1:100	Abcam (ab21990-100)
PAX6	Mouse monoclonal anti-PAX6	1:200	DSHB
SNAP25	Rabbit polyclonal anti-SNAP25	1:1000	Sigma-Aldrich (S9684)
SOX2	Rabbit polyclonal anti-SOX2	1:400	Millipore (ab5603)
TBR1	Rabbit polyclonal anti-TBR1	1:400	Millipore (ab9616)
TBR2	Rabbit polyclonal anti-TBR2	1:400	Millipore (ab2283)
TUJ1	Mouse monoclonal anti-TUJ1	1:4000	Covance (MMS-435P)
VGAT	Goat polyclonal anti-VGAT	1:600	Santa-Cruz (sc-49574)
VGLUT	Rabbit polyclonal anti VGLUT	1:500	Synaptic Systems (BNPI)
ZO1	Mouse monoclonal anti-Zo1	1:200	Zymed (33-9100)

Table 3-7 – **Immunohistochemistry secondary antibodies**.

Secondary Antibody	Dilution	Supplier
Donkey anti-goat, Alexa F594	1:400	Molecular Probes (A11056)
Donkey anti-mouse, Alexa F594	1:400	Molecular Probes (A21044)
Donkey anti-rat, Alexa F488	1:400	Molecular Probes (A21208)
Goat anti-mouse, Alexa F488	1:400	Molecular Probes (A11001)
Goat anti-rabbit, Alexa F594	1:400	Molecular Probes (A11012)
Goat anti-rabbit, Alexa F647	1:400	Molecular Probes (A21244)
Rabbit anti-mouse, Alexa F488	1:400	Molecular Probes (A11059)

3.3.4 RNA extraction and cDNA synthesis

Mouse Tissue

Total RNA was extracted from mice cortices, using RNeasy Lipid Tissue Mini Quit (Qiagen), according to the manufacturer's instructions. RNA concentration and purity was then evaluated by spectrophotometry based on optical density (OD), measurements at 260 and 280 mm (Model: NanoDrop-100; Thermo Scientific).

cDNA synthesis was performed in a 20µl reaction mixture. 2 µg of total RNA were mixed with 1 µl random primer hexamers (Amersham) and 1 µl each of dATP, dTTP, dCTP and dGTP (10 mM). This mix was incubated 5 minutes at 65˚C and after cooling for 2 minutes on ice, the remaining reagents were added (4 µl of 25 mM $MgCl_2$, 2 µl of 10x RT buffer, 2 µl of 0.1M DTT, 0.5 µl Superscript II Reverse Transcriptase (200U), all reagents from Invitrogen, Life Technologies). The reaction was incubated for 50 minutes at 42˚C and followed by 15 minutes incubation at 70˚C to inactivate the enzyme. Parallel reactions for each RNA sample were run without Superscript II to evaluate the degree of genomic DNA contamination. Completed reverse transcription (RT) reactions were stored at -20˚C until further used.

Neurons-derived from IPSCs and human brain tissue

A similar protocol was followed for RNA extraction and cDNA synthesis from neurons-derived from hIPSCs and human brain tissue, being described in this section the differences between them. RNeasy Mini Kit (QIAGEN) was used for total RNA isolation with DNase digestion on the column, to avoid DNA contamination, according to manufacturer's instructions. cDNA synthesis was performed with 0.5 µg of total RNA and the second mix was composed by 4 µl of 5x First-Strand Band Buffer, 2 µl of 0.1 DTT, 1 µl of RNase Out (40 units/µl) and 1 µl of Superscript II RT (all reagents from Invitrogen). Reaction mix was first incubated for 10 minutes at 25˚C followed by 50 minutes at 42˚C.

3.3.5 Quantitative PCR

Mouse Tissue

Gene expression level was addressed by quantitative PCR (qPCR) using Power SYBR® Green Master Mix (Life Technologies), and cDNA was used as template for the real-time PCR run in Rotor Gene 6000 (Corbett Life Science). The thermal cycler conditions were as follows: hold for 10 minutes at 95°C, followed by 40 cycles of a two-step PCR consisting of a 95°C step for 15 seconds followed by a 60°C step for 25 seconds. A final thermal ramp from 72 to 95 degrees was performed in each experiment. Negative control PCR samples were run with no template. Relative mRNA expression was calculated using $2^{-\Delta ct}$ method and primers were previously optimized in order to establish annealing temperature and primer efficiency (e=2±0.2), calculated after serial primer dilutions and construction of respective standard curve (slope and R^2 respectively around -3.3 and 0.99 described in Schmittgen and Livak 2008). Data were normalized to the expression of *PPIA peptidylprolyl isomerase A* (*cyclophilin A*) (*CypA*) and *ribosomal protein L13A* (*Rpl13A*). Data acquisition was performed with *Rotor-Gene Series* Software 1.7 (Corbett Life Science) and data analysis was performed with Microsoft Excel.

Neurons-derived from IPSCs and human brain tissue

Once again, the qPCR protocol was similar to the above described, being here mentioned the different steps. The real time-PCR was run in 7500 Fast (Applied Biosystems), with the same thermal cycler conditions as the described above, taking into account the annealing temperature for the primers used (Schmittgen and Livak, 2008). The normalization was done to *GAPDH* expression. Data acquisition was performed with *7500 software* v2.0.6 (Applied Biosystems) and data analysis was performed in Microsoft Excel.

Primers

Table 3-8 – **Primer sequence and annealing temperature for all primer pairs used for quantitative analysis.**

Org.		**Gene**	**Forward Primer (5'->3')**	**Reverse Primer (5'->3')**	**Annealing Temperature (˚C)**
Mouse	*$A_{2A}R$*	*Adenosine A_2A Receptor*	ATT CCA CTC CGG TAC AAT GG	AGT TGT TCC AGC CCA GCA T	60
	A_1R	*Adenosine A_1 Receptor*	TCG GCT GGC TAC CAC CCC TTG	CCA GCA CCC AAG GTC ACA CCA AAG C	60
	TrkB-FL	*TrkB-Full Lengh Receptor*	GAG CTG CTG ACC AAC CTC CA	GTC CCC GTG CTT CAT GTA CTC A	60
	TrkB-T1	*TrkB-T1 Receptor*	TAA GAT CCC CCT GGA TGG GTA G	AAG CAG CAC TTC CTG GGA TA	60
	CypA	*PPIA peptidylprolyl isomerase A (cyclophilin A)*	TAT CTG CAC TGC CAA GAC TGA GTG	CTT CTT GCT GGT CTT GCC ATT CC	60
	Rpl13A	*Ribosomal protein L13A*	GGA TCC CTC CAC CCT ATG ACA	CTG GTA CTT CCA CCC GAC CTC	60
Human, IPSCs	*A_1R*	*Adenosine A1 Receptor*	GCC ACA GAC CTA CTT CCA CA	CCT TCT CGA ACT CGC ACT TG	62
	$A_{2A}R$	*Adenosine A2A Receptor*	AAC CTG CAG AAC GTC AC	GTC ACC AAG CCA TTG TAC CG	62
	TrkB-FL	*TrkB-Full Length Receptor*	GGC CCA GAT GCT GTC ATT AT	TGC CTT TTG GTA ATG CTG TTT	62

TrkB-T1	*TrkB-T1 Receptor*	TCT ATG CTG TGG TGG TGA TTG	GAG TCC AGC TTA CAT GGC AG	62
BDNF	*Brain-derived neurotrophic factor*	TAA CGG CGG CAG ACA AAA AGA	GAA GTA TTG CTT CAG TTG GCC T	60
MAP2	*Microtubule-associated protein 2*	CAC GGA AGC TTA AGC AAA GG	CCC TCG GTG TTT GTA CTT TTC T	60
GAPDH	*Glyceraldehyde-3-phosphate dehydrogenase*	GGA GTC AAC GGA TTT GGT CG	GAC AAG CTT CCC GTT CTA G	60/62
GFAP	*Glial fibrillary acidic protein*	TGC TCG CCG CTC CTA CGT CT	ATC CAC CCG GGT CGG GAG TG	60
SNAP25	*Synaptosomal-associated protein 25*	CTG CTC GTG TAG TGG ACG AA	CGA TCT CAT TGC CAT ATC C	60
VGAT	*Vesicular GABA transporter*	CGT GAT GAC CTC CTT GGT CT	CAA GAA GTT CCC CAT CTC CA	60

Note: Primers were stocked at 100 µM and frozen at -20˚C. 0.4 µl of each primer were added for real-time PCR run, except for GFAP and MAP2 run where was added 0.2 µl

3.4 Electrophysiology

3.4.1 *Ex vivo* electrophysiological recordings

Hippocampus isolation and slice preparation

The animals were first anesthetized with isoflurane (1,2-Propylenglycol 50% (v/v)) in an anaesthesia chamber. When animals showed the first signs of anaesthesia state, like reduction of respiratory rate and lack of reflexes, they were sacrificed by decapitation. In order to have access to the brain, the skull was exposed by cutting the skin at the top of the head and then the brain was carefully removed and placed in ice-cold artificial cerebrospinal fluid (aCSF – Krebs' solution) containing: 124 mM NaCl; 3 mM KCl; 1.25 mM NaH_2PO_4, 26 mM $NaHCO_3$, 1 mM $MgSO_4$, 2 mM $CaCl_2$ and 10 mM glucose previously gassed with 95% O_2 and 5% CO_2, pH 7.4. The two brain hemispheres were separated through the midline and the hippocampus was isolated, taking care not to damage it with the spatulas. When isolated, the hippocampus was cut perpendicularly to the long axis into slices with 400 µm thickness with the McIlwain tissue chopper. Slices were then placed in a resting chamber in Krebs' solution permanently oxygenated at room temperature for one hour in order to recover.

Basal synaptic transmission

After functional and energetic recovery, slices were transferred to the recording chamber for submerged slices, being continuously superfused with bathing solution (Krebs' solution) gassed with 95% O_2 and 5% CO_2 at 32˚C. The flux of bathing solution was established at 3ml/min and the drugs used were added to this superfusion solution.

Recordings were obtained with Axoclamp 2B amplifier and digitized (Axon Instruments, Foster City, CA). Individual responses were monitored and averages of eight consecutive responses were continuously store on personal computer with *LTP program* (Anderson and Collingridge, 2001). Field excitatory post-synaptic potentials (fEPSPs) were recorded through an extracellular microelectrode (2-8 MW resistance, Harvard apparatus LTD, Fircroft way, Edenbridge, Kent) placed in the *stratum radiatum* of the CA1 area (*Figure 3.4* ***a)***). Stimulation (rectangular 0.1 ms pulses, once every 15 seconds) was delivered through a concentric electrode placed on the Schaffer collateral-commissural fibers, in the *stratum radiatum* near CA3-CA1 border. The stimulus intensity (80-200 µA) was initially adjusted to obtain a large fEPSP with a minimum population spike contamination (*Figure 3.4* ***b)***).

Alteration on synaptic transmission was evaluated as the % change in the average slope of the fEPSP in relation to the average slope of the fEPSP measured during the 10 minutes preceded the addiction of the drugs used in the experiment (baseline), as previously described (Diógenes et al., 2004).

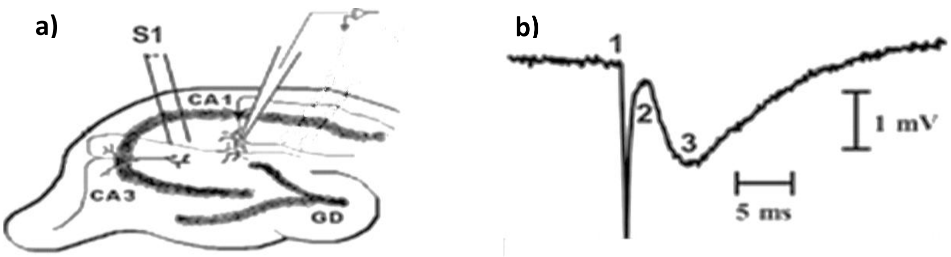

Figure 3.2 - **Extracellular recording from hippocampal slices. a)** Represents the stimulation of one set of the Shaffer collateral-commissural pathway (S1) in a hippocampal slice to record extracellular responses in the CA1 dendritic layer (*stratum radiatum*). **b)** Representative tracing obtained, composed by **1 -** stimulus artefact, followed by **2 -** presynaptic volley and **3 –** the field excitatory postsynaptic potentials (fEPSP) (adapted from Diógenes et al. 2011).

Pharmacological tools

Table 3-9 – **Drugs used in electrophysiology.**

Abbreviation	Designation	Function	Used Concentration	Supplier
DPCPX	1,3-Dipropyl-8-cyclopentylxanthine	A_1R selective antagonist	50 nM	Tocris (Natick, MA, USA)
ITU	5-iodotubercidin	ADK inhibitor	100 nM	Sigma (St. Louis, MO, USA)

Note: All drugs mentioned were aliquoted as stock solutions of 5mM (DPCPX) and 50 mM (ITU) and stored at -20ºC.

3.5 Data analysis

The values are presented in mean ± SEM of *n* number of independent experiments. Statistical significance was evaluated using non-paired Student's t-test. A *p-value*<0.05 represents differences that are statistically significant. *Prism GraphPad* software was used for statistical analysis.

4. Results

4.1 Characterization of adenosine receptors in *Mecp2 KO* mice model

This thesis was developed within a broader project that includes one PhD student (Sofia Duarte, co-supervisor of the present study) and another Master student (Cátia Palminha). Therefore, and for the sake of clarity, some of the here presented results were obtained by the above mentioned students and are clearly acknowledged throughout the thesis.

4.1.1 Rational

As described in section 1.3.3 of this manuscript, adenosine receptors alterations have already been reported in multiple disorders, some of them sharing common features with RTT. However, the adenosinergic system has never been explored in RTT. Then, our lab started to investigate this topic in order to understand whether changes in adenosinergic system, in RTT, could contribute to RTT pathophysiology.

Results obtained by Cátia Palminha (Palminha, 2014) suggest that hippocampal adenosine levels might be decreased in *Mecp2 KO* mice when compared with *WT* mice. Extracellular adenosine levels were studied by evaluating indirectly the disinhibition of synaptic transmission, caused by the selective A_1R antagonist, DPCPX (*Figure 4.1* ***a)*** adapted from Palminha, 2014). Hippocampal slices from *Mecp2 KO* mice showed a smaller disinhibition caused by DPCPX, which probably indicates that *Mecp2 KO* mice have lower levels of endogenous adenosine or decreased levels of $A_{1A}R$. To corroborate this hypothesis, synaptic transmission was also studied with de A_1R agonist, CPA. CPA causes a lower inhibitory effect upon synaptic transmission when endogenous levels of adenosine are higher or when $A_{1A}R$ levels are decreased. Testing progressively higher CPA concentrations, the inhibitory effect was significantly more pronounced in hippocampal slices taken from *Mecp2 KO* mice, indicating the possibility of the presence of lower levels of endogenous adenosine or/and higher levels of $A_{1A}R$ levels (*Figure 4.1* ***b)*** adapted from Palminha, 2014). Taken together, these data strongly suggest an impairment on endogenous levels of adenosine. As a consequence, inefficient activation of both $A_{2A}R$ and

A_1R might occur. Given the important role of $A_{2A}R$ on BDNF levels (Tebano et al., 2008) and on its synaptic activity (Fontinha et al., 2008; Diógenes et al., 2004) an impairment of endogenous $A_{2A}R$ activations could drastically compromise BDNF mediated signalling. Furthermore, impairment of the inhibitory A_1R activation could promote excitability (epilepsy).

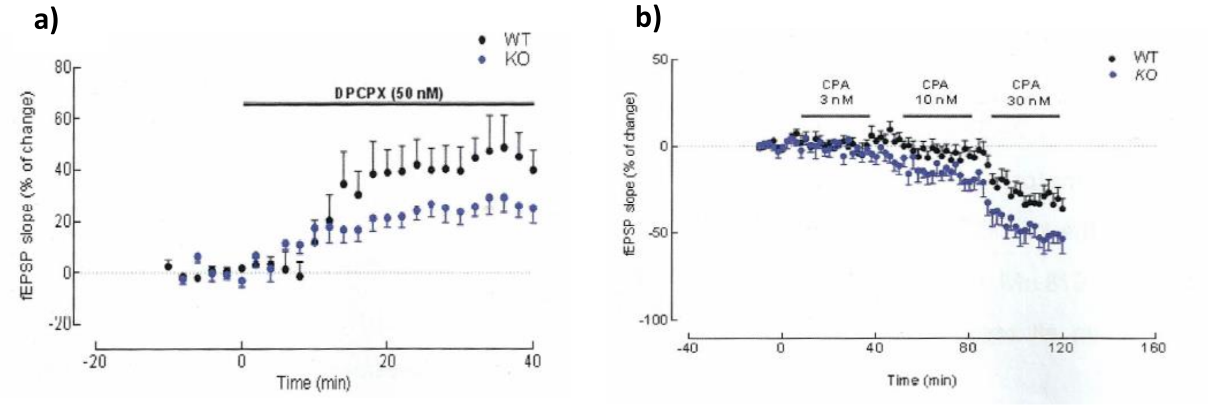

Figure 4.1 - **Changes in fEPSP induced by DPCPX and CPA**. **a)** averaged time course of changes in fEPSPs slope induced by application of DPCPX (50 nM) for 40 minutes and **b)** averaged time course of changes in fEPSP slope induced by application of three different concentrations of CPA (3 nM, 10 nM and 30 nM) for 120 minutes. *WT* (black symbols, n=4;7) and *Mecp2 KO* (blue symbols, n=8;7). The ordinates represent normalised fEPSP slopes, where 0% corresponds to the average slopes recorded 10 minutes before DPCPX/CPA application and the abscissa represents recording time in minutes. Adapted from Cátia Palminha master thesis (Palminha, 2014).

Moreover, changes in adenosine receptors were also detected. Binding protein assays showed increased A_1R protein expression level in *Mecp2 KO* mice when compared to *WT* animals (*Figure 4.2*, adapted from (Palminha, 2014)). Therefore, the following experiments were designed to further characterize the adenosinergic system in RTT.

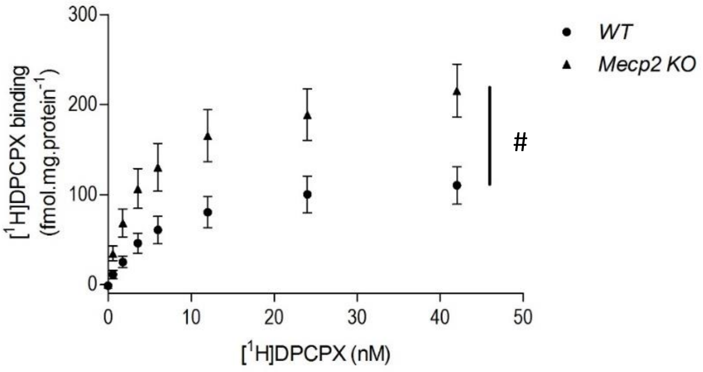

Figure 4.2 - **A_1R protein expression level in *Mecp2 KO* mice**. Graphic shows saturation isotherms for the binding of the selective A_1R receptor antagonist $[H^3]$DPCPX to the cortical homogenates of *WT* (circles, n=5) and *Mecp2 KO* (triangles, n=5) mice. Values are presented in mean ± SEM. # *p-value*<0.05 (F test) (Binding assays were performed and described in Cátia Palminha master thesis (Palminha, 2014)).

4.1.2 Adenosine receptors changes in *Mecp2 KO* mice

To better understand how the adenosinergic system was altered in the RTT animal model, the cortical *A_1R* and *$A_{2A}R$* mRNA expression and protein levels were evaluated.

As seen in *Figure 4.3*, *A_1R* mRNA relative expression showed no statistically significant difference between both genotypes (*WT*: 0.030 ± 0.0036, n=5 and *Mecp2 KO:* 0.025 ± 0.0040, n=5).

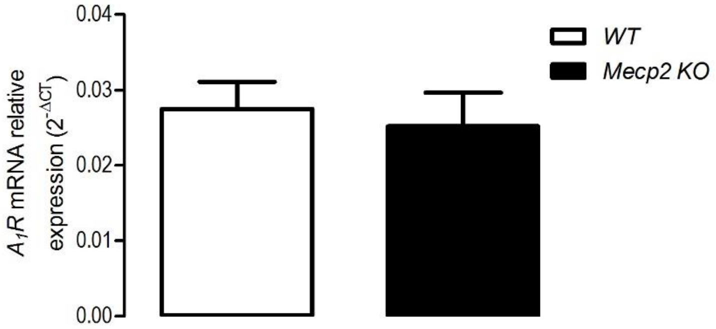

Figure 4.3 - ***A_1R* mRNA relative expression in *Mecp2 KO* mice**. *A_1R* mRNA expression level evaluated by qPCR in cortical samples of *WT* (white bars, n=5) and *Mecp2 KO* (black bars, n=5). *PPIA* and *RPL13A* were used as internal controls. Values are mean ± SEM.

In parallel, the analysis of *$A_{2A}R$* mRNA relative expression also revealed no statistically significant differences (*Figure 4.4* ***a)***) between genotypes (*Mecp2 KO*: 0.030 ± 0.005, n=5 and *WT*: 0.020 ± 0.006, n=5). Interestingly, Western-Blot analysis of cortical homogenates shows a significant decrease (*Figure 4.4* ***b);*** *p-value*<0.05) of $A_{2A}R$ protein expression level in cortical samples from *Mecp2 KO* mice (37.52% ± 11.30, n=6) when compared to *WT* (100% ± 24.80, n=6).

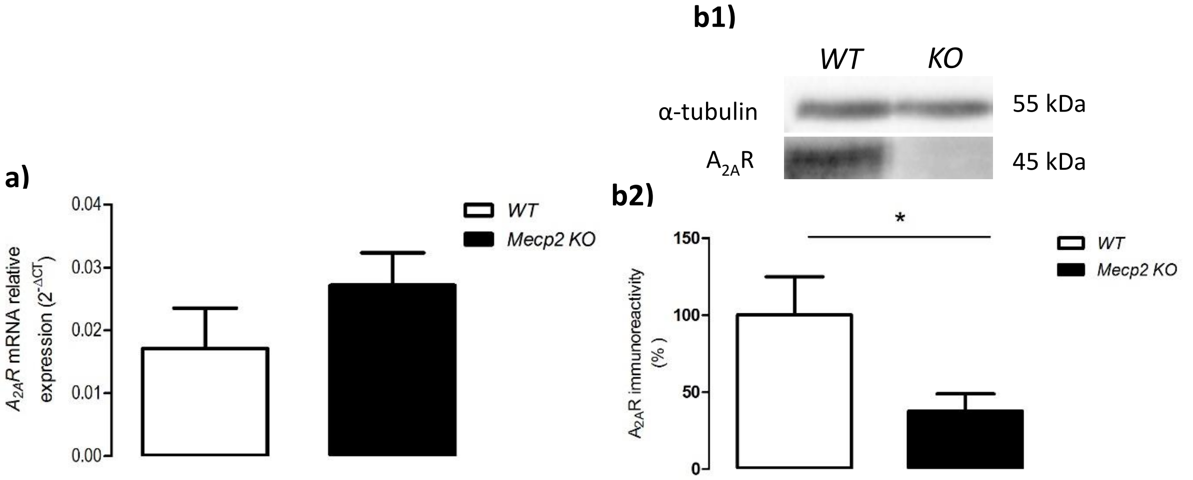

Figure 4.4 - ***$A_{2A}R$*** **mRNA relative expression and protein expression level in** ***Mecp2 KO*** **mice***.* **a)** Relative qPCR data showing *$A_{2A}R$* mRNA relative expression in cortical samples of *WT* (white bars, n=5) and *Mecp2 KO* (black bars, n=5). *PPIA* and *RPL13A* were used as internal controls. **b1)** representative Western-Blot of *WT* and *Mecp2 KO* mice, using primary antibody against $A_{2A}R$ (~45 kDa) and α-tubulin (~55 kDa), used as loading control. These bands were detected from cortical homogenates of *WT* (white bars, n=6) and *Mecp2 KO* (black bars, n=6) mice. **b2)** Quantification of $A_{2A}R$ immunoreactivity obtained by Western-Blot analysis. Immunoreactivity for *WT* was taken as 100% (baseline). All values presented are mean ± SEM; **p-value*<0.05 (Student's t-test).

4.1.3 Adenosine kinase as a possible cause of adenosine impairment in *Mecp2 KO* mice

4.1.3.1 ADK evaluation

As already mentioned in section 1.3.1, together with ADA, ADK is responsible for the degradation of adenosine in order to maintain its endogenous concentration within homeostatic levels (Boison, 2013). Changes in this enzyme have already been associated to multiple disorders, such as epilepsy (Gouder et al., 2004; Boison, 2012; Boison, 2013; Aronica et al., 2013). In particular, ADK levels are increased in epileptic mouse models and also in the human epileptic brain (Aronica et al., 2013), which leads to lower endogenous adenosine level and consequently a lower inhibition of synaptic transmission (Boison, 2013). Previous data from the lab points to a decrease of endogenous adenosine level in RTT mice model (Palminha, 2014), thus the possibility that changes in ADK could be involved was raised. Therefore, ADK protein expression level was evaluated by Western-Blot, and as shown in *Figure 4.5,* there was no significant differences between *Mecp2 KO* (121.5% ± 10.13, n=8) and *WT* (100.2 %± 3.611 n=8) mice.

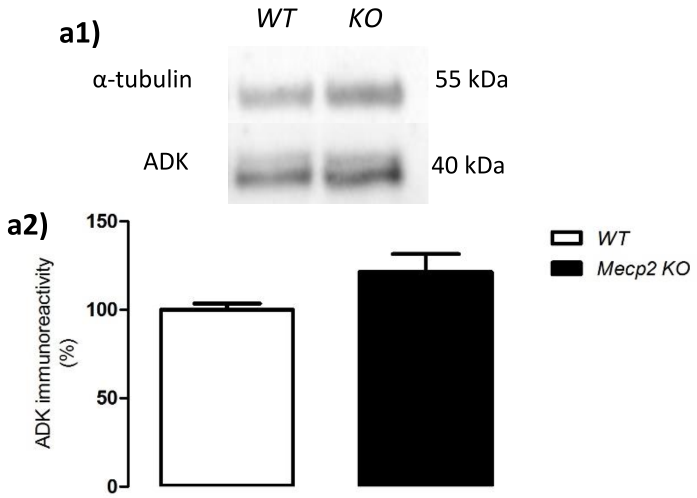

Figure 4.5 - **ADK protein expression level in *Mecp2 KO* mice**. **a1)** Representative Western-Blot of cortical tissue homogenates from *Mecp2 KO* and *WT* mice. Primary antibodies used recognize ADK isoforms (~40 kDa) and α-tubulin (~55 kDa), used as loading control. **a2)** average band intensity for ADK obtained from *WT* (white bars, n=8) and *Mecp2 KO* (black bars, n=8) cortical homogenates by Western-Blot analysis. All values presented are mean ± SEM, and are represented in % of *WT* protein (100%).

Although no significant alterations in ADK protein expression level have been detected, the evaluation of ADK function was considered to be a critical aspect to take into account.

Therefore, ADK function was, indirectly, evaluated by studying the effect of the ADK inhibitor, iodotubercidin (ITU) (Pak et al., 1994) upon synaptic transmission. ITU, by blocking ADK activity, increases adenosine levels promoting inhibition of synaptic transmission through A_1R activation. Therefore, the higher the activity of ADK, the lower the level of adenosine and as a consequence the higher the inhibition of synaptic transmission induced by ITU. Thus, if a higher activity of ADK was the cause of the reduced adenosine level in RTT, the ITU should induce a higher inhibition of synaptic transmission in hippocampal slices taken from *Mecp2 KO* mice. However this might not be the case. Hippocampal slices were superfused by Krebs' solution containing ITU (100 nM) by 84 minutes as described before (Diógenes et al. 2004). As shown in *Figure 4.6*, ITU caused a similar decrease on synaptic transmission in hippocampal slices from the two genotypes (*WT*: approximately 48% inhibition, n=7; *Mecp2 KO*: approx. 38% inhibition, n=2). Interestingly, the superfusion of the same slices with the selective $A_{1A}R$ antagonist, DPCPX (50 nM), caused a more pronounced disinhibition of synaptic transmission in hippocampal slices taken from *WT* animals (*WT*: approx. 50% desinhibition, n=7; *Mecp2 KO*: approx. 10% desinhibition, n=2). Although it is indispensable to increase the number of experiments, this data corroborate the hypothesis that endogenous adenosine level might indeed be decreased in RTT.

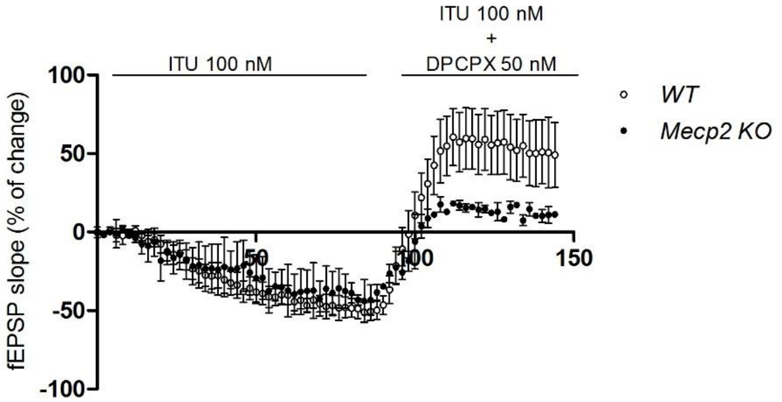

Figure 4.6 - **fEPSP changes induced by ITU and ITU+DPCPX**. Graphic shows the averaged time course of changes in fEPSP slope induced by ITU (100 nM) applied for 84 minutes followed by ITU (100 nM) + DPCPX (50 nM) for 60 minutes. Hippocampal slices were taken from *WT* (white circle, n=7) and *Mecp2 KO* mice (black circle, n=2). Ordinate axis represents normalised fEPSP slopes, where 0% corresponds to the averaged slopes 10 minutes before ITU application. Abscissa axis represents time.

4.2 BDNF signalling impairment in *Mecp2 KO* mice

4.2.1 Rational

BDNF, through TrkB-FL receptor activation, regulates neuronal survival, differentiation and synaptic plasticity (Huang and Reichardt, 2003) such as LTP, the neurophysiological basis for learning and memory (Bliss and Collingridge, 1993). It has been postulated that BDNF level is decreased in RTT (reviewed by Li and Pozzo-Miller, 2014) however less attention has been given to TrkB receptors. Recently, data from our lab (Duarte, 2015 in preparation) clearly demonstrated that the well-known facilitatory effect of exogenous BDNF upon hippocampal LTP is completely lost in hippocampal slices taken from *Mecp2 KO*. This data strongly suggest that together with the lower endogenous BDNF level, also the BDNF receptors could be affected. Indeed, recent data clearly show a significant decrease on TrkB-FL receptors in the hippocampus of *Mecp2 KO* when compared to *WT* animals (*Figure 4.7* **a)**, Duarte, 2015 in preparation). No significant alterations were detected in TrkB-Tc receptor level (*Figure 4.7* **b)**, Duarte, 2015 in preparation).

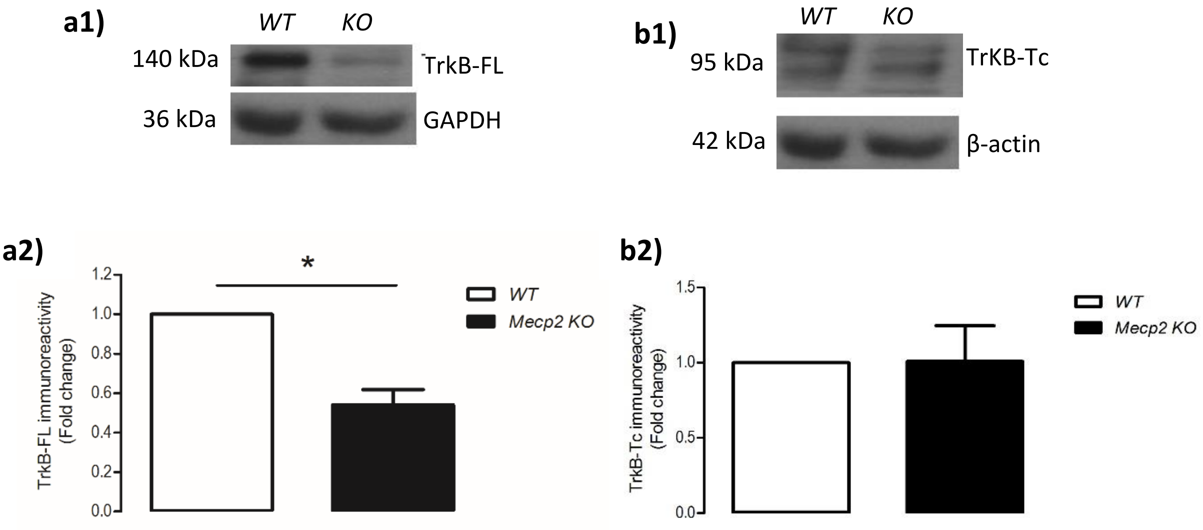

Figure 4.7 - **TrkB-FL and TrkB-Tc protein expression level in *Mecp2 KO* mice**. **a1)** Representative Western-Blot of cortical tissue homogenates from *Mecp2 KO* and *WT* mice. Primary antibodies used recognize TrkB-FL (~140 kDa) and GAPDH (~36kDa), used as loading control. **a2)** average band intensity for TrkB-FL obtained from *WT* (white bars, n=10) and *Mecp2 KO* (black bars, n=8) cortical homogenates by Western-Blot. Values obtained for *WT* samples in Western-Blot are considered as 1. All values presented are mean ± SEM. *p-*value*<0.05 (Student's t-test). **b1)** Representative Western-Blot of cortical tissue homogenates from *Mecp2 KO* and *WT* mice. Primary antibodies used recognize TrkB-Tc (~95 kDa) and β-actin (~42kDa), used as loading control. **b2)** average band intensity of TrkB-Tc obtained from *WT* (white bars, n=10) and *Mecp2 KO* (black bars, n=8) cortical homogenates by Western-Blot analysis. Values obtained for *WT* samples in Western-Blot are considered as 1. All values presented are mean ± SEM. (Duarte, 2015 in preparation).

In order to provide more detailed information about BDNF signalling, this chapter was devoted to the evaluation of *TrkB* mRNA expression and to the determination of BDNF protein expression level in this RTT animal model. Regarding to *TrkB* mRNA expression evaluation, only *TrkB-T1* truncated isoform was studied, once this truncated isoform is the most abundant and well characterized in human/mice brain.

4.2.2 BDNF protein expression level in *Mecp2 KO* mice

BDNF protein expression level was evaluated as described in methods section by ELISA assays. As expected, the results reveal a significant decrease (*p-value*<0.05) in BDNF protein expression level in homogenates prepared from *Mecp2 KO* mice cortex when compared to samples from *WT* animals (*Mecp2 KO*: 0.491 pg/mg ± 0.167, n=3; WT: 2.237 pg/mg ± 0.385, n=4; *Figure 4.8*).

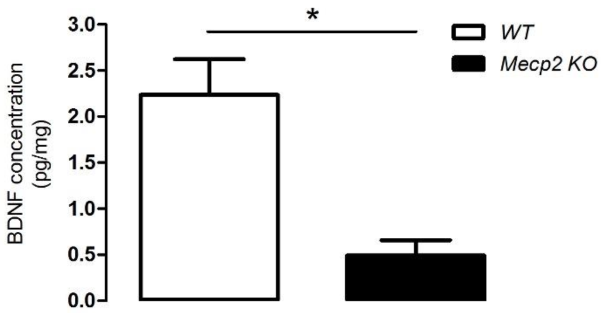

Figure 4.8 - **BDNF concentration in *Mecp2 KO* mice**. BDNF concentration (pg/mg), evaluated by ELISA assay, in cortical homogenates from *WT* (white bars, n=4) and *Mecp2 KO* (black bars, n=3) mice. All values are presented as mean ± SEM. **p-value* < 0.05 (Student's t-test).

4.2.3 TrkB receptors characterization in *Mecp2 KO* mice

Both *TrkB-FL* and *TrkB-T1 mRNA* relative expression were analysed by qPCR as described in the methods section. As shown in *Figure 4.9* ***a)*** there are no significant differences between *WT* (0.123 ± 0.026, n=5) and *Mecp2 KO* mice (0.180 ± 0.033, n=5). Regarding *TrkB-T1* mRNA expression, no significant changes were detected between *Mecp2 KO* (0.222 ± 0.026, n=5) and *WT* mice (0.178 ± 0.026, n=5) (*Figure 4.9* ***b)***).

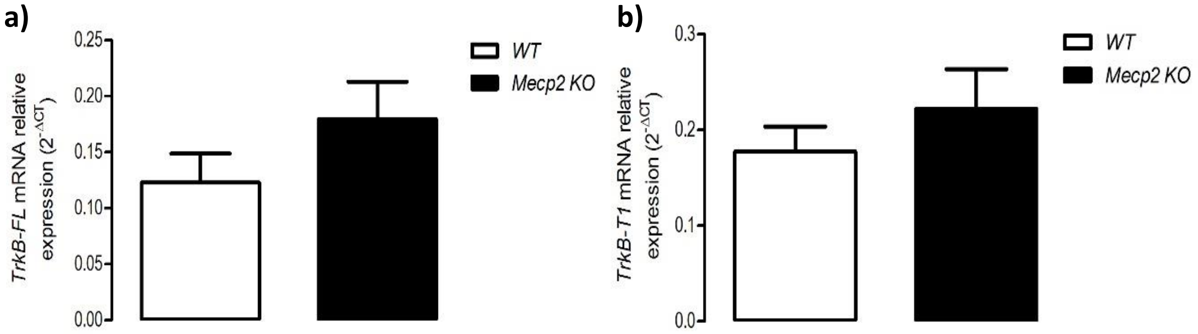

Figure 4.9 - ***TrkB-FL* and *TrkB-T1* mRNA relative expression in *Mecp2 KO* mice**. TrkB-FL (**a**)) and TrkB-T1 (**b)**) mRNA expression level evaluated by qPCR in cortical samples of *WT* (white bars, n=5) and *Mecp2 KO* (black bars, n=5). *PPIA* and *RPL13A* were used as internal loading controls. All values presented are mean ± SEM.

4.3 Exploring adenosinergic system through neurons-derived from hIPSCs and in human brain sample

4.3.1 Rational

Mouse models are widely chosen to study RTT, in particular *Mecp2 KO* mice. Like any model, it has benefits but also some limitations (discussed in section 1.2). Therefore, it is important to study more than one model to increase the likelihood of finding something relevant. Neurons-derived from hIPSCs have been recently used to model diseases, and offer the opportunity to compare, "*in vitro*", neurons-derived from RTT patients and healthy controls.

In this chapter, mRNA expression of adenosine receptors, BDNF and TrkB receptors will be studied and were quantified in neurons-derived from hIPSCs and in human brain sample. Protein expression level of TrkB receptors and BDNF will be also studied and were quantified only in neurons-derived from hIPSCs.

4.3.2 Characterization of hIPSCs

One crucial aspect that must be considered before using *in vitro* differentiated cortical neurons is to validate their identity. IPSCs are multipotent and able to differentiate into any of the 3 embryonic lineages: endoderm, mesoderm and ectoderm. Although, the dual SMAD inhibition protocol is quite efficient in directing cells along the neuroectoderm differentiation cascade, while inhibiting endodermal and mesodermal lineages, we have still to guarantee that the generated neuroprogenitors have anterior identity. Throughout neuronal differentiation several well-characterized stages can be identified by the expression of a set of proteins (Table 4-1). Immunofluorescence of these cell-type specific markers was performed at days 12, 20, 30 and 120 of neuronal differentiation (*Figure 4.10*).

Table 4-1 - **Neuronal markers used to characterize hIPSCs**. (Shi et al., 2012; Adams et al., 2007; Molyneaux et al., 2007; Thompson et al., 2005).

Marker	Expression	Description
OCT3/4	Pluripotent stem cells	Belongs to the core pluripotency network responsible for maintaining self-renewal and undifferentiated embryonic stem cells.
SOX2	Neuronal stem cells and neuronal progenitors	Expressed by developing cells from the neural tube and in neural progenitors in the CNS, being inactivated upon terminal differentiation.
PAX6	Neuronal stem cells and neuronal progenitors	Expressed in human neuroectoderm cells. Key role in the onset of human neuroectoderm differentiation into any region-specific neural progenitors.
OTX2	Neuronal Stem cells and neuronal progenitors	Expressed throughout the forebrain and midbrain, being an excellent marker of anterior specification.
FOXG1	Neuronal progenitors	Expressed only in the anterior neuroectoderm.
ZO1	Neuronal progenitors	Abundant in endothelial cells and the highly specialized epithelial junctions.
Nestin	Neuronal progenitors and early neurons	Intermediate filament protein type VI, expressed in neuronal progenitors.
GFAP	Astrocytes	Intermediate filament protein expressed in astrocytes.
TUJ1	Postmitotic neurons and differentiated neurons	Belong to the tubulin protein family and is exclusively expressed in neurons.
TBR1	Early neurons and deep-layer neurons	Regulates cortical development, specifically within layer VI of the human cortex.
TBR2	Early neurons	Expressed in basal neural progenitors.
BRN2	Progenitor cells and deep-layer neurons	Marker of human cortical layer II/III and V.
CTIP2	Deep-layer neurons	Expressed in deep-layer neurons with higher expression levels in subcerebral neurons of layer V.
MAP2	Early neurons and differentiated neurons	Belongs to the tubulin protein family and is exclusively expressed in neurons.
SNAP25	Presynaptic density	SNAP-25 is a component of the trans-SNARE complex, responsible for forming a tight complex that brings the synaptic vesicle and plasma membranes together.
VGAT	GABAergic neurons	Integral membrane protein involved in gamma-aminobutyric acid (GABA) and glycine uptake into synaptic vesicles.
VGLUT	Glutamatergic neurons	Responsible for the uptake of the excitatory amino acid, L-glutamate, into synaptic vesicles.

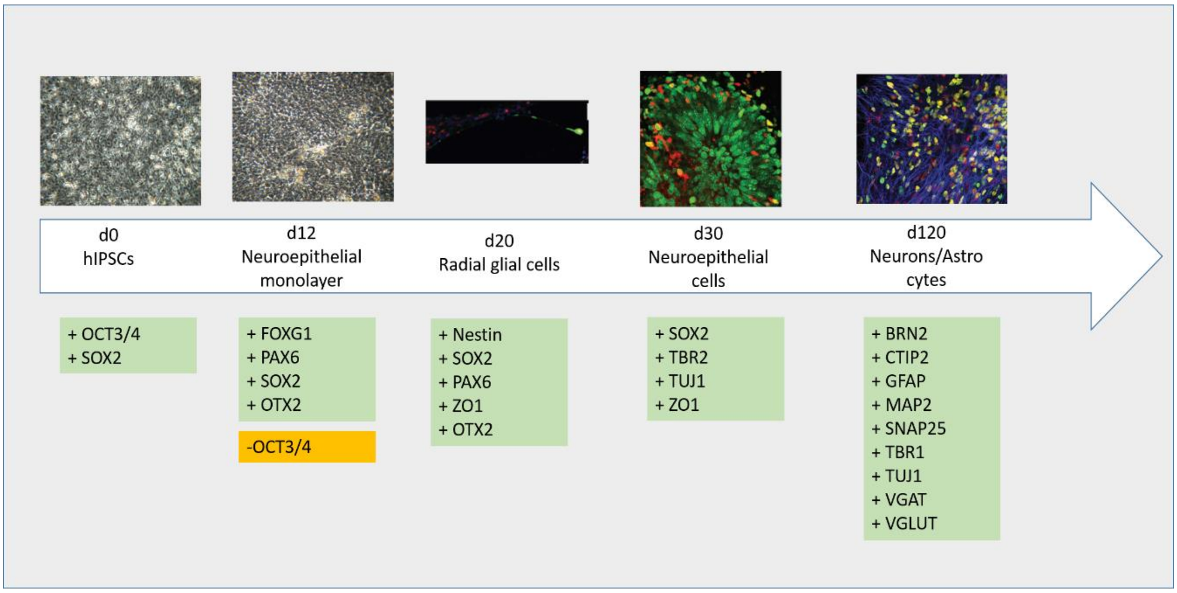
d0
hIPSCs
d12
Neuroepithelial monolayer
d20
Radial glial cells
d30
Neuroepithelial cells
d120
Neurons/Astro cytes
+ OCT3/4
+ SOX2
+ FOXG1
+ PAX6
+ SOX2
+ OTX2
-OCT3/4
+ Nestin
+ SOX2
+ PAX6
+ ZO1
+ OTX2
+ SOX2
+ TBR2
+ TUJ1
+ ZO1
+ BRN2
+ CTIP2
+ GFAP
+ MAP2
+ SNAP25
+ TBR1
+ TUJ1
+ VGAT
+ VGLUT

Figure 4.10 - **Stages of neuronal differentiation and cell type specific markers**. Represented in the arrow are the 5 main differentiation stages: **d0** – hIPSCs; **d12** – Neuroepithelial monolayer; **d20** – Radial glial cells; **d30** – Neuroepithelial cells and **d120** – Neurons and astrocytes. Cell type specific markers are depicted by their expression (green boxes) or absence (orange box) at a given step of neuronal differentiation. Images representing each stage were published in (Shi et al., 2012).

As expected, OCT3/4, expression is not detected at day 12 indicating that all cells have been able to exit into differentiation and have stopped expressing this pluripotency marker. Across the well highlands of PAX6 expressing cells, neuroprogenitors, were observed and anterior identity was verified using two distinct cell markers: OTX2 and FOXG1. In all cell lines, clusters of cells expressing PAX6 were highly abundant as well as OTX2 and FOXG1. No differences could be observed between the control and mutant cell lines demonstrating that induction of neuronal differentiation is not affected in *MECP2*-mutant cells. On day 20, the presence of PAX6-expressing cells was much lower, since it is a primary progenitor cell marker while the expression of Nestin is already present and becomes even more abundant at day 30. The appearance of neuronal rosettes was identified by the combination of SOX2 and ZO1. The neuroepithelial cells (SOX2+) were radially arranged and showed signs of polarization with apical ZO1 expression. Although, we could observe similar proportions of rosette formation for all cell lines, their appearance was variable ranging from d12 to d17. At day 30, substantial maturation of neuronal progenitors was observed, as shown by the appearance of TUJ1-expressing cells already displaying an intricate network of axonal projections, and TBR2-expressing cells, revealing the presence of cortical neuronal progenitors (*Figure 4.11*).

At the end of the differentiation process (*Figure 4.12*) neuronal maturation and glial differentiation were evaluated. A large number of GFAP-positive astrocytes could be seen interspersed with TUJ1-positive neurons and the same results were observed with MAP2. Layer-specific cortical markers, CTIP2, BRN2 and TBR1, were widely present in all cell lines further confirming the efficiency and specificity of the differentiation. Neuronal maturation was evaluated using antibodies against proteins involved in the transmission and regulations of the electrical impulse. The vast majority of neurons were SNAP25-positive indicating the formation of pre-synaptic complexes. Although the dual SMAD inhibition protocol aims at the production of glutamatergic neurons, observed by VGLUT staining, the appearance of some GABAergic neurons is still a reality. Immunofluorescence using VGAT allowed the identification of very few cells positive for this marker.

Immunofluorescence analysis of cell-type specific markers provides valuable information however, quantification is often difficult and cumbersome. In this regard mRNA quantification by real-time PCR (RT-PCR) using the same cell-type specific markers allowed a better characterization of the final cellular composition for each cell line. The differentiation process leads to the production of not only neurons but also glia, therefore we analysed the mRNA expression of *GFAP* and *MAP2* to find the ratio between neuronal and glial production. If the ratio of two cell types is variable between the different cell lines this could mask potentially relevant results, especially those involving proteins expressed in just one of the cell populations. Therefore, this step is important not to compromise further analysis. However, once all proteins studied (except SNAP25) are expressed in both cell populations, normalization was performed to a ubiquitously expressed transcript *GAPDH*. High variability was observed in the expression of *GFAP* and *MAP2* (*Figure 4.13* ***a)***). We, also analysed mRNA expression of late markers such as *VGAT* and *SNAP25* (*Figure 4.13* ***b)***). *VGAT* expression is very low, in agreement with the results obtained with the low abundance of VGAT-positive cells by Immunofluorescence. *SNAP25* has higher expression, indicating, indirectly, the presence of glutamatergic mature neurons, as expected.

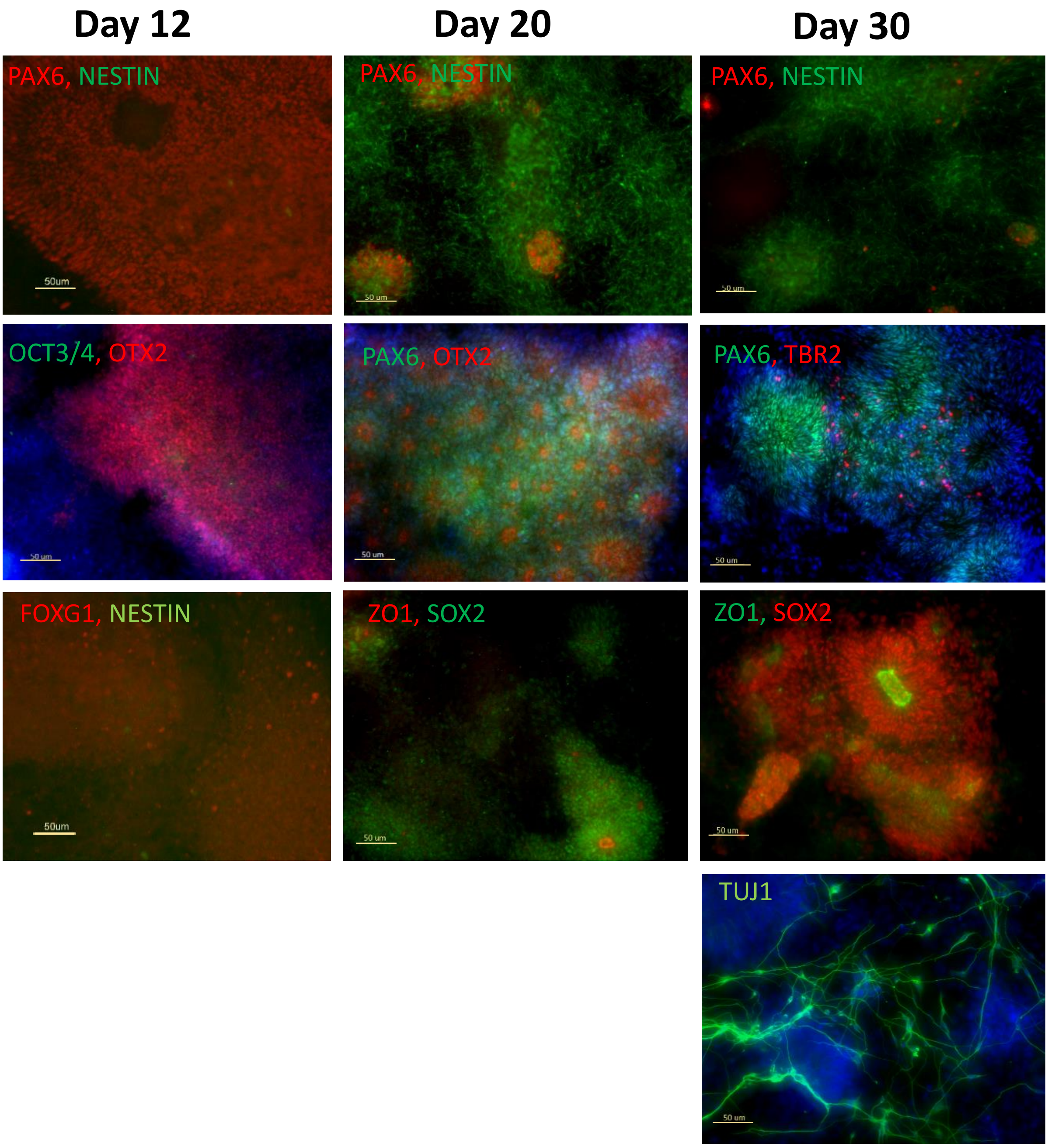
Day 12
Day 20
Day 30
PAX6, NESTIN
PAX6, NESTIN
PAX6, NESTIN
OCT3/4, OTX2
PAX6, OTX2
PAX6, TBR2
FOXG1, NESTIN
ZO1, SOX2
ZO1, SOX2
TUJ1
50um
50 um

Figure 4.11 - **Characterization of the first 3 stages of neuronal induction**. In left column, representative images of day 12 (d12) staining are shown, positive for OTX2, SOX2 and FOXG1. In the middle column, representative images for d20 are shown, with positive signal to SOX2, PAX6, Nestin and ZO1. Finally, in the right column are represented the markers for day 30, with positive signal for PAX6, Nestin, TUJ1, ZO1, SOX2, TBR2. Images were acquired by fluorescent microscopy, with 20x objective. Scale bars, 50 µm.

Day 120

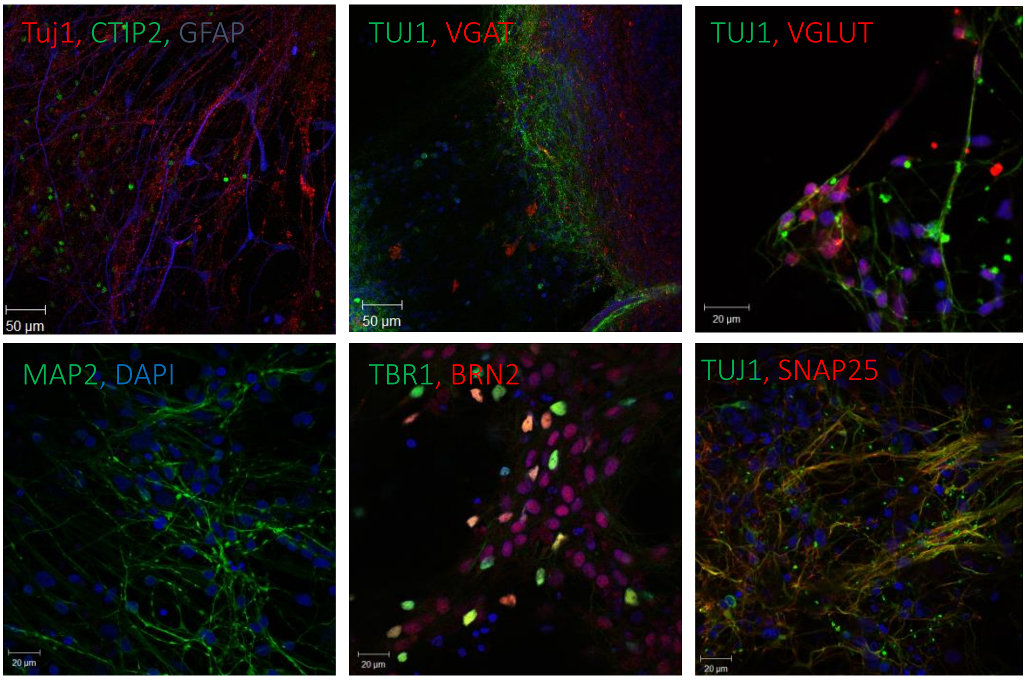
Tuj1, CTIP2, GFAP
50 µm
TUJ1, VGAT
50 µm
TUJ1, VGLUT
20 µm
MAP2, DAPI
20 µm
TBR1, BRN2
20 µm
TUJ1, SNAP25
20 µm

Figure 4.12 - **Characterization of final neuronal differentiation stage**. Representative images of day 120 (d120) staining are shown with positive signal for TUJ1, CTIP2, GFAP, VGAT, VGLUT, SNAP25, MAP2, TBR1 and BRN2. Images were acquired by confocal microscopy, with 20x objective. Scale bars, 20/50 µm.

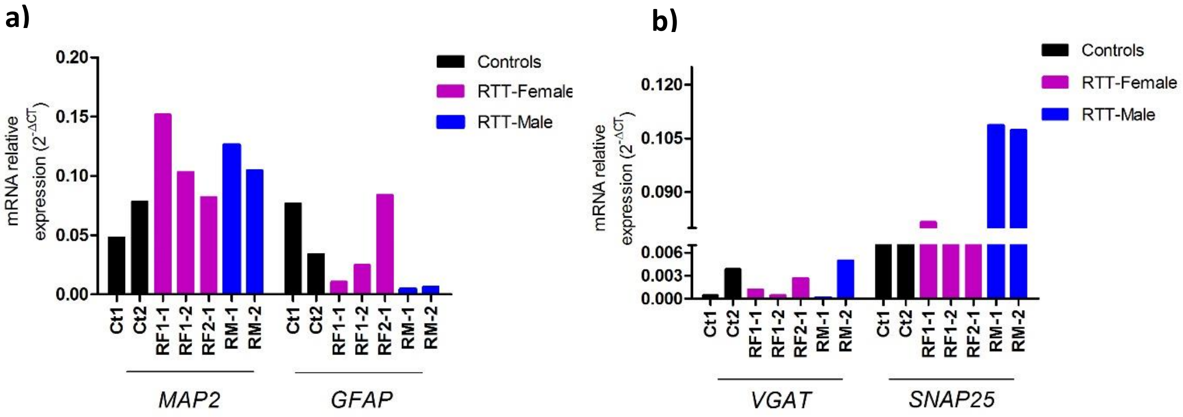

Figure 4.13 **Neuronal and glia-marker expression in cells derived from hIPSCs**. **a)** Histogram shows relative expression obtained by qPCR showing mRNA levels of *MAP2*, a neuronal marker, and *GFAP*, a glial marker; **b)** for *VGAT* and *SNAP25*. *GAPDH* was used as internal loading control.

4.3.3 Adenosine receptors expression in hIPSCs and human brain sample

After the appropriate hIPSCs characterization, mRNA of adenosine receptors was evaluated. In addition, we had the opportunity to perform the same analysis using human patient material.

The results obtained from RTT female neurons show a tendency for an increase in *A_1R* mRNA (0.005 ± 0.001, n=3), when compared to control lines (0.003 ± 0.001, n=2) (*Figure 4.14* ***a1,2)***). However, given the striking degree of variability within each group and the reduced number of experiments (*n*), statistical analysis could not be performed. Surprisingly, even though the two control cell lines are of different gender, the variability between them is not high, suggesting that there are no gender specific differences. Interestingly, mRNA expression evaluated in a human temporal cortical sample obtained from a RTT patient showed higher *A_1R* mRNA expression levels as compared to an equivalent cortical area from a healthy control (*Figure 4.14* ***b)***). This is in accordance with the results obtained in i) cortical samples from the RTT mice model, which revealed increased levels of A_1R protein and in 2) neurons from RTT female-derived hIPSCs, which revealed a tendency for increased *A_1R* mRNA expression.

$A_{2A}R$ mRNA expression level in neurons-derived from hIPSCs revealed that lines RF1-1, RF2-1 and RM-2 (RTT lines) have a tendency for a higher expression levels than controls. However, these results present high variability depending on the differentiation round of the same cell line. In spite of that, there is a trend to have increased $A_{2A}R$ mRNA expression levels in RTT female lines (0.0003 ± 6.7e-005, n=3) when compared to the control group (0.0002 ± 1.1e-005, n=2) (*Figure 4.15* ***a1,2)***).

The analysis of the human brain tissue revealed the opposite pattern in line with the results obtained at the protein level in the mouse cortex (*Figure 4.15* ***b)***).

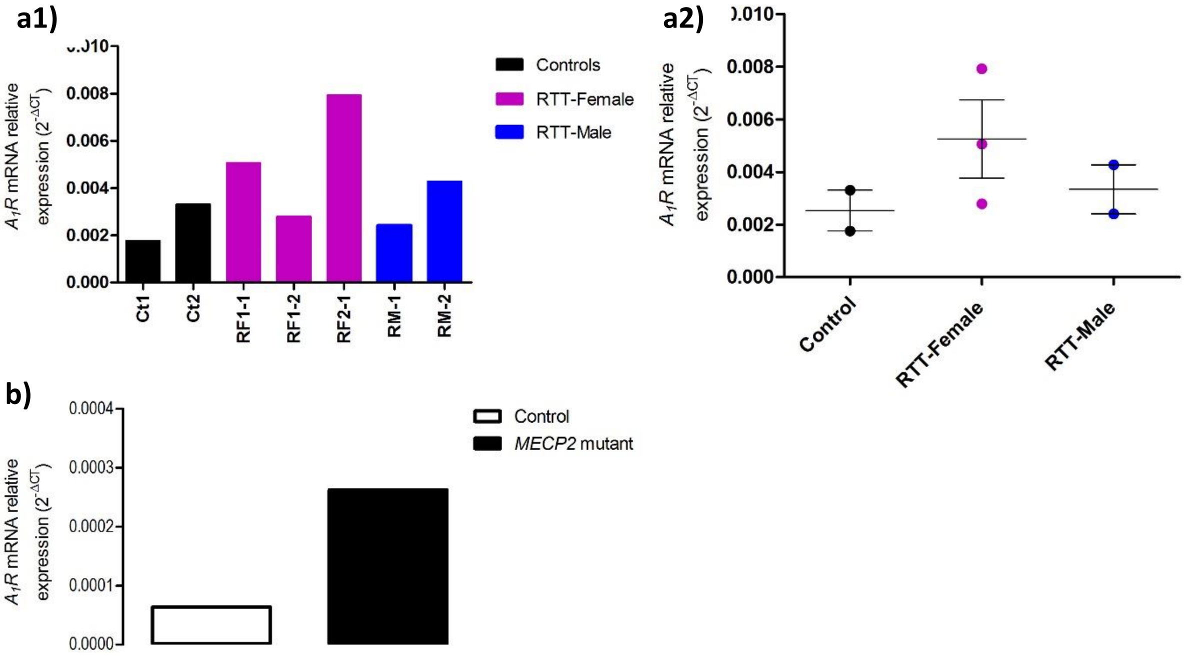

Figure 4.14 - ***A_1R* mRNA relative expression in neurons-derived from hIPSCs and in RTT human brain**. **a1)** *A_1R* mRNA relative expression for each cell line. *GAPDH* was used as internal loading control. **a2)** Grouped *A_1R* mRNA expression: controls (Ct1, Ct2; black); RTT-Female (RF1-1, RF1-2, RF2; purple) and RTT-Male (RM-1, RM-2; blue). Values are presented in mean ± SEM. **b)** *A_1R* relative expression in samples taken from healthy human temporal cortex (white bar) and RTT-female cortex (black bar).

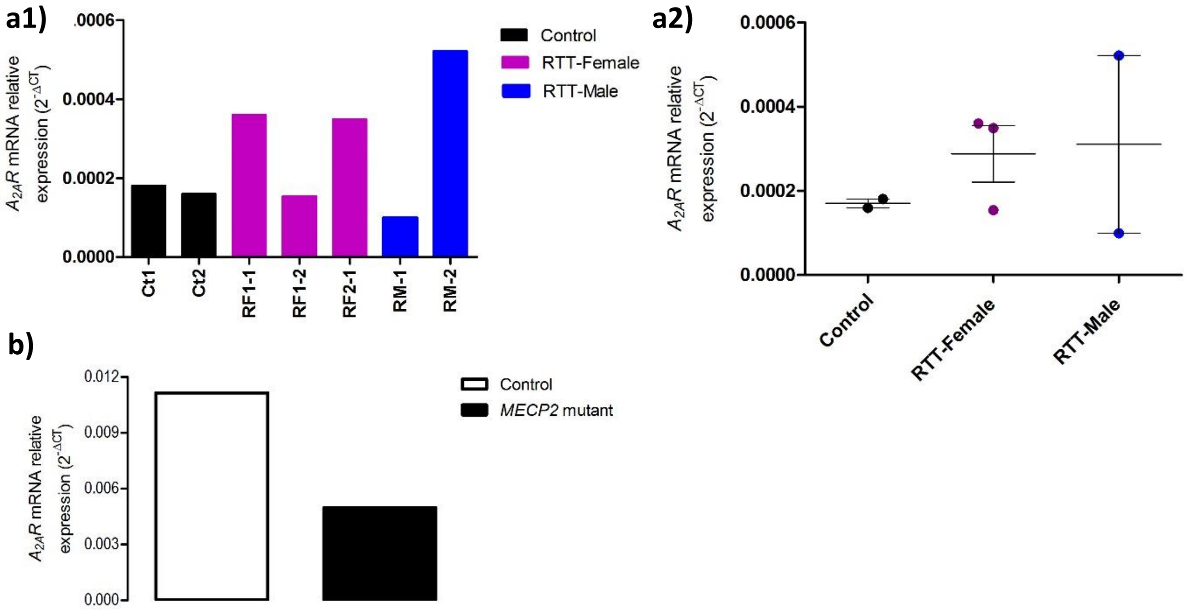

Figure 4.15 - **$A_{2A}R$ mRNA relative expression in neurons-derived from hIPSCs and in RTT human brain**. **a1)** $A_{2A}R$ mRNA relative expression for each cell line. *GAPDH* was used as internal loading control. **a2)** Grouped $A_{2A}R$ mRNA expression: controls (Ct1, Ct2; black); RTT-Female (RF1-1, RF1-2, RF2; purple) and RTT-Male (RM-1, RM-2; blue). Values are presented in mean ± SEM. **b)** $A_{2A}R$ relative expression in samples taken from healthy human temporal cortex (white bar) and RTT-female cortex (black bar).

In parallel, ADK protein expression level was also evaluated in neurons-derived from hIPSCs to explore if molecular changes in this enzyme could be related with adenosinergic changes in RTT as detailed before. Western-Blot analysis showed high variability in ADK immunoreactivity and therefore no inference can be made (*Figure 4.16 **a1,2)***). However, in *Mecp2 KO* mice, statistical analysis has already provided evidence for non-altered ADK levels in RTT model when compared to *WT*.

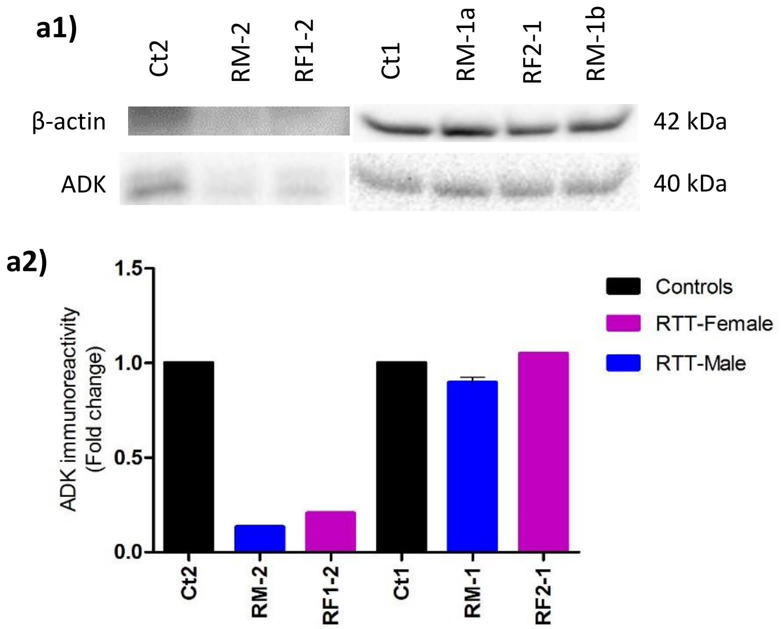

Figure 4.16 - **ADK protein expression level in neurons-derived from hIPSCs**. **a1)** Western-Blot analysis using primary antibodies recognizing ADK isoforms (~40 kDa) and β-actin (~42 kDa), used as loading control. **a2)** Immunoreactivity intensity of the ADK isoforms obtained in neuronal lines. Data were normalized to respective control (fold change). RM-1a and RM-1b are technical replicates.

4.3.4 BDNF signalling impairment

Protein levels of BDNF, TrkB-FL and TrkB-Tc receptors were evaluated in neurons-derived from IPSCs.

BDNF mRNA expression was quantified by qPCR as described in methods. Low BDNF mRNA expression level in both RTT-females (0.001 ± 0.001, n=3) and in the control group (0.003 ± 0.001, n=2) was detected. On the contrary, in the RTT-male lines there was higher expression of BDNF mRNA (0.102 ± 0.090, n=2) in both rounds of differentiation (*Figure 4.17* ***a1,2)***). Contrary to what was observed for mRNA quantification of other target genes, the variability within each group is much lower. In the human cortical sample, the *BDNF* mRNA expression is similar in both the patient and the control (*Figure 4.17* ***b)***). In conclusion, *BDNF* mRNA expression level might have a tendency to be increased in male RTT lines but not in female lines which show a small decrease.

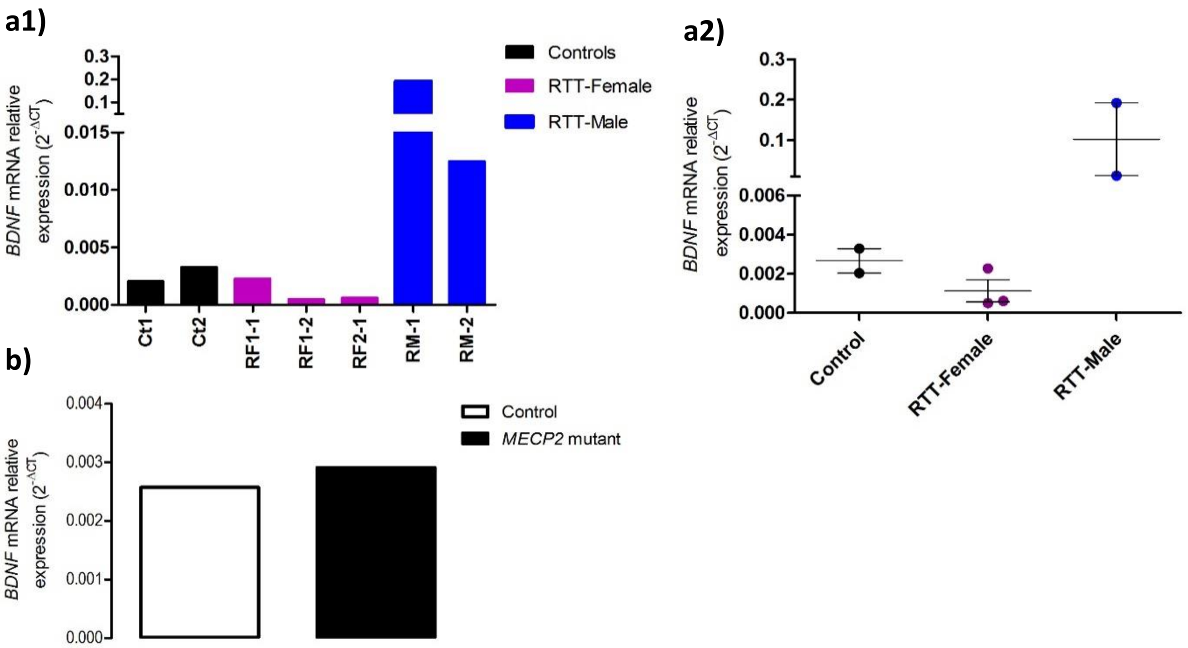

Figure 4.17 – ***BDNF* mRNA relative expression in neurons-derived from hIPSCs and in RTT human brain**. **a1)** *BDNF* mRNA relative expression for each cell line. *GAPDH* was used as internal loading control. **a2)** Grouped *BDNF* mRNA expression: controls (Ct1, Ct2; black); RTT-Female (RF1-1, RF1-2, RF2; purple) and RTT-Male (RM-1, RM-2; blue). Values are presented in mean ± SEM. **b)** *BDNF* relative expression in samples taken from healthy human temporal cortex (white bar) and RTT-female cortex (black bar).

BDNF protein expression level was also quantified using the ELISA assay in 3 lines: Ct2, RM-2 and RF1-2. As seen in *Figure 4.18*, BDNF protein expression level are increased in both female and male mutant lines, contradictory to what has been previously described for female line. The *BDNF* transcript level in RTT female lines shows a clear tendency to be downregulated when compared to the control group and furthermore, in *Mecp2 KO* mice BDNF protein expression level seem to be also downregulated.

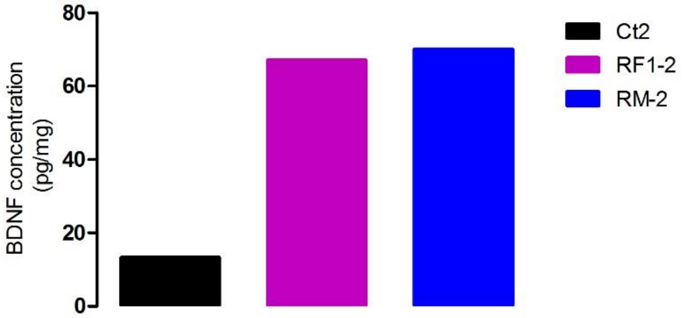

Figure 4.18 - **BDNF concentration in neurons-derived from hIPSCs**. BDNF concentration (pg/mg), evaluated by ELISA assay, in neurons-derived from three different lines: WT (blue), R1-2 (purple) and RM-2 (blue).

TrkB-FL mRNA expression analysis in neurons-derived from hIPSCs shows a tendency for lower expression in RTT lines with the exception of RF2-1 where a small increase is observed (*Figure 4.19* ***a1)***). Overall, there seems to be a slight tendency in RTT-females to have decreased expression of TrkB-FL (0.013 ± 0.003, n=3) when compared to the control samples (0.015 ± 0.001, n=2). No conclusion can be withdrawn from the RTT-male group since variability is too high (0.009 ± 0.005, n=3) (*Figure 4.19* ***a2)***). *TrkB-FL* mRNA expression in the temporal cortex of RTT patient shows a small increase when compared with the control (*Figure 4.19* ***b)***), in contradiction to what was observed in *Mecp2 KO.*

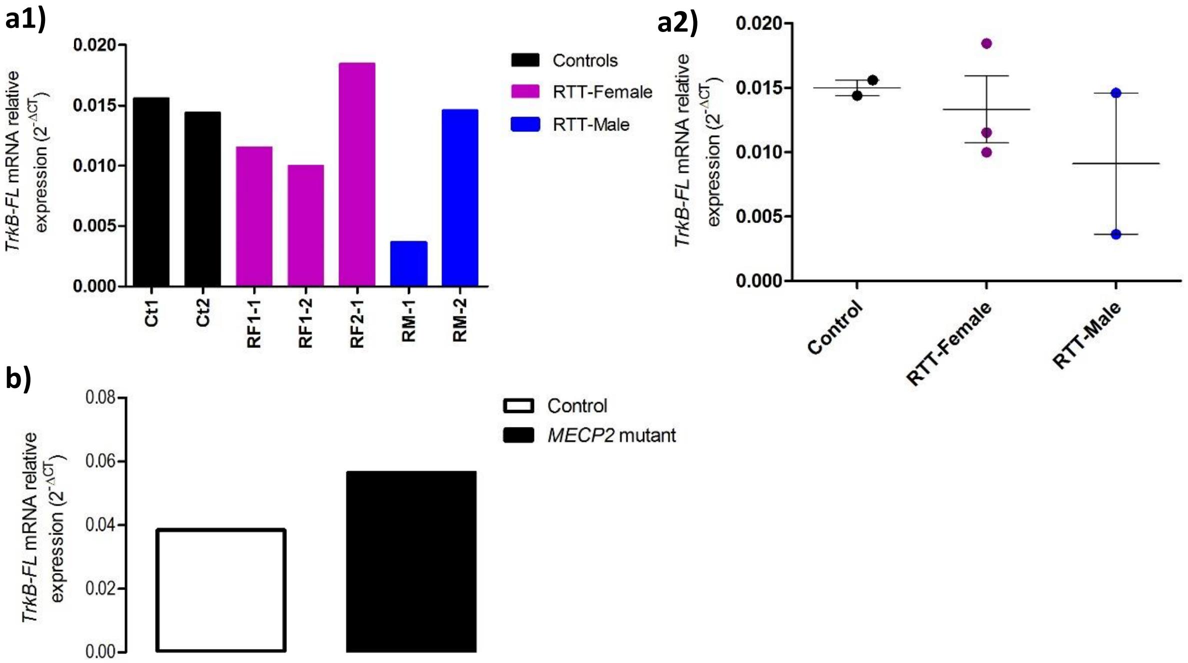

Figure 4.19 – ***TrkB-FL* mRNA relative expression in neurons-derived from hIPSCs and in RTT human brain**. **a1)** *TrkB-FL* mRNA relative expression for each cell line. *GAPDH* was used as internal loading control. **a2)** Grouped *TrkB-FL* mRNA expression: controls (Ct1, Ct2; black); RTT-Female (RF1-1, RF1-2, RF2; purple) and RTT-Male (RM-1, RM-2; blue). Values are presented in mean ± SEM. **b)** *TrkB-FL* relative expression in samples taken from healthy human temporal cortex (white bar) and RTT-female cortex (black bar).

TrkB-FL protein expression level is consistently decreased in all RTT cell lines (*Figure 4.20* ***a1,2)***) in agreement to what was observed in cortical samples in *Mecp2 KO* mice.

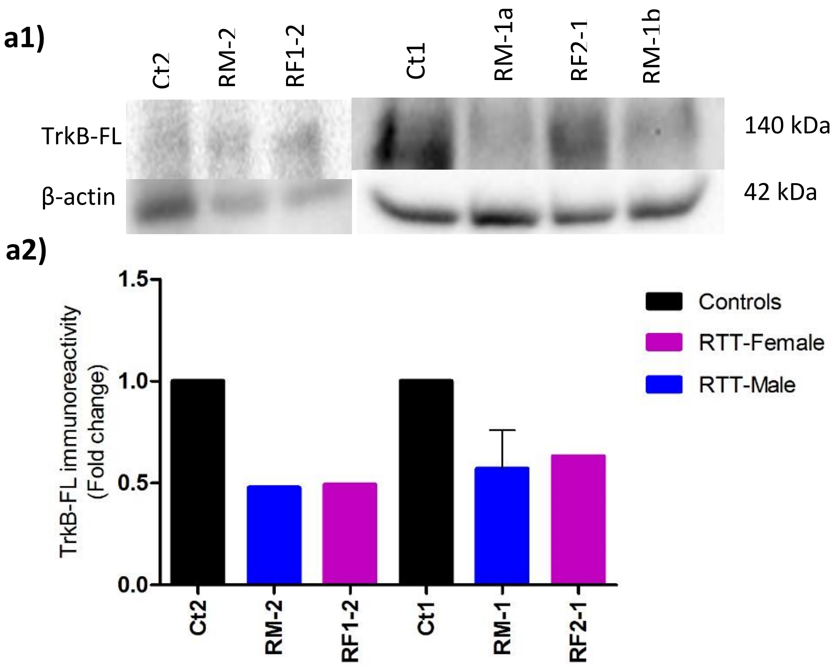

Figure 4.20 – **TrkB-FL protein expression level in neurons-derived from hIPSCs**. **a1)** Western-Blot analysis using primary antibodies recognizing TrkB-FL (~140 kDa) and β-actin (~42 kDa), used as loading control. **a2)** Immunoreactivity intensity of the TrkB-FL obtained in neuronal lines. Data were normalized to respective control (fold change). RM-1a and RM-1b are technical replicates.

Finally, *TrkB-T1* mRNA expression level is decreased in all lines, except in RF2-1 that shows similar transcript levels when compared to the controls (*Figure 4.21 **a1)***). Strikingly, RTT-male (0.026 ± 0.002, n=2) *TrkB-T1* mRNA expression is largely decreased when compared with control group (0.223 ± 0.030, n=2). The RTT-female group also shows lower *TrkB-T1* receptor expression (0.137 ± 0.037, n=3) when compared with control, but with higher expression when compared with RTT-male group (*Figure 4.21 **a2)***). No changes were observed when mRNA expression levels were assessed between the patient temporal cortex and the healthy control (*Figure 4.21 **b)***).

TrkB-Tc protein expression level is consistently decreased in all RTT cell lines with the exception of RF2-1 (*Figure 4.22 **a1,2)***) contrasting with the data obtained in cortical samples from *Mecp2 KO* mice, where no differences were observed.

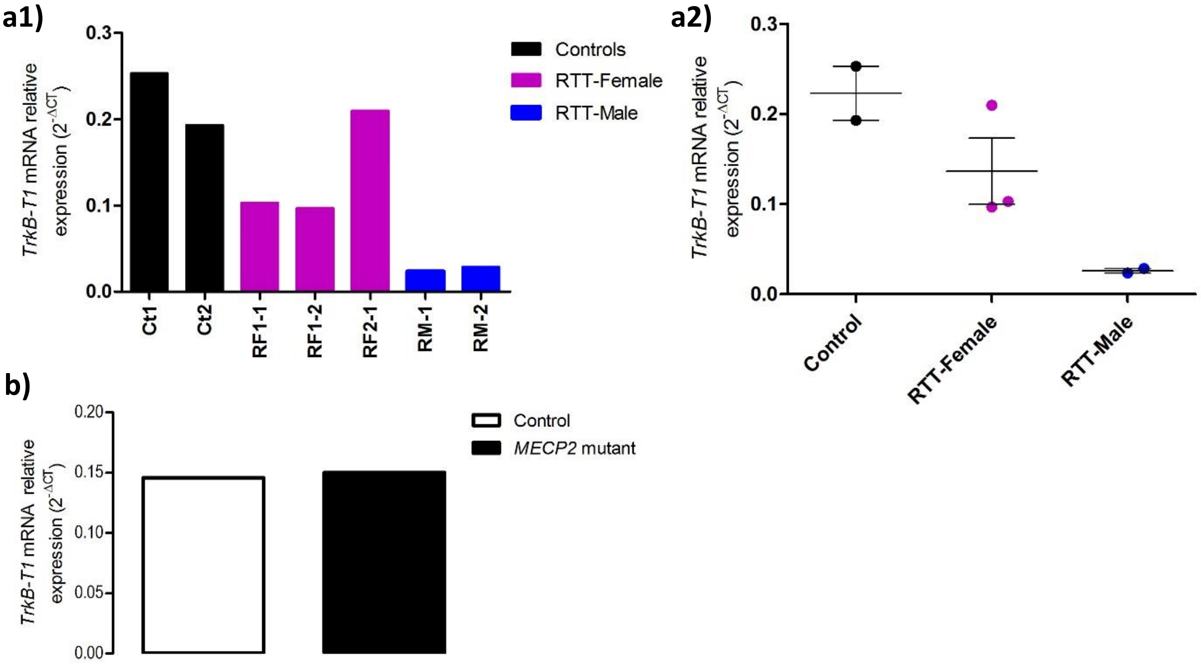

Figure 4.21 - ***TrkB-T1* mRNA relative expression in neurons-derived from hIPSCs and in RTT human brain**. **a1)** *TrkB-T1* mRNA relative expression for each cell line. *GAPDH* was used as internal loading control. **a2)** Grouped *TrkB-T1* mRNA expression: controls (Ct1, Ct2; black); RTT-Female (RF1-1, RF1-2, RF2; purple) and RTT-Male (RM-1, RM-2; blue). Values are presented in mean ± SEM. **b)** *TrkB-T1* relative expression in samples taken from healthy human temporal cortex (white bar) and RTT-female cortex (black bar).

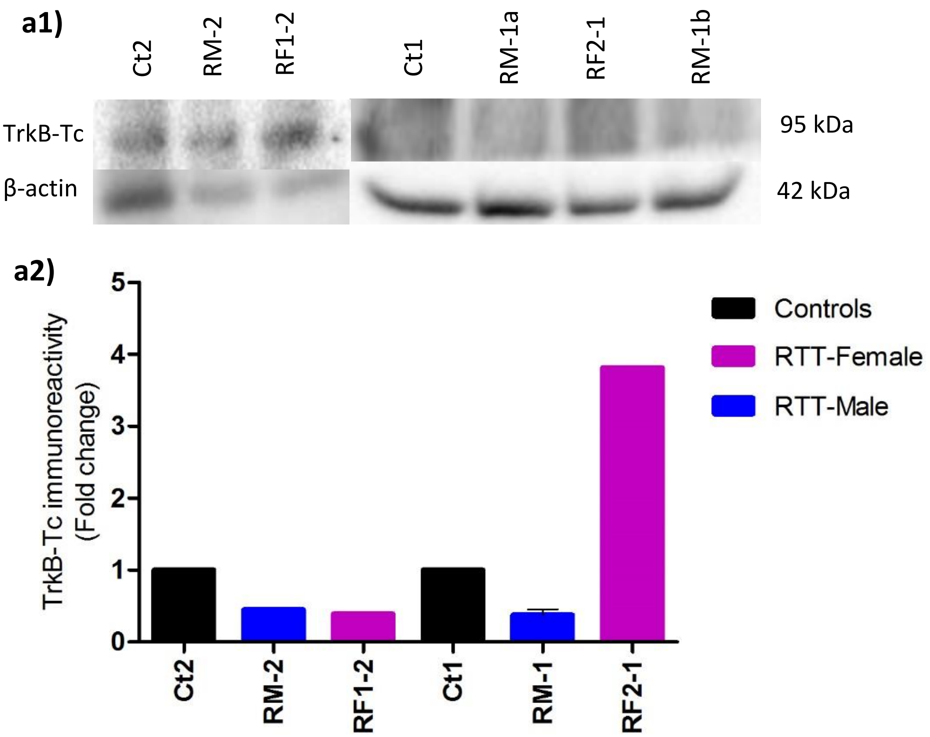

Figure 4.22 – **TrkB-Tc protein expression level in neurons-derived from hIPSCs**. **a1)** Western-Blot analysis using primary antibodies recognizing TrkB-Tc (~95 kDa) and β-actin (~42 kDa), used as loading control. **a2)** Immunoreactivity intensity of the TrkB-Tc obtained in neuronal lines. Data were normalized to respective control (fold change). RM-1a and RM-1b are technical replicates.

5. Discussion

In the present work, characterization of the adenosinergic system and BDNF signalling using different models, provided evidence that both are affected in RTT (see Table 5-1). However, given the high variability and low number of experiments using human material, and the discrepancy between the human and the mouse model, the conclusions are only speculative.

Table 5-1 **Summary of the obtained results**. Full symbols represent results submitted to statistical analysis. Dashed symbols represent tendencies. ↓ decrease; ↑increase; = no statistical significant differences; ? - inconclusive; n.d. - not determined.

*For TrkB-Tc mRNA expression only TrkB-T1 truncated isoform was analysed.

		A_1R	*$A_{2A}R$*	*ADK*	*BDNF*	*TrkB-FL*	*TrkB-Tc**
 ***Mecp2 KO* mice**	**mRNA**	=	=	n.d.	n.d.	=	=
	Protein	↑	↓	=	↓	↓	=
 RTT human brain	**mRNA**	⇡	⇣	n.d.	=	⇡	=
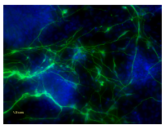 **RTT-hIPSCs neurons**	**mRNA**	F ⇡ M ?	F ⇡ M ?	n.d.	F ⇣ M ⇡	F ⇡ M ?	⇣
	Protein	n.d.	n.d.	?	⇡	⇣	F ? M ⇣

Adenosinergic system

The involvement of the adenosinergic system in neurological disorders has been receiving increased attention since A_1R and $A_{2A}R$ modulation have been shown to attenuate some symptoms of several disorders (see for review Gomes et al., 2011; Chen et al., 2007; Sebastião and Ribeiro, 2009). This suggests that the adenosinergic signalling is affected in these pathologies. Our lab was the pioneer exploring the involvement of the adenosinergic system in RTT.

The results presented in this thesis demonstrate that mRNA expression level for *A_1R* is unaffected in the cortex of *Mecp2 KO* mice. However, previous data clearly demonstrated that A_1R protein expression level was significantly increased in cortex of *Mecp2 KO* (Palminha, 2014). There is a clear discrepancy between A_1R mRNA and protein expression levels. This could be explained by decreased degradation of A_1R and/or increased translation by post-transcriptional modulation. In fact, it is known that MeCP2 modulates protein synthesis through the AKT/mTOR system, a pathway known to be impaired in RTT (Li et al., 2013).

Interestingly, in neurons produced from RTT-derived hIPSCs, the female lines show a tendency to exhibit increased level of *A_1R* mRNA. In addition, in one cortical *post-mortem* sample of a RTT patient, *A_1R* mRNA expression level is also increased when compared to an age matched control. The mechanism underlying the overall increased levels of A_1R remains undisclosed so far. However, we can speculate that this could be a compensatory mechanism in order to decrease the excitability associated to this pathology. Accordingly, in the brain of *Mecp2 KO* mice there is a tendency for hyperexcitability as changes in basal inhibitory rhythms have been observed (Calfa et al., 2011a) as well as pre- and postsynaptic defects in GABAergic synapses (Medrihan et al., 2008). Moreover, data from our lab, input output curves recorded from hippocampal slices of *Mecp2 KO* mice, show an increased basal synaptic transmission. In addition, hippocampal electrophysiological experiments performed using A_1R agonist and antagonist strongly suggest decreased endogenous adenosine level resulting in failure to control excitation. As mentioned before, the increase in A_1R protein could be a compensatory mechanism to fine tune inhibitory adenosine activity in spite of its low levels. Remarkably, this tendency was also seen in mRNA expression level on RTT-derived neurons and in the human brain sample. Quantification of protein expression level in human material will be important to validate these results.

To understand how and why adenosine levels are decreased in *Mecp2 KO* mice, among other possible scenarios, we looked at alterations in ADK expression levels and in its activity. This enzyme, together with ADA, is responsible for adenosine degradation, and is found altered in some disorders associated with impaired inhibitory transmission, such as epilepsy (Aronica et al., 2011; Boison, 2013). Our results, however, do not show significant differences in ADK cortical levels in the RTT animal model and in neurons-derived from RTT-hIPSCs. Functionally, it is not easy to evaluate whether ADK activity is altered, given other alterations in the adenosinergic signalling such as increased A_1R protein expression, which can perturb result interpretation. Electrophysiological recordings performed in the presence of an inhibitor of ADK show a similar decrease in synaptic transmission in the hippocampal slices from *Mecp2 KO and WT* mice. This could mean that 1) the decreased level of endogenous adenosine is not due to an exacerbated ADK activity in RTT (otherwise ADK would have mediated an exacerbated depression of synaptic transmission in RTT model); and/or that 2) even with higher level of A_1R, the increased adenosine level, resultant from inhibition of its degradation by ADK, is not sufficient to produce a similar decrease on synaptic transmission as seen in *WT* animals. Moreover, the increased desinhibition induced by DPCPX, a selective A_1R antagonist, observed in the presence of ADK in *WT* animals reinforces the possibility of adenosine level being decreased in the RTT animal model.

Nevertheless, it will be interesting to explore the effect of other molecules involved in adenosine metabolism, such as ADA, and find the mechanism behind reduced adenosine levels. Some studies, describe the downregulation of mitochondrial gene expression, which results in reduced electron transport chain units and also reduced glucose metabolism. Lower levels of ATP, highly related with adenosine formation, could explain adenosine reduction (Li et al., 2013; Krishnan et al., 2015). Impaired adenosine levels could also be related with upstream steps in adenosine biosynthesis, like ATP endogenous levels.

The $A_{2A}R$ mRNA expression level, in *Mecp2 KO* mice, is not significantly affected however, protein expression level is severely decreased. In RTT human brain, mRNA expression is decreased, but in neurons-derived from female RTT-hIPSCs there is a tendency to have increased $A_{2A}R$ mRNA expression. These discrepancies could be related to the variability observed in the different cell lines. Alterations in $A_{2A}R$ in RTT need therefore further exploration. Interestingly, in spite of the possible reduction of protein expression level of this adenosine receptor, its activation is still efficient in rescuing BDNF effects upon synaptic plasticity (Duarte, 2015 in preparation).

How adenosine alterations occur in RTT and how they underlie RTT's pathology is a critical issue that must be explored since it could provide important clues on how RTT symptoms could ameliorate.

BDNF signalling

BDNF deregulation is a recurrent topic in RTT. The modulation of this neurotrophin expression is controlled by the MeCP2 protein, found to be mutated in RTT in more than 90% of the cases. Several studies showed decreased *Bdnf* mRNA expression as well as decreased protein levels in *MeCP2 KO* mice (Chang et al., 2006; Abuhatzira et al., 2007; Wang et al., 2006; Li et al., 2013) but similar *BDNF* mRNA expression in human RTT brain samples (Deng et al., 2007). At the same time, the overexpression of this neurotrophin can improve some of RTT symptoms, demonstrating the high impact of BDNF in this pathology (Chang et al., 2006). Our results obtained from *Mecp2 KO* mice were concordant with the majority of literature where *Mecp2 KO* mice present lower expression levels of BDNF protein. Surprisingly, when we looked at BDNF expression levels, in RTT-derived neurons, there was a tendency to have increased BDNF expression protein level. If confirmed, these results could reveal different BDNF expression pattern in humans.

Little was known about TrkB receptor expression in RTT. One study has shown increased *TrkB-FL* mRNA expression level in *Mecp2 KO* mice and in RTT human cortical brain samples, which could be a compensatory mechanism promoted by low BDNF protein levels (Abuhatzira et al., 2007) while the other described no differences in *TrkB-FL* mRNA between mutant human neurons and control neurons (Li et al., 2013). In line with the last study, our data shows no significant differences in *TrkB-FL* mRNA level in *Mecp2 KO* mice. However, TrkB-FL protein expression level in *Mecp2 KO* mice hippocampi is decreased (Duarte, 2015 in preparation) as wells as in RTT-derived neurons.

No changes were observed in TrkB truncated receptors in *Mecp2 KO* both at the mRNA (truncated isoform T1) and the protein expression levels (TrkB-Tc) and the same was observed for the TrkB-T1 mRNA in the cortical human sample. However, in neurons-derived from RTT-hIPSCs, both TrkB-T1 receptor mRNA and protein expression levels (TrkB-Tc) show a tendency to be decreased, without the typical variability seen for the other observations increasing the validity of the results. An interesting hypothesis is that the increased levels of BDNF in RTT-derived neurons could be the result of a compensatory mechanism induced by the decreased level of TrkB.

One interesting observation, that holds true both for the adenosinergic system and for the BDNF signalling is that, in *Mecp2 KO* mice, mRNA expression levels are not altered (A_1R, $A_{2A}R$ and TrkB receptors) while quantification of the respective proteins are clearly changed. This observation might be related to post-translational and degradation mechanisms, as previously mentioned. However, another possible explanation is that the severity inherent to the *Mecp2 KO* model probably does not allow for compensatory mechanisms, acting at the transcriptional level that could restore normal protein expression.

hIPSCs as RTT model

The appearance of hIPSCs as a disease model is very recent, with no more than 6 years of development. In this work, the biggest issue was the variability found not only between gender-matched lines but also between independent rounds of differentiation from the same parental hIPSCs line. Part of this variability could be related to the multiple genetic and epigenetic alterations that occur during the reprogramming and differentiation procedures, such as the fixation of sporadic random mutations and the random X chromosome inactivation in female lines (Dajani et al., 2013). Another important source of variability is the efficiency of cortical neuron production that is prone to fluctuate and thus compromising the results.

Even though we found some concordant tendencies between the human and the mouse models, we cannot truly understand what the real tendency in RTT-derived neurons is. This is further aggravated by the small sample size that, in the future, could be solved by increasing not only the number of patient-derived hIPSCs lines but also by increasing the amount of independent rounds of differentiation.

Cerebral cortex processes are not the result of the activity of one isolated type of neurons but of the interaction of both stimulatory and inhibitory neurons. One important pitfall of this approach is that the protocol used generates mainly cortical glutamatergic neurons failing to recapitulate the functional complexity of the brain (Buxbaum and Hof, 2013). This is likely to contribute to the differences found between the hIPSCs model, the human *post-mortem* sample and the *Mecp2* KO mice.

Overall, the results clearly point towards a dysfunction in BDNF and the adenosinergic system. Despite this, pharmacological activation of $A_{2A}R$ is able to rescue BDNF actions upon LTP in *Mecp2* KO mice (Duarte, 2015 in preparation). Thus, adenosine receptor pharmacological manipulation is a promising therapeutic strategy to rescue BDNF-mediated dysfunctions in RTT.

6. Acknowledgments

Aproximando-se o fim desta jornada, não posso deixar de agradecer a todos aqueles que de alguma forma me ajudaram neste percurso.

Começo por agradecer à Professora Ana Sebastião pela sua recetividade e pela disponibilidade que sempre demonstrou ter quando necessário.

Às minhas orientadoras, um gigante obrigada que nunca será suficiente. Cada uma, à sua maneira, contribuiu para o meu enriquecimento profissional mas também pessoal. Particularizando, começo por agradecer à Mizé por me ter aceitado como sua aluna, ajudando-me a iniciar e a evoluir na carreira de investigação científica. Agradeço pelo seu entusiasmo e motivação, pelos seus conselhos e por toda a preocupação e compreensão que sempre teve ao longo de todo o ano. À Cláudia, por toda a partilha de conhecimento e conselhos dados mas também pelo apoio, preocupação e motivação que sempre me transmitiu. À Sofia, pela receção inicial ao trabalho de laboratório e pela ajuda que foi dando ao longo deste ano.

Deixo também uma palavra de agradecimento a todos os colegas de laboratório, sempre dispostos a ajudar, criando um bom ambiente na nossa unidade. Em especial ao Rui Gomes que me ajudou na execução inicial de qPCR, e ao seu grupo (LLopes) que disponibilizou alguns dos primers necessários. À Sara Ferreira pelo apoio no trabalho de bancada e por executar as genotipagens dos nossos animais. Um agradecimento também à Alexandra, pela disponibilidade e ajuda em todas as burocracias.

Aos meus colegas de sala, pela boa disposição e animação. Em especial à Mariana que para além de ser a minha companheira de bancada por uns bons meses se tornou também uma boa amiga.

Às minhas amiguinhas de Neurociências: Sara, Margarida e Mariana! Ajudaram, sem dúvida, a tornar tudo isto mais fácil com as vossas gargalhadas, conversas e passeios. Uma muito obrigada pela vossa amizade.

Ao João, que é incansável e está sempre do meu lado. Obrigada pelo teu companheirismo em todas as etapas pelas quais temos passado.

Aos meus pais, irmã e avó por todo o apoio e força que sempre me deram. Obrigada por estarem sempre comigo.

7. Bibliographic references

Abbracchio, M.P. et al., 1995. G protein-dependent activation of phospholipase C by adenosine A3 receptors in rat brain. *Molecular pharmacology*, 48(6), pp.1038–45.

Abreu, L.C. De, 2014. Quantification of functional abilities in Rett syndrome : a comparison between stages III and IV. , pp.1213–1222.

Abuhatzira, L. et al., 2007. MeCP2 deficiency in the brain decreases BDNF levels by REST/CoREST-mediated repression and increases TRKB production. *Epigenetics*, 2(December), pp.214–222.

Adams, V.H. et al., 2007. Intrinsic disorder and autonomous domain function in the multifunctional nuclear protein, MeCP2. *Journal of Biological Chemistry*, 282(20), pp.15057–15064.

Allen, S.J. et al., 1994. Cloning of a non-catalytic form of human trkB and distribution of messenger RNA for trkB in human brain. *Neuroscience*, 60(3), pp.825–834.

Amenduni, M. et al., 2011. iPS cells to model CDKL5-related disorders. *European Journal of Human Genetics*, 19(12), pp.1246–1255.

Amir, R.E. et al., 1999. Rett syndrome is caused by mutations in X-linked MECP2, encoding methyl-CpG-binding protein 2. *Nature genetics*, 23(october), pp.185–188.

Amir, R.E. and Zoghbi, H.Y., 2000. Rett syndrome: Methyl-CpG-binding protein 2 mutations and phenotype-genotype correlations. *American Journal of Medical Genetics - Seminars in Medical Genetics*, 97(2), pp.147–152.

Ananiev, G. et al., 2011. Isogenic pairs of wild type and mutant induced pluripotent stem cell (iPSC) lines from rett syndrome patients as In Vitro disease model. *PLoS ONE*, 6(9).

Anderson, W.W. and Collingridge, G.L., 2001. The LTP Program: A data acquisition program for on-line analysis of long-term potentiation and other synaptic events. *Journal of Neuroscience Methods*, 108, pp.71–83.

Aronica, E. et al., 2013. Glial adenosine kinase - A neuropathological marker of the epileptic brain. *Neurochemistry International*, 63(7), pp.688–695.

Aronica, E. et al., 2011. Upregulation of adenosine kinase in astrocytes in experimental and human temporal lobe epilepsy. , 52(9), pp.1645–1655.

Autry, A.E. and Monteggia, L.M., 2012. Brain-derived neurotrophic factor and neuropsychiatric disorders. *Pharmacological reviews*, 64(2), pp.238–58.

Banerjee, A., Castro, J. and Sur, M., 2012. Rett syndrome: Genes, synapses, circuits, and therapeutics. *Frontiers in Psychiatry*, 3(May), pp.1–13.

Barker, P. a., 2004. p75NTR is positively promiscuous: Novel partners and new insights. *Neuron*, 42(4), pp.529–533.

Bedogni, F. et al., 2014. Rett syndrome and the urge of novel approaches to study MeCP2 functions and mechanisms of action. *Neuroscience and Biobehavioral Reviews*, 46, pp.187–201.

Berman, R.F. et al., 2000. Evidence for increased dorsal hippocampal adenosine release and metabolism during pharmacologically induced seizures in rats. *Brain Research*, 872(1-2), pp.44–53.

Binder, D.K. and Scharfman, H.E., 2004. Brain-derived neurotrophic factor. *Growth factors (Chur, Switzerland)*, 22(3), pp.123–131.

Bliss, T.V. and Collingridge, G.L, 1993. A synaptic model of memory: long-term potentiation in the hippocampus. , pp.361(6407):31–9.

Boison, D., 2012. Adenosine Dysfunction in epilepsy. *Glia*, 29(6), pp.997–1003.

Boison, D., 2013. Adenosine kinase: exploitation for therapeutic gain. *Pharmacological reviews*, 65(July), pp.906–43.

Boison, D., Chen, J.F. and Fredholm, B.B., 2010. Adenosine Signalling and Function in Glial Cells Detlev. *Cell Death Differ*, 17(7), pp.1071–1082.

Bontemps, F., Van den Berghe, G. and Hers, H.G., 1983. Evidence for a substrate cycle between AMP and adenosine in isolated hepatocytes. *Proceedings of the National Academy of Sciences of the United States of America*, 80(10), pp.2829–2833.

Bontemps, F., Vincent, M.F. and Van den Berghe, G., 1993. Mechanisms of elevation of adenosine levels in anoxic hepatocytes. *The Biochemical journal*, 290 (Pt 3, pp.671–677.

Buxbaum, J.D. and Hof, P.R., 2013. *The Neuroscience of Autism Spectrum Disorders*, Elsevier.].

Calfa, G., Hablitz, J.J. and Pozzo-Miller, L., 2011a. Network hyperexcitability in hippocampal slices from Mecp2 mutant mice revealed by voltage-sensitive dye imaging. *Journal of neurophysiology*, 105(4), pp.1768–1784.

Calfa, G., Percy, A. and Pozzo-Miller, L., 2011b. On experimental models of Rett Syndrome based on Mecp2 Dysfunction. *Experimental Biology and Medicine*, 236(1), pp.3–19.

Chahrour, M. et al., 2008. MeCP2, a key contributor to neurological disease, activates and represses transcription. *Science (New York, N.Y.)*, 320(5880), pp.1224–1229.

Chahrour, M. and Zoghbi, H.Y., 2007. The Story of Rett Syndrome: From Clinic to Neurobiology. *Neuron*, 56(MIM 312750), pp.422–437.

Chailangkarn, T., Acab, A. and Renato Muotri, a, 2012. Modeling neurodevelopmental disorders using human neurons. *Current opinion in neurobiology*, 22(5), pp.785–790.

Chang, Q. et al., 2006. The disease progression of Mecp2 mutant mice is affected by the level of BDNF expression. *Neuron*, 49, pp.341–348.

Chen, J.F. et al., 2007. Adenosine A2A receptors and brain injury: Broad spectrum of neuroprotection, multifaceted actions and “fine tuning” modulation. *Progress in Neurobiology*, 83, pp.310–331.

Chen, R.Z. et al., 2001. Deficiency of methyl-CpG binding protein-2 in CNS neurons results in a Rett-like phenotype in mice. *Nature genetics*, 27(3), pp.327–331.

Cheng, T. and Qiu, Z., 2014. MeCP2 : multifaceted roles in gene regulation and neural development. , 30(4), pp.601–609.

Cheung, A.Y.L. et al., 2012. X-chromosome inactivation in Rett syndrome human induced pluripotent stem cells. *Frontiers in Psychiatry*, 3(MAR), pp.1–16.

Cohen-cory, S. et al., 2011. Brain-Derived Neurotrophic Factor and the Development of Structural Neuronal Connectivity. *Neurobiology*, 70(5), pp.271–288.

Connor, B. and Dragunow, M., 1998. The role of neuronal growth factors in neurodegenerative disorders of the human brain. *Brain research. Brain research reviews*, 27(1), pp.1–39.

Corvol, J.C. et al., 2001. Gαolf is necessary for coupling D1 and A2a receptors to adenylyl cyclase in the striatum. *Journal of Neurochemistry*, 76(5), pp.1585–1588.

Costenla, A.R., Mendonça, A de,. and Ribeiro, J.A., 1999. Adenosine modulates synaptic plasticity in hippocampal slices from aged rats. *Brain Research*, 851(1-2), pp.228–234.

Cunha, R. A. and Agostinho, P.M., 2010. Chronic caffeine consumption prevents memory disturbance in different animal models of memory decline. *Journal of Alzheimer’s Disease*, 20(SUPPL.1).

Cunha, R.A., Constantino, M.D. and Ribeiro, J.A., 1999. G protein coupling of CGS 21680 binding sites in the rat hippocampus and cortex is different from that of adenosine A1 and striatal A2A receptors. *Naunyn-Schmiedeberg’s archives of pharmacology*, 359(4), pp.295–302.

Dajani, R. et al., 2013. Investigation of Rett syndrome using pluripotent stem cells. *Journal of cellular biochemistry*, 114(11), pp.2446–53.

Deng, V. et al., 2007. FXYD1 is an MeCP2 target gene overexpressed in the brains of Rett syndrome patients and Mecp2-null mice. *Human Molecular Genetics*, 16(6), pp.640–650.

Diógenes, M.J. et al., 2004. Activation of adenosine A2A receptor facilitates brain-derived neurotrophic factor modulation of synaptic transmission in hippocampal slices. *The Journal of neuroscience : the official journal of the Society for Neuroscience*, 24(12), pp.2905–2913.

Diógenes, M.J. et al., 2011. Enhancement of LTP in aged rats is dependent on endogenous BDNF. *Neuropsychopharmacology : official publication of the American College of Neuropsychopharmacology*, 36, pp.1823–1836.

Duarte, S., 2015. *PhD thesis (Synaptic dysfunction in early encephalopathies: from genes to function)*.

Dunwiddie, T. V and Masino, S.A., 2001. The role and regulation of adenosine in the central nervous system. *Annual review of neuroscience*, 24, pp.31–55.

During, M.J. and Spencer, D.D., 1992. Adenosine: a potential mediator of seizure arrest and postictal refractoriness. *Annals of neurology*, 32(5), pp.618–624.

Eide, F.F., 1996. naturally occuring truncated trkb receptors have dominant inhibitory effects on brain-derived neurotrophic factor signaling. *J neurosci.*, 16(10), pp.3123–3129.

Ekonomou, A. et al., 2000. Reduction of A1 adenosine receptors in rat hippocampus after kainic acid-induced limbic seizures. *Neuroscience letters*, 284(1-2), pp.49–52..

Evans, J.C. et al., 2005. Early onset seizures and Rett-like features associated with mutations in CDKL5. *European journal of human genetics : EJHG*, 13(10), pp.1113–1120.

Fontinha, B.M. et al., 2009. Adenosine A(2A) receptor modulation of hippocampal CA3-CA1 synapse plasticity during associative learning in behaving mice. *Neuropsychopharmacology : official publication of the American College of Neuropsychopharmacology*, 34(7), pp.1865–1874.

Fontinha, B.M. et al., 2008. Enhancement of long-term potentiation by brain-derived neurotrophic factor requires adenosine A2A receptor activation by endogenous adenosine. *Neuropharmacology*, 54, pp.924–933.

Fredholm, B.B. et al., 2005. Adenosine and brain function. *International review of neurobiology*, 63, pp.191–270.

Fredholm, B.B. et al., 2001. International Union of Pharmacology. XXV. Nomenclature and classification of adenosine receptors. *Pharmacological reviews*, 53(4), pp.527–552.

Freitas, B.C.G. et al., 2012. Stem cells and modeling of autism spectrum disorders. *Experimental Neurology*, 260, pp.33–43.

Galvão, T.C. and Thomas, J.O., 2005. Structure-specific binding of MeCP2 to four-way junction DNA through its methyl CpG-binding domain. *Nucleic Acids Research*, 33(20), pp.6603–6609.

Girard, M. et al., 2001. Parental origin of de novo MECP2 mutations in Rett syndrome. *European journal of human genetics : EJHG*, 9(3), pp.231–236.

Glass, M. et al., 1996. Loss of A1 adenosine receptors in human temporal lobe epilepsy. *Brain research*, 710(1-2), pp.56–68.

Gomes, C. V et al., 2011. Adenosine receptors and brain diseases: neuroprotection and neurodegeneration. *Biochimica et biophysica acta*, 1808(5), pp.1380–1399.

Gouder, N. et al., 2004. Overexpression of adenosine kinase in epileptic hippocampus contributes to epileptogenesis. *The Journal of neuroscience : the official journal of the Society for Neuroscience*, 24(3), pp.692–701.

Greene, R.W., 2011. Adenosine: Front and center in linking nutrition and metabolism to neuronal activity. *Journal of Clinical Investigation*, 121(7), pp.2548–2550.

Greene, R.W. and Haas, H.L., 1991. The electrophysiology of adenosine in the mammalian central nervous system. *Progress in Neurobiology*, 36(4), pp.329–341.

Guy, J. et al., 2001. A mouse Mecp2-null mutation causes neurological symptoms that mimic Rett syndrome. *Nature genetics*, 27(3), pp.322–326.

Guy, J. et al., 2007. Reversal of neurological defects in a mouse model of Rett syndrome. *Science (New York, N.Y.)*, 315(2007), pp.1143–1147.

Hagberg, B. et al., 1983. A progressive syndrome of autism, dementia, ataxia, and loss of purposeful hand use in girls: Rett's syndrome: report of 35 cases. *Annals of neurology*, 14(4), pp.471–9.

Hauser, R. A., Hubble, J.P. and Truong, D.D., 2003. Randomized trial of the adenosine A(2A) receptor antagonist istradefylline in advanced PD. *Neurology*, 61(3), pp.297–303.

Hotta, A. et al., 2009. Isolation of human iPS cells using EOS lentiviral vectors to select for pluripotency. *Nature methods*, 6(5), pp.370–376.

Huang, E.J. and Reichardt, L.F., 2003. Trk receptors: roles in neuronal signal transduction. *Annual review of biochemistry*, 72, pp.609–642.

Itoh, M. et al., 2012. Methyl CpG-binding protein isoform MeCP2-e2 is dispensable for rett syndrome phenotypes but essential for embryo viability and placenta development. *Journal of Biological Chemistry*, 287(17), pp.13859–13867.

Jacobson, K. A. and Gao, Z.-G., 2012. Adenosine receptors as therapeutic targets. *Nature review. Drug discovery*, 5(3), pp.247–264.

Jacobson, K.A., 1998. Adenosine A3 receptors: novel ligands and paradoxical effects. *Trends in pharmacological sciences*, 19(5), pp.184–91.

Jang, J. et al., 2014. Induced pluripotent stem cells for modeling of pediatric neurological disorders. *Biotechnology Journal*, 9(7), pp.871–891.

Jerónimo-Santos, A. et al., 2014. Impact of in vivo chronic blockade of adenosine A2A receptors on the BDNF-mediated facilitation of LTP. *Neuropharmacology*, 83, pp.99–106.

Katz, D.M. et al., 2012. Preclinical research in Rett syndrome: setting the foundation for translational success. *Disease Models & Mechanisms*, 5, pp.733–745.

Kim, K.Y., Hysolli, E. and Park, I.-H., 2011. Neuronal maturation defect in induced pluripotent stem cells from patients with Rett syndrome. *Proceedings of the National Academy of Sciences of the United States of America*, 108(34), pp.14169–14174.

Klose, R.J. et al., 2005. DNA binding selectivity of MeCP2 due to a requirement for A/T sequences adjacent to methyl-CpG. *Molecular Cell*, 19(5), pp.667–678.

Klose, R.J. and Bird, A.P., 2004. MeCP2 behaves as an elongated monomer that does not stably associate with the Sin3a chromatin remodeling complex. *The Journal of biological chemistry*, 279(45), pp.46490–6.

Kolbeck, R. et al., 1999. Brain-derived neurotrophic factor levels in the nervous system of wild-type and neurotrophin gene mutant mice. *Journal of neurochemistry*, 72(5), pp.1930–1938.

Krishnan, N. et al., 2015. PTP1B: a new therapeutic target for Rett syndrome. *Journal of Clinical Investigation*, 125(8), pp.2931–2934.

Kudo, S. et al., 2003. Heterogeneity in residual function of MeCP2 carrying missense mutations in the methyl CpG binding domain. *Journal of medical genetics*, 40(7), pp.487–93.

Lee, F.S. and Chao, M. V, 2001. Activation of Trk neurotrophin receptors in the absence of neurotrophins. *Proceedings of the National Academy of Sciences of the United States of America*, 98(6), pp.3555–3560.

Lee, R. et al., 2001. Regulation of cell survival by secreted proneurotrophins. *Science (New York, N.Y.)*, 294(5548), pp.1945–1948.

Lewis, J.D. et al., 1992. Purification, sequence, and cellular localization of a novel chromosomal protein that binds to methylated DNA. *Cell*, 69(6), pp.905–914.

LeWitt, P. A. et al., 2008. Adenosine A2A receptor antagonist istradefylline (KW-6002) reduces off time in Parkinson’s disease: A double-blind, randomized, multicenter clinical trial (6002-US-005). *Annals of Neurology*, 63(3), pp.295–302.

Li, W. and Pozzo-Miller, L., 2014. BDNF deregulation in Rett syndrome. *Neuropharmacology*, 76, pp.737–746.

Li, Y. et al., 2013. Global transcriptional and translational repression in human-embryonic-stem-cell-derived Rett syndrome neurons. *Cell Stem Cell*, 13, pp.446–458.

Linden, J. et al., 1999. Characterization of human A(2B) adenosine receptors: radioligand binding, western blotting, and coupling to G(q) in human embryonic kidney 293 cells and HMC-1 mast cells. *Molecular pharmacology*, 56(4), pp.705–713.

Liyanage, V.R.B. and Rastegar, M., 2014. Rett syndrome and MeCP2. *NeuroMolecular Medicine*, 16(2), pp.231–264.

Lopes, L.V. et al., 2002. Adenosine A(2A) receptor facilitation of hippocampal synaptic transmission is dependent on tonic A(1) receptor inhibition. *Neuroscience*, 112(2), pp.319–29.

Lopes, L.V., Cunha, R.A. and Ribeiro, J.A., 1999. Cross talk between A(1) and A(2A) adenosine receptors in the hippocampus and cortex of young adult and old rats. *Journal of neurophysiology*, 82(6), pp.3196–3203.

Luberg, K. et al., 2010. Human TrkB gene: Novel alternative transcripts, protein isoforms and expression pattern in the prefrontal cerebral cortex during postnatal development. *Journal of Neurochemistry*, 113(4), pp.952–964.

Luikart, B.. et al., 2003. In vivo role of truncated trkb receptors during sensory ganglion neurogenesis. *Neuroscience*, 117(4), pp.847–858.

Maia, L. and Mendonça, A. de, 2002. Does caffeine intake protect from Alzheimer ' s disease ? , pp.377–382.

Marchetto, M.C.N.M. et al., 2010. A model for neural development and treatment of Rett syndrome using human induced pluripotent stem cells. *Cell*, 143(4), pp.527–39.

Martinowich, K. et al., 2003. DNA methylation-related chromatin remodeling in activity-dependent BDNF gene regulation. *Science (New York, N.Y.)*, 302(5646), pp.890–893.

Mccauley, M.D. et al., 2011. Mice : Implication for Therapy in Rett Syndrome. , 3(113).

Medrihan, L. et al., 2008. Early defects of GABAergic synapses in the brain stem of a MeCP2 mouse model of Rett syndrome. *Journal of neurophysiology*, 99(1), pp.112–121.

Mendonça, A. de, Sebastião, A.M. and Ribeiro, J.A., 1995. Inhibition of NMDA receptor-mediated currents in isolated rat hippocampal neurones by adenosine A1 receptor activation. *Neuroreport*, 6(8), pp.1097–100.

Molyneaux, B.J. et al., 2007. Neuronal subtype specification in the cerebral cortex. *Nature reviews. Neuroscience*, 8(6), pp.427–437.

Nagata, H. et al., 1984. Regional and subcellular distribution in mammalian brain of the enzymes producing adenosine. *Journal of neurochemistry*, 42(4), pp.1001–7.

Neul, J.L. et al., 2011. Rett syndrome: revised diagnostic criteria and nomenclature. , 68(6), pp.944–950.

Nikitina, T. et al., 2007. Multiple modes of interaction between the methylated DNA binding protein MeCP2 and chromatin. *Molecular and cellular biology*, 27(3), pp.864–77.

Nitta, A. et al., 2002. Diabetic neuropathies in brain are induced by deficiency of BDNF. *Neurotoxicology and teratology*, 24(5), pp.695–701.

Numakawa, T., 2014. Possible protective action of neurotrophic factors and natural compounds against common neurodegenerative diseases. *Neural regeneration research*, 9(16), pp.1506–8.

Pak, M.A. et al., 1994. Inhibition of adenosine kinase increases endogenous adenosine and depresses neuronal activity in hippocampal slices. *Neuropharmacology*, 33(9), pp.1049–53.

Palminha, C., 2014. *Master thesis (Characterization of adenosine receptors in a Rett Syndrome model)*.

Percy, A.K. and Lane, J.B., 2005. Rett syndrome: model of neurodevelopmental disorders. *Journal of child neurology*, 20(9), pp.718–21.

Philippe, C. et al., 2010. Phenotypic variability in Rett syndrome associated with FOXG1 mutations in females. *Journal of medical genetics*, 47(1), pp.59–65.

Phillips, E. and Newsholme, E.A., 1979. Maximum activities, properties and distribution of 5' nucleotidase, adenosine kinase and adenosine deaminase in rat and human brain. *Journal of neurochemistry*, 33(2), pp.553–8.

Popoli, P. et al., 2002. Blockade of striatal adenosine A2A receptor reduces, through a presynaptic mechanism, quinolinic acid-induced excitotoxicity: possible relevance to neuroprotective interventions in neurodegenerative diseases of the striatum. *The Journal of neuroscience : the official journal of the Society for Neuroscience*, 22(5), pp.1967–75.

Pratte, M. et al., 2011. Progressive motor and respiratory metabolism deficits in post-weaning Mecp2-null male mice. *Behavioural Brain Research*, 216(1), pp.313–320.

Rajagopal, R. et al., 2004. Transactivation of Trk neurotrophin receptors by G-protein-coupled receptor ligands occurs on intracellular membranes. *The Journal of neuroscience : the official journal of the Society for Neuroscience*, 24(30), pp.6650–6658.

Ralevic, V. and Burnstock, G., 1998. Receptors for purines and pyrimidines. *Pharmacological reviews*, 50(3), pp.413–492.

Rebola, N. et al., 2008. Adenosine A2A receptors are essential for long-term potentiation of NMDA-EPSCs at hippocampal mossy fiber synapses. *Neuron*, 57(1), pp.121–134.

Rebola, N. et al., 2003. Enhanced adenosine A2A receptor facilitation of synaptic transmission in the hippocampus of aged rats. *Journal of neurophysiology*, 90(2), pp.1295–1303.

Rett, A., 1966. [On a unusual brain atrophy syndrome in hyperammonemia in childhood]. *Wiener medizinische Wochenschrift (1946)*, 116(37), pp.723–6.

Ribeiro, J.A., Sebastião, A.M. and Mendonça, A. de, 2002. Adenosine receptors in the nervous system: pathophysiological implications. *Progress in Neurobiology*, 68(6), pp.377–392.

Robinson, L. et al., 2012. Morphological and functional reversal of phenotypes in a mouse model of Rett syndrome. *Brain*, 135, pp.2699–2710.

Rogel, A. et al., 2005. Phospholipase C is involved in the adenosine-activated signal transduction pathway conferring protection against iodoacetic acid-induced injury in primary rat neuronal cultures. *Neuroscience Letters*, 373(3), pp.218–221.

Rose, C.R. et al., 2003. Truncated TrkB-T1 mediates neurotrophin-evoked calcium signalling in glia cells. *Nature*, 426(6962), pp.74–8.

Sachdeva, S. and Gupta, M., 2013. Adenosine and its receptors as therapeutic targets: An overview. *Saudi Pharmaceutical Journal*, 21(3), pp.245–253.

Saporta, M.A., Grskovic, M. and Dimos, J.T., 2011. Induced pluripotent stem cells in the study of neurological diseases. *Stem Cell Research & Therapy*, 2(5), p.37.

Scanziani, M. et al., 1992. Presynaptic inhibition of miniature excitatory synaptic currents by baclofen and adenosine in the hippocampus. *Neuron*, 9(5), pp.919–27.

Schmittgen, T.D. and Livak, K.J., 2008. Analyzing real-time PCR data by the comparative C(T) method. *Nature protocols*, 3(6), pp.1101–1108.

Sebastião, A.M. and Ribeiro, J.A., 2009. Tuning and fine-tuning of synapses with adenosine. *Current neuropharmacology*, 7, pp.180–194.

Sebastião, A.M. and Ribeiro, J.A., 2009. Triggering neurotrophic factor actions through adenosine A2A receptor activation: implications for neuroprotection. *British journal of pharmacology*, 158(1), pp.15–22.

Shahbazian, M.D. et al., 2002. Insight into Rett syndrome: MeCP2 levels display tissue- and cell-specific differences and correlate with neuronal maturation. *Human molecular genetics*, 11(2), pp.115–124.

Shi, Y., Kirwan, P. and Livesey, F.J., 2012. Directed differentiation of human pluripotent stem cells to cerebral cortex neurons and neural networks. *Nature Protocols*, 7(10), pp.1836–1846.

Smeets, E. et al., 2005. Rett syndrome in females with CTS hot spot deletions: A disorder profile. *American Journal of Medical Genetics*, 132 A(2), pp.117–120.

Stearns, N. a. et al., 2007. Behavioral and anatomical abnormalities in Mecp2 mutant mice: A model for Rett syndrome. *Neuroscience*, 146, pp.907–921.

Stuss, D.P. et al., 2013. Impaired in vivo binding of MeCP2 to chromatin in the absence of its DNA methyl-binding domain. *Nucleic Acids Research*, 41(9), pp.4888–4900.

Takahashi, K. et al., 2007. Induction of Pluripotent Stem Cells from Adult Human Fibroblasts by Defined Factors. *Cell*, 131(5), pp.861–872.

Takahashi, K. and Yamanaka, S., 2006. Induction of Pluripotent Stem Cells from Mouse Embryonic and Adult Fibroblast Cultures by Defined Factors. *Cell*, 126(4), pp.663–676.

Tarditi, A. et al., 2006. Early and transient alteration of adenosine A2A receptor signaling in a mouse model of Huntington disease. *Neurobiology of disease*, 23(1), pp.44–53.

Tebano, M.T. et al., 2008. Adenosine A2A receptors are required for normal BDNF levels and BDNF-induced potentiation of synaptic transmission in the mouse hippocampus. *Journal of Neurochemistry*, 104(1), pp.279–286.

Thompson, C.M. et al., 2005. Inhibitor of the glutamate vesicular transporter (VGLUT). *Current medicinal chemistry*, 12(18), pp.2041–2056.

Thomson, J. a et al., 1998. Embryonic stem cell lines derived from human blastocysts. *Science (New York, N.Y.)*, 282(5391), pp.1145–1147.

Trappe, R. et al., 2001. MECP2 mutations in sporadic cases of Rett syndrome are almost exclusively of paternal origin. *American journal of human genetics*, 68(5), pp.1093–1101.

Varani, K. et al., 2001. Aberrant amplification of A(2A) receptor signaling in striatal cells expressing mutant huntingtin. *FASEB journal : official publication of the Federation of American Societies for Experimental Biology*, 15(7), pp.1245–7.

Wan, M. et al., 1999. Rett syndrome and beyond: recurrent spontaneous and familial MECP2 mutations at CpG hotspots. *American journal of human genetics*, 65(6), pp.1520–1529.

Wang, H. et al., 2006. Dysregulation of brain-derived neurotrophic factor expression and neurosecretory function in Mecp2 null mice. *The Journal of neuroscience : the official journal of the Society for Neuroscience*, 26(42), pp.10911–10915.

Warlich, E. et al., 2011. Lentiviral vector design and imaging approaches to visualize the early stages of cellular reprogramming. *Molecular therapy : the journal of the American Society of Gene Therapy*, 19(4), pp.782–789.

El Yacoubi, M. et al., 2008. Evidence for the involvement of the adenosine A2A receptor in the lowered susceptibility to pentylenetetrazol-induced seizures produced in mice by long-term treatment with caffeine. *Neuropharmacology*, 55(1), pp.35–40.

Yamanaka, S. and Blau, H.M., 2010. Nuclear reprogramming to a pluripotent state by three approaches. *Nature*, 465(7299), pp.704–712.

Zachariah, R.M. et al., 2012. Novel MeCP2 Isoform-Specific Antibody Reveals the Endogenous MeCP2E1 Expression in Murine Brain, Primary Neurons and Astrocytes. *PLoS ONE*, 7(11), pp.24–28.